21st Nordic Process Control Workshop

Welcome to the 21st Nordic Process Control Workshop (NPCW) held at Åbo Akademi University, Åbo (Turku), Finland, 18–19 January 2018. The workshop brings together the Nordic Process Control (NPC) community to present and discuss research topics, including recent advances, on-going work, and future trends, and to consolidate and expand networking in the field of process control. Typical workshop participants are doctoral students, researchers, academics and professionals from academia, industry and research organisations.

The workshop is organised every one-and-a-half year by the NPC Working Group, the venue alternating between Denmark, Norway, Sweden and Finland. Current working group members are:

Prof. Kurt-Erik Häggblom, Åbo Akademi, Finland (chair)
Dr. Gürkan Sin, DTU, Denmark (co-chair)
Dr. Elling W. Jacobsen, KTH, Sweden (previous chair)
Prof. Sigurd Skogestad, NTNU, Norway (penultimate chair)
Dr. Jenő Kovács, Sumitomo SHI SW, Finland
Dr. John Bagterp Jørgensen, DTU, Denmark
Dr. Jan Peter Axelsson, Vascaia AB, Sweden
Prof. Bjarne Foss, NTNU, Norway
Dr. Annika Leonard, Vattenfall AB, Sweden
Dr. Alf Isaksson, ABB AB, Sweden
Prof. Bernt Lie, University College Southeast, Norway
Dr. Hans Aalto, Neste Engineering Solutions Oy, Finland
Dr. Bjørn Glemmestad, Yara Technology Centre, Norway
Prof. Tore Hägglund, LTH, Sweden
Docent Torsten Wik, CTH, Sweden
Dr. Krister Forsman, Perstorp AB, Sweden
Dr. Christer Utzen, GEA Process Engineering A/S, Denmark
Dr. Iiro Harjunkoski, Aalto University, Finland / ABB AG, Germany

The NPC Working Group awards the "Nordic Process Control Award" to persons who have made "lasting and significant contributions to the field of process control". The recipient of the 2018 NPC Award is Professor Dale E. Seborg, University of California, Santa Barbara, USA. We warmly congratulate Prof. Seborg and look forward to his award lecture "A Process Control Odyssey".

Previous recipients of the NPC Award are:

Howard H. Rosenbrock (Åland, Finland, 21 August 1995)
Karl Johan Åström (Wadahl, Norway, 13 January 1997)
F. Greg Shinskey (Stockholm, Sweden, 24 August 1998)
Jens G. Balchen (Lyngby, Denmark, 14 January 2000)
Charles R. Cutler (Åbo, Finland, 23 August 2001)
Roger W. Sargent (Trondheim, Norway, 9 January 2003)
Ernst Dieter Gilles (Gothenburg, Sweden, 19 August 2004)
Manfred Morari (Lyngby, Denmark, 26 January 2006)
Jacques Richalet (Espoo, Finland, 23 August 2007)
John MacGregor (Porsgrunn, Norway, 29 January 2009)
Graham Goodwin (Lund, Sweden, 26 August 2010)
Lawrence T. Biegler (Lyngby, Denmark, 26 January 2012)
James B. Rawlings (Oulu, Finland, 22 August 2013)
Rudolf Kalman (Trondheim, Norway, 15 January 2015)
Wolfgang Marquardt (Sigtuna, Sweden, 25 August 2016)

Prior to the workshop, on 17 January 2018, there is a full-day tutorial on "Recent Developments of Optimization in Process Systems Engineering". It is given by people with a background in the Optimization and Systems Engineering (OSE) group at Åbo Akademi University.

The Laboratory of Process Control in the Department of Chemical Engineering, Faculty of Science and Engineering at the Åbo Akademi University, is responsible for the local arrangements this year. The local organising committee consists of

Kurt-Erik Häggblom
Annika Fougstedt
Jari Böling

We wish to thank Ms. Henna Sucksdorff for setting up the registration site and for handling incoming registrations. Help from doctoral students and postdoctoral researchers at the Laboratory of Process Control and the Laboratory of Process Design and Systems Engineering is gratefully acknowledged.

We wish you all an enjoyable workshop!

Åbo, 15 January 2018

Kurt-Erik Häggblom

Contents

Program Outline

Tutorial:

Recent Developments of Optimization in Process Systems Engineering

Wednesday 17 January

09.30–10.10 Registration with coffee & sandwich

10.10–10.15 Opening words

10.15–11.55 Modeling in Process Control and Systems Engineering from a Sparse Perspective

12.00–13.00 Lunch

13.10–14.10 Optimization in Process Systems Engineering

14.15–15.15 Semidefinite Programming — Basics

15.15–15.30 Coffee break

15.30–17.00 Semidefinite Programming — Advanced Topics and Application

19.00– Dinner

Workshop

Thursday 18 January

08.15–08.50 Registration

08.50–09.00 Welcome to the 21st NPCW

09.00–09:15 Nordic Process Control Award presented to Prof. Dale Seborg

09.15–10.00 Award Lecture by Prof. Dale Seborg

10.00–10.20 Coffee break

10.20–12.00 Session 1: Optimization and Control

12.10–13.10 Lunch

13.20–15.00 Session 2: Performance and Diagnostics

15.00–15.20 Coffee break

15.20–17.00 Session 3: Use of Soft Sensors in Process Control

17.00–18.00 Poster Session with refreshments

17.30–18.30 NPC Working Group Meeting

19.00–20.00 Guided tour at Aboa Vetus Museum of History

20.00– Workshop Dinner at the museum restaurant

Friday 19 January

08.20–10.00 Session 4: Control Structures and Strategies

10.00–10.20 Coffee break

10.20–12.00 Session 5: Modelling

12.10–13.10 Lunch

13.20–14.40 Session 6: System Identification

14.40–15.00 Closing Ceremony and Welcome to 22nd NPCW

List of Participants

Denmark (7+3=10)

Ricardo Caroço	Technical University of Denmark	rcar@kt.dtu.dk
Eskild S Fleischer	GEA Process Engineering	eskild.s.fleischer@gea.com
John Bagterp Jørgensen	Technical University of Denmark	jbjo@dtu.dk
Jørgen K H Knudsen	2-control Aps	joek@2-control.dk
Frederico Montes	Technical University of Denmark	fmon@kt.dtu.dk
Emil Krabbe Nielsen	Technical University of Denmark	ekrani@elektro.dtu.dk
Merve Öner	Technical University of Denmark	meon@kt.dtu.dk
Gürkan Sin	Technical University of Denmark	gsi@kt.dtu.dk
Robert Spann	Technical University of Denmark	rosp@kt.dtu.dk
Christer Utzen	GEA Process Engineering	christer.utzen@geagroup.com

Finland (24+10+4=38)

Hans Aalto	Neste Engineering Solutions Oy	hans.aalto@neste.com
Merja Aartovaara	Borealis Polymers Oy	merja.aartovaara@borealisgroup.com
Bernt Åkesson	Finnish Defence Research Agency	bernt.akesson@mil.fi
Jari Böling	Åbo Akademi University	jboling@abo.fi
Mats Friman	Metso Flow Control	mats.friman@metso.com
Sten Gustafsson	Åbo	sten.gustafsson@abo.fi
Tore Gustafsson	Åbo	togustaf@gmail.com
Kurt-Erik Häggblom	Åbo Akademi University	khaggblo@abo.fi
Iiro Harjunkoski	Aalto University / ABB AG, Germany	iiro.harjunkoski@aalto.fi
Alia Joko	Åbo Akademi University	carolyn.joko@abo.fi
Kaj Juslin	Enbuscon Oy	kaj.juslin@enbuscon.com
Jenő Kovács	Sumitomo SHI SW	jeno.kovacs@shi-g.com
Jan Kronqvist	Åbo Akademi University	jan.kronqvist@abo.fi
Mikael Kurula	Åbo Akademi University	mkurula@abo.fi
Antton Lahnalammi	Aalto University	antton.lahnalammi@aalto.fi
Rinat Landman	Aalto University	rinat.landman@aalto.fi
Esa Lappi	National Defence University	esa.lappi@mil.fi
Andreas Lundell	Åbo Akademi University	andreas.lundell@abo.fi
Mikael Manngård	Åbo Akademi University	mmanngar@abo.fi
Erkka Moilanen	Stora Enso International Oy	erkka.moilanen@storaenso.com
Minh Nguyen	Aalto University	minh.dn.nguyen@aalto.fi
Antti Pelkola	Neste Engineering Solutions Oy	antti.pelkola@neste.com
Frank Pettersson	Åbo Akademi University	frank.pettersson@abo.fi
Ray Pörn	Åbo Akademi University	rporn@abo.fi
Ilkka Rytkölä	Wärtsilä Finland Oy	Ilkka.rytkola@wartsila.com
Henrik Saxén	Åbo Akademi University	hsaxen@abo.fi
John-Eric Saxén	Åbo Akademi University	john-eric.saxen@abo.fi
István Selek	University of Oulu	istvan.selek@oulu.fi
Amir Shirdel	Neste Engineering Solutions Oy	amir.shirdel@neste.com
Anders Skjäl	Åbo Akademi University	anders.skjal@abo.fi
Bei Sun	Aalto University	bei.sun@aalto.fi
Hannu Toivonen	Åbo Akademi University	htoivone@abo.fi

Stefan Tötterman	Neste Engineering Solutions Oy	stefan.totterman@neste.com
Ann-Christin Waller	Åland	ann-christin.waller@aland.net
Kurt Waller	Åland	kurt.waller@aland.net
Matias Waller	Åland University of Applied Sciences	matias.waller@ha.ax
Tapio Westerlund	Åbo Akademi University	twesterl@abo.fi
Kai Zenger	Aalto University	kai.zenger@aalto.fi

Iran (1)

| Bijan Moaveni | Iran Univ. of Science and Technology | b_moaveni@iust.ac.ir |

Norway (19+1=20)

Muhammad Faisal Aftab	Norwegian Univ. of Science and Technology	muhammad.faisal.aftab@ntnu.no
Christoph Backi	Norwegian Univ. of Science and Technology	christoph.backi@itk.ntnu.no
Timur Bikmukhametov	Norwegian Univ. of Science and Technology	timur.bikmukhametov@ntnu.no
Tamal Das	Norwegian Univ. of Science and Technology	tamal.das@ntnu.no
Bjørn Glemmestad	Yara Technology Centre	bjorn.glemmestad@yara.com
Johannes Jäschke	Norwegian Univ. of Science and Technology	johannes.jaschke@ntnu.no
Jonatan Klemets	Norwegian Univ. of Science and Technology	jonatan.klemets@itk.ntnu.no
Dinesh Krishnamoorthy	Norwegian Univ. of Science and Technology	dinesh.krishnamoorthy@ntnu.no
Torstein T Kristoffersen	Norwegian Univ. of Science and Technology	torstein.t.kristoffersen@ntnu.no
Bernt Lie	University College Southeast	bernt.lie@usn.no
Pedro Lira-Parada	Norwegian Univ. of Science and Technology	pedro.a.l.parada@ntnu.no
Bahareh Nikparvar	Norwegian Univ. of Science and Technology	bahareh.nikparvar@ntnu.no
Sveinung Ohrem	Norwegian Univ. of Science and Technology	sveinung.j.ohrem@ntnu.no
Marius Reed	Norwegian Univ. of Science and Technology	mariusre@stud.ntnu.no
Sigurd Skogestad	Norwegian Univ. of Science and Technology	skoge@ntnu.no
Julian Straus	Norwegian Univ. of Science and Technology	julian.straus@ntnu.no
Mandar Thombre	Norwegian Univ. of Science and Technology	mandar.thombre@ntnu.no
Adriaen Verheyleweghen	Norwegian Univ. of Science and Technology	adriaen.verheyleweghen@ntnu.no
Ludmila Vesjolaja	University College Southeast	ludmila.vesjolaja@usn.no
Cristina Zotica	Norwegian Univ. of Science and Technology	cristina.f.zotica@ntnu.no

Sweden (8+3=11)

Khalid Atta	Luleå University of Technology	khalid.atta@ltu.se
Jan Peter Axelsson	Vascaia AB	jan.peter.axelsson@vascaia.se
Fredrik Bengtsson	Chalmers University of Technology	fredben@chalmers.se
Wolfgang Birk	Luleå University of Technology	wolfgang.birk@ltu.se
Krister Forsman	Perstorp AB	krister.forsman@perstorp.com
Tore Hägglund	Lund University	tore@control.lth.se
Elling W Jacobsen	Royal Institute of Technology	jacobsen@ee.kth.se
Michael Lundh	ABB AB	michael.lundh@se.abb.com
Simon Pedersen	Chalmers University of Technology	pesimon@chalmers.se
Olle Trollberg	Royal Institute of Technology	olletr@kth.se
Torsten Wik	Chalmers University of Technology	tw@chalmers.se

USA (2)

| Dale Seborg | University of California, Santa Barbara | dale.seborg@gmail.com |
| Judy Seborg | Santa Barbara, California | seborgj@gmail.com |

Tutorial Program

Recent Developments of Optimization in Process Systems Engineering

Wednesday 17 January

09.30–10.10 Registration with coffee & sandwich

10.10–10.15 Opening words

10.15–11.55 Modeling in Process Control and Systems Engineering from a Sparse Perspective
Hannu Toivonen and Mikael Manngård, Åbo Akademi

12.00–13.00 Lunch

13.10–14.10 Optimization in Process Systems Engineering
Jan Kronqvist, Åbo Akademi

14.15–15.15 Semidefinite Programming — Basics
Ray Pörn, Åbo Akademi

15.15–15.30 Coffee break

15.30–17.00 Semidefinite Programming — Advanced Topics and Applications
Ray Pörn, Åbo Akademi

19.00– Dinner

You are encouraged to bring your own laptop to the tutorial with programs and toolboxes installed as explained in the topic outlines.

Sparse modeling in process control and process systems engineering

Hannu Toivonen and Mikael Manngård

Developments in sparse optimization during the last twenty years have made it possible to address certain combinatorial optimization problems, which were previously deemed intractable. The purpose of this tutorial is to describe some applications of sparse optimization in process control and systems engineering. These include variable selection for predictive models, identification of switching systems, system identification in the presence of trends, and identification of low-order dynamic models.

The structure of the presentation is as follows:

1) **Background: examples of combinatorial optimization problems**
   - Variable selection, i.e., finding a small subset from a given set of variables which explains data. For example, for predictive models, or to explain fault situations.
   - Change detection in data or model. For example: identification of switching systems, which switch between a number of modes at unknown time instants, or estimation of piecewise linear trends in data.

2) **A basic problem: selection of independent variables in regression model**
   Here we describe how a combinatorial problem can be solved, either exactly or approximately, by relaxing it to a convex l1-constrained problem. The most important properties of this approach are reviewed.

3) **System identification in the presence of trends and level shifts**
   Here we identify a system model and structured disturbances (such as trends, outliers and level shifts) simultaneously using sparse optimization. Results are demonstrated on numerical examples.

4) **Identification of low-order system models**
   System order can be characterized in terms of the rank of a Hankel matrix associated with the system's impulse response. Identification of a low-order model can therefore be formulated as a rank-constrained optimization problem. These are numerically hard problems, but can be relaxed by replacing the matrix rank by its nuclear norm, defined as the sum of the matrix singular values. The nuclear norm relaxation results in a convex optimization problem, for which efficient solvers exist.

For the numerical examples in the tutorial the cvx toolbox in Matlab will be used.

Optimization in process systems engineering

Jan Kronqvist

In this workshop we present some important types of optimization problems, with focus on how to solve these problems. We present some basic theory, methods and some problem formulations. We demonstrate how these problems can be solved efficiently in Matlab by the state-of-the-art solvers Gurobi and IPOPT.

1) **A brief introduction to optimization**

2) **Integer programming**
   We present techniques for solving linear problems containing integer variables, mainly the branch and bound method and some cutting planes.

3) **Disjunctive programming**
   How to incorporate logic decisions in optimizations problems.

4) **Solving optimization problems in Matlab**
   We show how to solve linear problems with integer variables in Matlab using Gurobi. We also give a brief illustration on how to use the nonlinear solver IPOPT with Matlab.

5) **Optimization problems with nonlinear functions**
   How can we solve optimization problems with both nonlinear functions and integer variables?

In this workshop we will use the solvers Gurobi and IPOPT in Matlab. There are free Academic licenses available for both solvers and we encourage participant to obtain these in advance.

Opti toolbox which contains IPOPT and some other powerful solvers can be obtained from:
https://www.inverseproblem.co.nz/OPTI/

Gurobi which is one of the most powerful solvers for linear and quadratic optimization problems can be obtained directly from:
http://www.gurobi.com/
There is an interface to Matlab which is easy to set up. Obtaining the Academic license takes less than 5 minutes (can only be done with a university network connection).

Semidefinite programming – basics and applications

Ray Pörn

Semidefinite programming (SDP) is one of the most exciting developments in mathematical programming during the last 20 years. SDP has applications in very diverse fields such as convex constrained optimization, control theory, combinatorial optimization, statistics, differential geometry and many more. SDPs are often solved using interior-point methods and many applications can be solved fairly efficiently in practice. The structure of this workshop is as follows:

1) **Introduction and some applications**

2) **Representability**
   What can be expressed as SDPs? Many different things can be expressed using linear matrix inequalities (LMIs) and solved with SDP methods. Some tools from linear algebra are given in order to represent different constraints in correct form.

3) **Relaxation and randomization**
   SDP provides tight approximation of different non-convex optimization problems. The SDP solution can also be used as a basis for a fast randomization procedure in order to obtain a good quality solution for the non-convex problem.

4) **Reformulation**
   Combinatorial problems can be reformulated in many ways, a typical technique is linearization. SDP can be used to obtain an optimal reformulation of certain combinatorial problem.

5) **More applications**

6) **Computer exercises**
   The participants are encouraged to bring their own laptop with matlab and the cvx toolbox (http://cvxr.com/cvx/download/) installed.

Workshop Program

Thursday 18 January

08.15–08.50 Registration

08.50–09.00 Welcome to the 21st NPCW

09.00–09:15 Nordic Process Control Award presented to Prof. Dale Seborg

09.15–10.00 Award Lecture by Prof. Dale Seborg
Chair: Elling W. Jacobsen, KTH

1. A Process Control Odyssey [Abstract]
   Dale Seborg
   University of California, Santa Barbara, USA

10.00–10.20 Coffee break

10.20–12.00 Session 1: Optimization and Control
Chair: Sigurd Skogestad, NTNU

2. On Handling Non-Linearity for Model-Based Predictive Control and Optimization [Paper]
   Hans Aalto and Antti Pelkola
   Neste Engineering Solutions Oy, Finland

3. Industrial Implementation of Nonlinear Model Predictive Controllers [Paper]
   Jørgen K.H. Knudsen[1] and John Bagterp Jørgensen[2]
   [1]2-control Aps, Denmark, [2]Technical University of Denmark (DTU)

4. A Novel Approach to Steady-State Gradient Estimation Using Transient Measurements [Abstract]
   Dinesh Krishnamoorthy, Esmaeil Jahanshahi, and Sigurd Skogestad
   Norwegian University of Science and Technology (NTNU)

5. Steady-State Optimization Using Phase-Lag Information [Abstract]
   Olle Trollberg and Elling W. Jacobsen
   Royal Institute of Technology (KTH), Sweden

6. State of the Art of Integration of Scheduling and Control — Remaining Challenges [Abstract]
   Iiro Harjunkoski
   Aalto University, Finland, and ABB AG, Germany

12.10–13.10 Lunch

13.20–15.00 Session 2: Performance and Diagnostics
Chair: John Bagterp Jørgensen, DTU

7. Intelligent Vessels [Abstract]
   Ilkka Rytkölä and Fredrik Östman
   Wärtsilä Finland Oy

8. Analysis of Indirect Fire System Effectiveness Using Simulation and Data Farming [Abstract]
   Miika Haataja[1], Esa Lappi[2], and Bernt Åkesson[1]
   [1]Finnish Defence Research Agency; [2]National Defence University, Finland

9. Assessment of the Control Performance of Combustion-Thermal Power Plants [Abstract]
   István Selek[1] and Jenö Kovács[2]
   [1]University of Oulu, Finland; [2]Sumitomo SHI FW, Finland

10. Detection and Characterization of Oscillations in Control Loops using Multivariate Empirical Mode Decomposition: An Overview [Abstract]
    Muhammad Faisal Aftab and Morten Hovd
    Norwegian University of Science and Technology (NTNU)

11. Using Multilevel Flow Modeling for Fault Diagnosis of Produced Water Treatment [Abstract]
    Emil Krabbe Nielsen, Jerome Frutiger, Gürkan Sin, Ole Ravn, and Morten Lind
    Technical University of Denmark (DTU)

15.00–15.20 Coffee break

15.20–17.00 Session 3: Use of Soft Sensors in Process Control

Chair: Jenö Kovács, Sumitomo SHI SW, Finland

12. Fault-Tolerant Control of Actuators [Abstract]
    Mats Friman
    Metso Flow Control, Finland

13. Analysis of Influence of Sensor Degradation on Flowrate Estimates by Virtual Flow Metering Systems [Abstract]
    Timur Bikmukhametov and Johannes Jäschke
    Norwegian University of Science and Technology (NTNU)

14. Model-Based Process Development and Monitoring of Lactic Acid Bacteria Fermentations [Abstract]
    Robert Spann[1], Anna Eliasson Lantz[1], Christophe Roca[2], Krist V. Gernaey[1], and Gürkan Sin[1]
    [1]Technical University of Denmark (DTU); [2]Chr. Hansen, Denmark

15. Comparative Study of Kalman Filter-Based Observers with Simplified Tuning Procedures [Abstract]
    Christoph Josef Backi and Sigurd Skogestad
    Norwegian University of Science and Technology (NTNU)

16. State and Parameter Estimation for a Gas-Liquid Cylindrical Cyclone [Abstract]
    Torstein Thode Kristoffersen and Christian Holden
    Norwegian University of Science and Technology (NTNU)

17.00–18.00 Poster Session with refreshments

17.30–18.30 NPC Working Group Meeting

19.00–20.00 Guided tour at Aboa Vetus Museum of History

20.00–   Workshop Dinner at the museum restaurant

Friday 19 January

08.20–10.00 Session 4: Control Structures and Strategies

Chair: Kurt-Erik Häggblom, ÅA

17. A New Efficient Ratio Control Structure [Abstract]
    Tore Hägglund
    Lund University, Sweden

18. Discrete PI Controller Design for Linear Measurement Combinations in Self-Optimizing Control [Abstract]
    Jonatan Klemets and Morten Hovd
    Norwegian University of Science and Technology (NTNU)

19. Risk-Based Health-Aware Control of Subsea System [Abstract]
    Adriaen Verheyleweghen and Johannes Jäschke
    Norwegian University of Science and Technology (NTNU)

20. Resolving Issues of Scaling for Gramian Based Input-Output Pairing Methods [Abstract]
    Fredrik Bengtsson[1], Torsten Wik[1], and Elin Svensson[2]
    [1]Chalmers University of Technology, Sweden; [2]CIT Industriell Energi AB, Sweden

21. On the Modified Hankel Interaction Index Array for Control Configuration Selection [Abstract]
    Bijan Moaveni[1] and Wolfgang Birk[2]
    [1]Iran University of Science and Engineering; [2]Luleå University of Technology, Sweden

10.00–10.20 Coffee break

10.20–12.00 Session 5: Modelling

Chair: Bernt Lie, UCS

22. Surrogate Model Generation Using the Concepts of Self-Optimizing Control [Paper]
    Julian Straus and Sigurd Skogestad
    Norwegian University of Science and Technology (NTNU)

23. Scale-Up Modeling of a Pharmaceutical Crystallization Process via Compartmentalization Approach [Abstract]
    Merve Öner[1], Getachew S. Molla[1], Michael F. Freitag[2], Stuart M. Stocks[2], Jens Abildskov[1], and Gürkan Sin[1]
    [1]Technical University of Denmark (DTU); [2]LEO Pharma A/S, Denmark

24. Nonsmooth Modelling Methods in Chemical Engineering [Abstract]
    Marius Reed, Marlene Lund, and Johannes Jäschke
    Norwegian University of Science and Technology (NTNU)

25. Neural Network-Based Model Reduction and Sensitivity Analysis of Apoptosis [Abstract]
    C. Alia Joko, Frank Pettersson, and Henrik Saxén
    Åbo Akademi University, Finland

26. A Dynamic Model of the Response of Foodborne Pathogenic Bacteria to High Pressure Processing [Abstract]
    Bahareh Nikparvar[1], Nils Nieuwenkamp[2], and Nadav Bar[1]

    [1]Norwegian University of Science and Technology (NTNU); [2]University of Amsterdam, the Netherlands

12.10–13.10 Lunch

13.20–14.40 Session 6: System Identification

Chair: Tore Hägglund, LTH

27. Input PRBS Design for Identification of Multivariable Systems [Paper]
    Winston Garcia-Gabin and Michael Lundh
    ABB AB, Sweden

28. Experiment Designs to Obtain Uncorrelated Outputs in MIMO System Identification [Abstract]
    Kurt-Erik Häggblom
    Åbo Akademi University, Finland

29. Data-based Testing for Nonlinearity in Dynamical Systems: Surrogate Data Compared with Nonlinear Distortion [Paper]
    Matias Waller
    Åland University of Applied Sciences, Finland

30. Identification of Low Order Output-Error Models [Abstract]
    Mikael Manngård, Jari M. Böling, and Hannu T. Toivonen
    Åbo Akademi University, Finland

14.40–15.00 Closing Ceremony and Welcome to 22nd NPCW

List of Posters

Presentations for the poster session were selected based on submission preferences or degree of difficulty to classify the topic of the contribution as one for the oral sessions.

P1. Comparison of Two Classes of Observers in a Biochemical Process [Abstract]
R.F. Caroço[1], J. Abildskov[1], T. López-Arenas[2], and J.K. Huusom[1]
[1]Technical University of Denmark (DTU); [2]Universidad Autónoma Metropolitana-Cuajimalapa, Mexico

P2. Control Strategy Based on Radial Basis Function for an Ibuprofen Batch Crystallization Process under Upstream Uncertainty [Abstract]
Frederico Montes, Krist V. Gernaey, and Gürkan Sin
Technical University of Denmark (DTU)

P3. Modelling of the Prehydrolysis Kraft Process for Process Control [Paper]
Antton Lahnalammi, Herbert Sixta, and Sirkka-Liisa Jämsä-Jounela
Aalto University, Finland

P4. Fault Propagation Analysis Combining a Nonparametric Multiplicative Regression Causality Estimator with Process Connectivity Information [Paper]
Rinat Landman and Sirkka-Liisa Jämsä-Jounela
Aalto University, Finland

P5. A Receding Horizon Optimal Control Approach for Solution Purification Process [Paper]
Bei Sun[1], Sirkka-Liisa Jämsä-Jounela[1], and Chunhua Yang[2]
[1]Aalto University, Finland; [2]Central South University, Changsha, China

P6. Spectroscopic Method for Bacterial Quantification in Suspension [Abstract]
Minh Nguyen[1], Jarmo Alander[2], and Kai Zenger[1]
[1]Aalto University, Finland; [2]Vaasa University, Finland

P7. Estimation of the Regulating Power Potential of the Grocery Store S-Market Tuira [Abstract]
István Selek and Enso Ikonen
University of Oulu, Finland

P8. Methods and Software for Solving Convex Mixed Integer Nonlinear Programming Problems [Abstract]
Jan Kronqvist
Åbo Akademi University, Finland

P9. Profile Based Analysis for Automatic Feature Extraction from Time Series Data [Abstract]
John-Eric Saxén, Jerker Björkqvist, and Hannu T. Toivonen
Åbo Akademi University, Finland

P10. A Control Oriented Model for Inline Deoiling Hydrocyclone [Abstract]
Tamal Das and Johannes Jäschke
Norwegian University of Science and Technology (NTNU)

P11. SIMC-Tuned PID Feedback Control Strategy in Fed-Batch Bioreactors [Abstract]
Pedro A. Lira-Parada and Nadav Bar
Norwegian University of Science and Technology (NTNU)

P12. Combining Safety and Control using System Theoretic Process Analysis and Adaptive Control [Abstract]
Sveinung Ohrem, Hyangju Kim, Christian Holden, and Mary Ann Lundteigen
Norwegian University of Science and Technology (NTNU)

P13. Optimal Operation using Classical Advanced Control Structures [Abstract]
Adriana Reyes-Lúa, Cristina Zotica, and Sigurd Skogestad
Norwegian University of Science and Technology (NTNU)

P14. Robust Optimization of a Gasoline Blending System [Abstract]
Mandar Thombre and Johannes Jäschke
Norwegian University of Science and Technology (NTNU)

P15. Future Directions in Control Relevant Models for Granulation Loop in Fertilizer Production [Paper]
Ludmila Vesjolaja[1], Bjørn Glemmestad[2], and Bernt Lie[1]
[1]University College of Southeast Norway; [2]Yara Technology Centre, Norway

P16. Comparing Water Treatment Topologies in Recirculating Aquaculture Plants [Abstract]
Simon Pedersen and Torsten Wik
Chalmers University of Technology, Sweden

P17. Utilization of Generic Consumer Modeling in Planning and Optimization of District Heating and Cooling Systems [Abstract]
Khalid Tourkey Atta and Wolfgang Birk
Luleå University of Technology, Sweden

P18. Integrating Microbial Genome-Scale Flux Balance Models with JModelica and the Bioprocess Library for Modelica [Abstract]
Jan Peter Axelsson
Vascaia AB, Sweden

Submitted Abstracts and Papers

In addition to the Award Lecture abstract submitted by Prof. Dale Seborg, 47 contributions were submitted and accepted to the workshop. After final revisions, there are 9 full papers and 39 abstracts or extended abstracts.

There are 35 submissions from academia (5 papers, of which 3 from Aalto University), 7 submissions with authors from both academia and industry (2 papers), 5 submissions from industry (2 papers), and 1 submission from a research agency. Five contributions have an author with an affiliation outside the Nordic countries.

A Process Control Odyssey

by

Dale E. Seborg
Professor Emeritus and Research Professor
University of California
Santa Barbara, California, U.S.A

This presentation will provide a personal perspective on the development of the field of process control, including process control education, during the past 50 years. Much of the talk will be anecdotal, based on my research and teaching experience at the University of Alberta (U of A) and the University of California, Santa Barbara (UCSB). It will also be based on industrial control issues encountered during industry-sponsored research, consulting, and short courses.

My early research at the U of A emphasized the development of novel advanced process control techniques and their application to pilot-scale equipment, using first-generation real-time computers. I was fortunate to be able to collaborate on these research and education projects with two very talented and collegial colleagues, Grant Fisher and Reg Wood.

My research projects at both universities have typically included experimental applications to university pilot-scale equipment, in addition to theoretical analysis and computer simulation. These applications featured critical evaluations of new control techniques and experimental comparisons with existing methods. All but a few of my Ph.D. students were required to do some experimental work as part of their thesis projects. Also, about one half of my M.Sc. students included experimental results in their theses. The early research projects resulted in some of the first published process control applications of modern control multivariable control techniques such as Kalman filtering, LQG optimal control, and model-reference adaptive control. Later experimental studies were increasingly concerned with applications to larger scale industrial equipment, as well as biochemical and biomedical applications. At UCSB, I was fortunate to be able to collaborate with two very talented and collegial colleagues, Duncan Mellichamp and Frank Doyle, on both research projects and our textbook.

In general, publications on experimental applications in process control (and other fields) present glowing reports of successful research projects. By contrast, unsuccessful applications are seldom published, for obvious reasons. But unsuccessful projects can provide valuable insight into the limitations and shortcomings of advanced control techniques. Several such "failures", and the resulting insights gained from them, will be described.

In many ways, process control education has changed significantly over the past 50 years, with respect to curriculum and computer applications. In other ways, the basic methodology, classroom lectures and few, if any experiments, has changed very little. Current trends in process control education, as well as the evolution of my *Process Dynamics and Control* textbook, will be discussed.

On Handling Non-Linearity for Model-Based Predictive Control and Optimization

Hans Aalto
Neste Engineering Solutions Oy, NAPCON, PB 310, 06101 Porvoo
phone +358504583373, telefax +358104587221, hans.aalto@neste.com

Antti Pelkola
Neste Engineering Solutions Oy, NAPCON, PB 310, 06101 Porvoo
phone +358504583768, telefax +358104587221, antti.pelkola@neste.com

ABSTRACT

Two methods are brought about which extend the robust and industry-adopted linear model-predictive control (LMPC) towards non-linear cases. In addition, we present a simple formulation of model-predictive dynamic real-time optimization (DRTO) which is a equivalent with the widely used term economic MPC.

The LMPC algorithm is set up in such a way that it offers opportunities to incorporate the non-linear behaviour of the target process response, the most obvious being the prediction of the process response, using an internal model, prior to the calculation of the optimal control solution. Further on, iterative refinement of the optimal control solution to better match process non-linearity can be used. Such solutions can be built as extensions to existing LMPC which has value in industrial applications.

DRTO can be derived from MPC by replacing the cost function, i.e. the predicted control error, with a cost function reflecting the process economics or with a negative benefit function. This means that control close to targets in terms of the control error minimization is no longer done, but the control task is re-formulated so as to keep the controlled variables between suitable minimum and maximum limits, in other words, the set of constraints of the original MPC is extended.

The two methods presented above are developed and tested in simulation environments with a distillation column and natural gas pipelines as target process models.

1 INTRODUCTION

Non-linear dynamic process models can be represented as first-principles non-linear ordinary or partial differential equations or obtained by experimental, data-driven methods. Hybrid representations also exist where these two models are combined to describe the overall behavior of some complex process. First-principles models often need parameter estimation (or model output validation, or both) against true measured data from the process, so the models may be augmented with a linear or non-linear estimator part so that the combined model and estimator are operating in either off-line or on-line mode.

Straightforward implementations of non-linear model-predictive control (NL-MPC) use either first-principles or experimental non-linear models when iterating towards the optimum control solution i.e. the optimum profile of present and future manipulated variables (MV). This approach almost always means long execution times from which long control cycles follows and quite often convergence problems also need to be addressed. Of course, non-linear model means non-linear optimization methods to be used in NL-MPC. A plethora of publications exist on utilizing particular model constructs such as polynomials to make the NL-MPC somewhat easier. In practical industrial applications, the linear MPC (LMPC) seems to be much more popular than NL-MPC because LMPC, which uses linear (or linearized) dynamical models, the calculation of the optimum MV profiles is accomplished by solving a quadratic programming (QP) problem which is much easier.

MPC executes three steps at each control cycle : 1) calculate, using a model, the "free response" M-vector y_{pre} of all controlled variables (CV) based on MV moves, measured disturbance variables (DV) and measured CV values and 2) make a "bias" correction of the CV predictions based on the freshest available process output data and define either the reference value M-vectors for CV's y_{ref} or minimum/maximum limits and 3) calculate the optimum (predicted control error minimizing) profile $u*$ of MV's from present time into the future honouring the constraints. The additivity of free response and the optimized part of the response to form the optimal output (CV) response M-vector , $y^* = \tilde{h}_1 u^* + y_{pre}$, is valid for LMPC but in principle not for the non-linear case. M is the length of the prediction horizon and $\tilde{h}_1$ is a matrix of impulse response coefficients.

See Section 2.1 and Figure 2 below for definition of bias and other terms used.
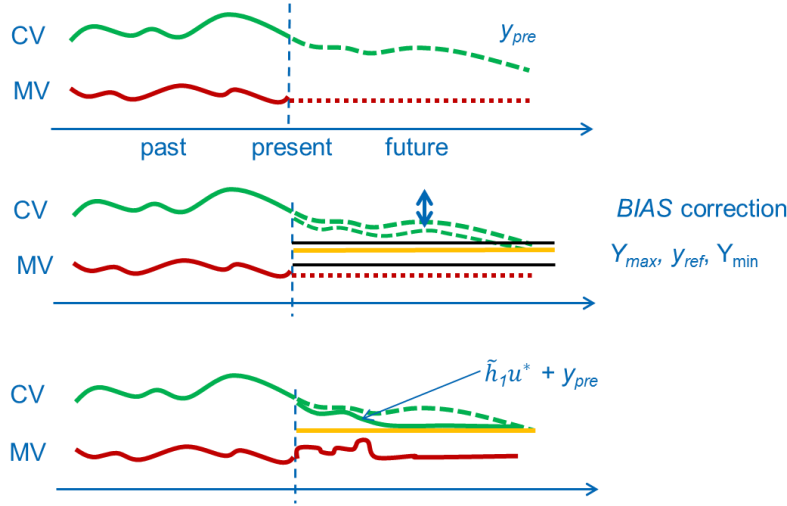
Figure 1.   The three steps of the MPC control cycle

A first-principles model is essentially a black box accepting inputs and producing outputs, while access to internal state variables may or may not be possible. A number of adjustable parameters affect the state and output behavior.

A general framework for empirical non-linear models is the Volterra series representation (Schetzen, 1980, among others):

$$y(k) = \left\{ \sum_{j=0}^{M} h_1(j) u(k-j) \right\}_{LIN} + \qquad (1)$$

$$\left\{ \sum_{h=2}^{r_0} \left(\sum_{j_1=0}^{M} \sum_{j_2=0}^{M} ... \sum_{j_h=0}^{M} h_h(j_1, j_2,..., j_h) u(k-j_1) u(k-j_2)...u(k-j_h) \right) \right\}_{NL},$$

where the first term represents the linear part of the process. The second term covers all the process nonlinearities. This model structure corresponds to the general Wiener model representation, where the linear part and the nonlinear part are additive to each other. In practice this nonlinear part is too complicated and heavy to be implemented in real time controls. Further the Volterra series has quite limited convergence. To avoid this problem Wiener suggested utilizing orthogonal functionals in his general Wiener representation (Wiener N., 1958). Due to space limitations we shall not present any of the numerous reduction techniques available to make the model structure more suitable for real-time MPC.

2 NON-LINEARITY WITH LINEAR MPC

2.1 Non-linear MPC with Wiener model structure

The full order Volterra series representation in SISO case (see Eq. 1) can be rewritten as follows:

$$y = \sum_{h=1}^{\infty} y^{(h)} = \sum_{h=1}^{\infty} \tilde{h}_h[h_h; u] = \tilde{h}[u] \qquad (2)$$

where $y^{(h)}$ is the h:th degree contribution to the overall response y and $\tilde{h}$ is a nonlinear Volterra operator that maps the input u into the output variable y. A single component $\tilde{h}_h[h_h; u]$ of this operator represents the h:th order Volterra kernel, where for each time instant k the following holds:

$$\tilde{h}_h[h_h; u(k)] = \sum_{j_1=0}^{M} \sum_{j_2=0}^{M} \cdots \sum_{j_h=0}^{M} h_h(j_1, j_2, \cdots, j_h) u(k - j_1) u(k - j_2) \cdots u(k - j_h). \qquad (3)$$

The total nonlinear Volterra operator $\tilde{h}$ can be written in the following operator form in case the inverse of the linear part of this series $\tilde{h}_1^{-1}$ exists:

$$\tilde{h} = \sum_{h=1}^{\infty} \tilde{h}_h = \tilde{h}_1 + \tilde{h}_2 + \tilde{h}_3 \cdots = \tilde{h}_1 \left(I + \tilde{h}_1^{-1} (\tilde{h}_2 + \tilde{h}_3 + \cdots) \right). \qquad (4)$$

Further the total inverse can be derived into the form (Doyle et al., 1995):

$$\tilde{h}^{-1} = \left(I + \tilde{h}_1^{-1} (\tilde{h}_2 + \tilde{h}_3 + \cdots) \right)^{-1} \tilde{h}_1^{-1}. \qquad (5)$$

This inverse of the whole Volterra operator (5) can be defined as the controller operator. The inverse of the total model requires first the inversion of only the first term $\tilde{h}_1^{-1}$, which is the linear part of the model, and secondly it requires the internal feedback from the controller output via the nonlinear terms of the model as shown in Eq (5).The resulting nonlinear internal model controller structure is shown in Figure 2, which corresponds to the linear internal model controller presented by Deshpande (1989) and others. This nonlinear controller synthesis yields the controller output as:

$$u = \left(I + \tilde{h}_1^{-1} (\tilde{h}_2 + \tilde{h}_3 + \cdots) \right)^{-1} \tilde{h}_1^{-1}[e]. \qquad (6)$$

This non-linear MPC in Figure 2 is an infinite sequence of operators. The first term is the linear model inverse, which is the only inverse operator in the subsequent terms. The terms are totally decoupled, which means that the linear operator inversion is all that is required initially and subsequent terms depend only on this linear inverse, previous terms in the operator series and the original model operator series. Feedback signal lines in the nonlinear MPC block are drawn as shown to emphasize that they are invoked by iteration and not simultaneously.

The key issues from the controller synthesis point of view are the convergence of the controller operator sequence, the way to implement a practical controller and the existence and the realizing of the inverse $\tilde{h}_1^{-1}$, which is not often implementable (Doyle et al., 1995).
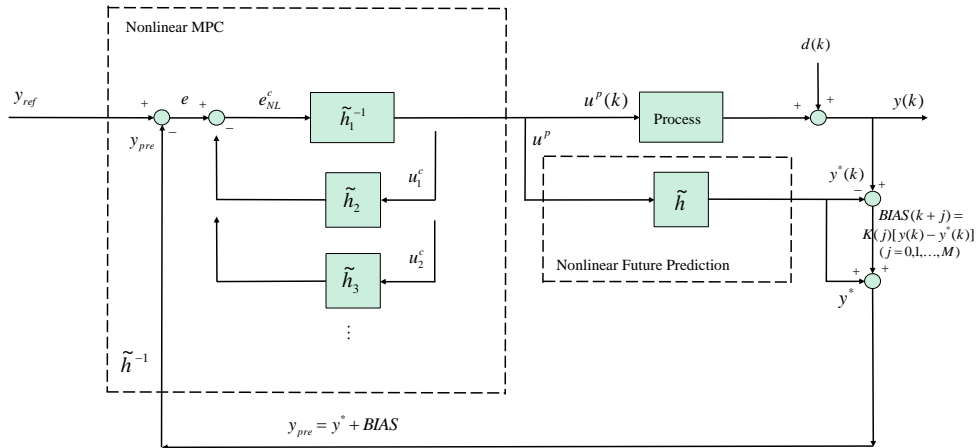
Figure 2. Nonlinear problem setting of MPC with Volterra model structure in SISO case.

As described earlier the linear part and the nonlinear part of the model are additive to each other and consequently they can be totally separated and identified separately. On the controller synthesis this can utilized in the same way as principally already shown in Figure 2. When the nonlinear terms are lumped together into an appropriate NN-model structure, the nonlinear predictive controller gets in general more simplified structure.

The two main parts of the controller structure are first the nonlinear prediction, which is the past contribution of the linear and the nonlinear NN-model predictions based on the process input history vector u^p. Secondly the nonlinear MPC structure, where the future contribution of the prediction based the nonlinear NN-model ($\tilde{h}_2 + \tilde{h}_3 + \cdots$) and the future control scenario $u^c = u_1^c + u_2^c + \cdots$, is subtracted from the predicted control error e. The remaining linear part of the error e_{NL}^c is minimized by the feedback controller, which approximates the inverse of the linear part of the model h_1^{-1}.

The total nonlinear past contribution of the prediction y^* based on the process input history vector u^p is:

$$y^* = y_{LIN}^* + y_{NL}^*, \tag{7}$$

where the linear part of the prediction y_{LIN}^* is based on any kind of linear model identified by any well-known identification techniques. The nonlinear part of the prediction y_{NL}^* can be totally described e.g. by an appropriate neural network structure. In order to introduce feedback from the true process, the predicted output $y^*(k)$ at the first prediction time step from the previous cycle is subtracted from the measured process output $y(k)$ and multiplied by a (gain) M-vector K to obtain a bias correction to be added to the non-linear prediction. This is a standard procedure for MPC.

2.2 Linear MPC with external black-box model

A black-box model does not reveal the model structure, but still it can be used to calculate the non-linear future predictions y^* in Figure 2. The non-linear corrections of the non-linear MPC : $\tilde{h}_2, \tilde{h}_3, \ldots$ cannot be formed so the LMPC is left alone to control the non-linear process although being supplied with non-linear predictions y^*. The linear models within LMPC do not match the non-linear predictions for most of the time but the control performance can still be good because LMPC is known to be robust against modelling error. If the degree of non-linearity of the process and the black-box model is significant, parameter adaptation within LMPC can be used, which then has a certain analogy with the non-linear corrections $\tilde{h}_2, \tilde{h}_3, \ldots$ in Figure 2.

It is actually quite self-evident to bring up the idea of augmenting LMPC with a black-box model, however, this idea is not widely discussed in literature and when brought up, it is hidden in more complicated model structures and concepts, (Gattu and Zafiriou, 1992 and 1995). From a practical standpoint, the concept is very appealing because a dynamic process simulator can be used to provide y^* and a suitable simulator model may be readily

available from e.g. previous process and control design tasks. Of course, interlinking LMPC and simulator needs software work such as time synchronization and modification of LMPC so that it can receive free response predictions from the simulator. The bias correction (see Figure 2) can be done within LMPC or in the simulator, if such a feature is available.

3   FROM LINEAR MPC TO DRTO

The basic idea to "upgrade" MPC to DRTO is to replace the control error cost function with a cost function which describes the process economy such as energy consumption. The DRTO optimization solver (QP for LMPC and some nonlinear solver for NL-MPC) can trivially be set to maximize a profit function. The MV, CV and DV variables involved and their dynamical relationships do not need any new conceptual definitions, only the selection of those variables may differ from a regular MPC set of variables. The MV's, CV's and DV's enter into the quadratic or non-linear cost (profit) function in an obvious way. If some CV constraints need to be obeyed they are easily incorporated into the set of constraints of the DRTO problem, either as linear (linearized) or non-linear constraints.

In the case of linear dynamic models and quadratic cost/profit, the attractive positive definiteness of the quadratic control error may be lost, so the QP solver must be able to copy with non-convex optimization.

An example is given in section 4.2 below.

4   METHODS VERIFICATIONS BY SIMULATIONS

Two case examples are presented: Non-linear MPC of a heavy oil fractionator using non-linear corrections within the MPC controller (Figure 2) and a DRTO for a natural gas pipeline system using a black-box model without the non-linear corrections.

## 4.1   Heavy Oil Fractionator

Crude oil and heavy oil fractionators are multi-product columns, where crude oil feed or in cracking reactors treated heavy oil feed is separated into several product cuts. The energy comes to the column with the vaporized feed and the separation is controlled by manipulating the cooling, the internal liquid reflux flow rate in the column and the outflow rates. Usually these columns are also strongly integrated to the energy recycle system of the plant. In the following a typical heavy oil fractionator is introduced for modeling and controls study purposes.

A full scale multivariable nonlinear control problem is introduced by Prett and Garcia (1988). As explained by the authors, it contains all the practical elements included in multivariable control applications. The process considered here is a heavy oil fractionator as shown in Figure 3.
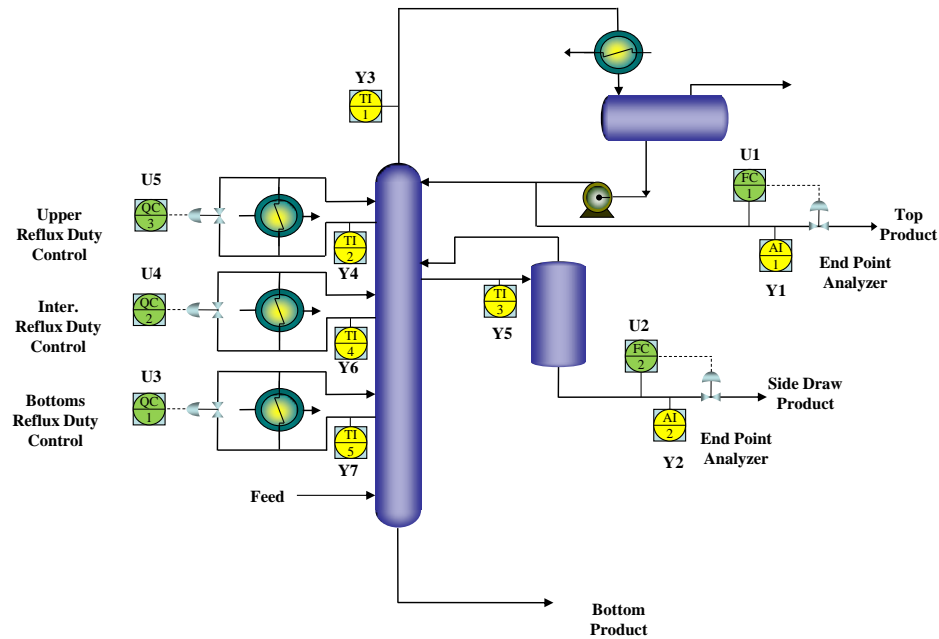
Figure 3.   Heavy Oil Fractionator with 5 MV's (=U's) and 7 CV's (=Y's).

The energy is fed into the Heavy Oil Fractionator only with the feed and is removed by the overhead and side coolers. The material balance is handled by the feed and product flow rates. The column separation can be maintained optimal continuously with these elements. The MV's are the main product flows (U1 and U2) and the duties of the side reflux duties (U3, U4 and U5). The CV's are the end points of the two main products (Y1 and Y2) and the specific column temperatures (Y3, Y4, Y5, Y6 and Y7) (Prett and Garcia, 1988).
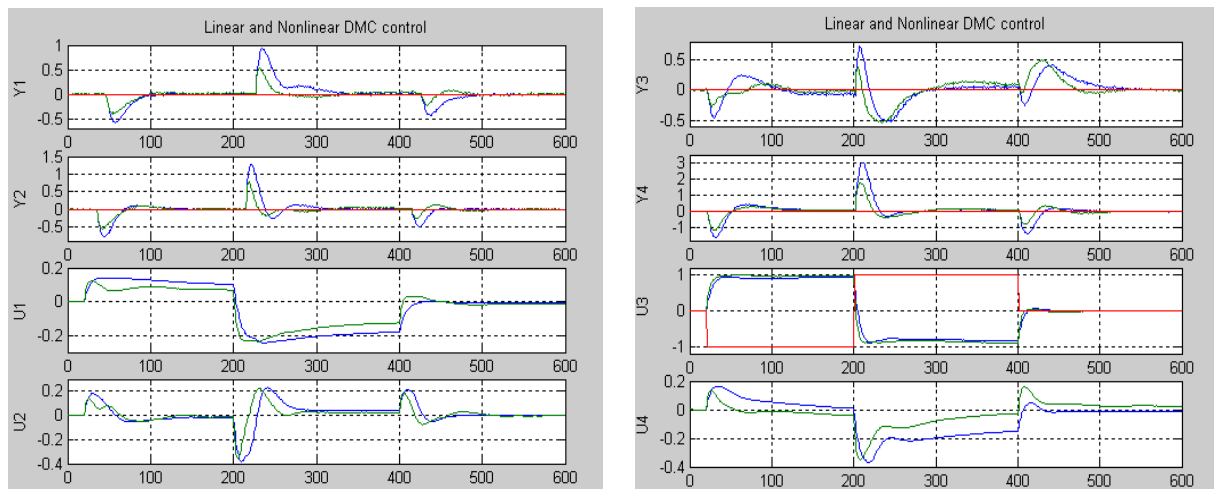
Figure 4.   Linear and nonlinear MPC control in case of measured step disturbances in the bottoms reflux duty U3 occur (Pelkola A., 2016).

In Figure 4 the linear MPC (blue lines) and the nonlinear MPC with orthogonal Wiener NN model structure (green lines) have been simulated in a case, where the step disturbances in the bottoms reflux duty U3 (red line) occur. In both cases the tunings of the MPC's are the same. These sizes of disturbances are quite dramatic in the operation of the column separation. It can be clearly seen that the control performance of the presented nonlinear MPC is better and stabilizes the process quicker than the corresponding linear MPC. Also the product quality and temperature deviations from the targets are smaller with the nonlinear MPC with orthogonal Wiener NN model structure (Pelkola A. 2016). The presented simulation period is 10 h's (600 minutes).

4.2 Natural gas pipeline network

The dynamics of natural gas pipeline networks is just slightly nonlinear (Aalto, 2008) which means that linear dynamical models can be used to model the behavior between MV's, typically discharge pressures of compressor stations and CV's, typically pressures and gas flows along the pipeline network. The DV's are the numerous gas off-take flow rates in the network which typically are accurately measured and for which, in several cases, forecasts are available. The DRTO task in this case is to minimize the energy used by compressor stations while fulfilling constraints on gas flow to clients (off-takes) and pressures in the pipeline.

The non-linear expression for energy used by a compressor can with good accuracy be approximated by a expression as follows:

$$kF\left[\left(\frac{P_d}{P_s}\right)^{\gamma} - 1\right] \approx kF(a\Delta P_d + b\Delta P_s + c) \qquad (8)$$

where k, a, b and c are constants , F is the gas flow through the compressor, γ is the polytropic exponent, P_d is compressor discharge pressure and P_s is compressor suction pressure.

Because P_d is an MV and F and P_s are CV's linearly dependent on MV's, (8) is a quadratic expression and as such usable in LMPC instead of the quadratic control error.

Each compressor must operate in a given window in the (F, P_d/P_s) coordinate system, the operating envelope, which act as non-linear constraints but may be linearized with reasonable accuracy, see Figure 5.
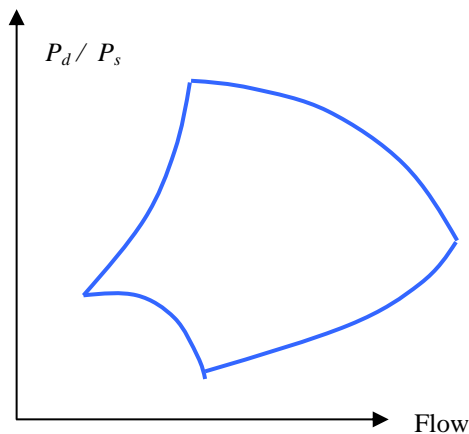

Figure 5.   Non-linear compressor envelope

DRTO for the Finnish natural gas pipeline network was tested in a simulation test-bench. A first-principles dynamical model produced the non-linear predictions (see figure 2 above) and the linearization and quadratic approximation steps from above were used. The pipeline network has three compressor stations with two compressors in each one and is presented in Figure 6.
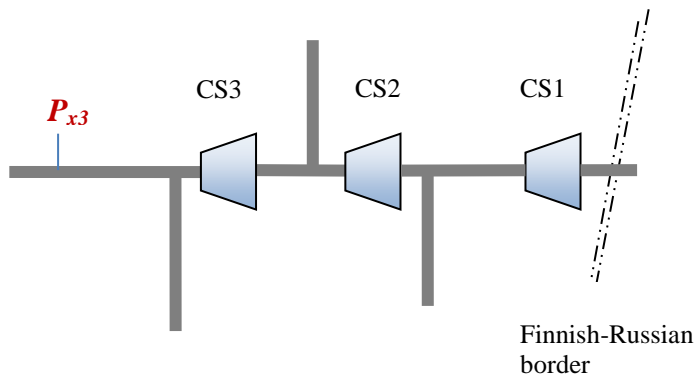
Figure 6. Schematic of the Finnish natural gas pipeline network with 3 compressor stations (CS). Total pipeline length is around 1000 kilometers.

Gas consumption forecasts are available and enter the non-linear prediction calculations directly. The target is to minimize total energy consumption of all three compressor stations. A test run using true pipeline data from year 2003 showed that 5% energy decrease is achieved. Figure 7 shows the behavior the pipeline pressure of a remote location at the end of the last pipeline segment. The pressure is moving very close to the minimum limit 29 bar compared to how the pipeline was really operated during the same time period. Lower pressure P_{x3} also mean less energy consumption of CS3. The three MV's, i.e. discharge pressures for compressor stations behaved as expected for simple transmission pipeline networks: discharge pressure of CS3 is minimized against constraints and CS1 and CS2 maximized against constraints. For details, see (Aalto, 2008).
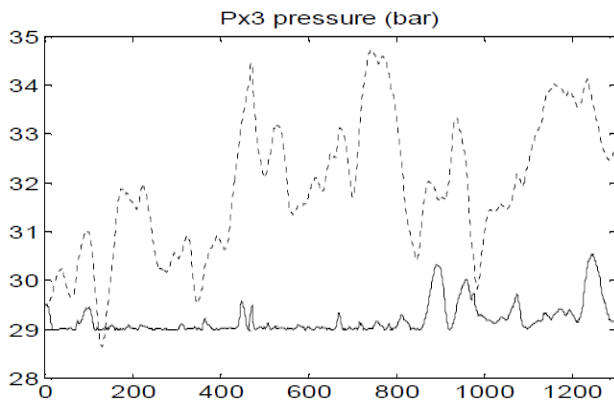
Figure 7. Pressure P_{x3} kept close to the minimum 29 bar by DRTO in simulation test-bench (solid line) and as controlled in the true pipeline system (dashed line). Time axis is in minutes.

5 CONCLUSIONS

The two methods to handle non-linearity in MPC presented in this paper adds to the multitude of existing methods however, our belief is that industrial users value the *additivity* or *modularity* of the approaches: if an LMPC exists, then add the non-linearity handling methods and continue operations with improved performance. If non-linearity creates some problems - not rarely seen in practical applications - then turn off the non-linear parts and continue with the LMPC until problems are rectified.

The method of using and external first principles model has an extra added value in such applications normally found in energy systems, where a large number of measurable disturbance variables (DV) exists and for which

forecasted DV profiles exist. The first-principles model automatically invokes these DV's and their forecasts without the need to do experimental modeling of the DV to CV responses.

6   REFERENCES

Aalto H. (2008), Optimal Control of Gas Pipeline Networks, a real-time, model-based, receding horizon optimisation approach, 186 pages, VDM Verlag Dr. Müller Aktiengesellschaft & Co. KG, Saarbrücken, Germany, ISBN 978-3-639-09111-3

Deshpande P.B. (1989), Multivariable Process Control, Instrument Society of America.

Doyle F. J., Ogunnaike B. A. O. and Pearson R. K. (1995), Nonlinear Model-based Control Using Second-order Volterra Models, Automatica, Vol 31, No. 5, pp. 697-714.

Gattu G. and E. Zafiriou (1992), Nonlinear Quadratic Dynamic Matrix Control with State estimation, Ind. Eng. Chem. Res., Vol. 31, pp. 1096-1104.

Gattu G. and E. Zafiriou (1995), Observer Based Nonlinear Quadratic Dynamic Matrix Control for State Space and Input/Output Models. The Canadian Journal of Chemical Engineering, Vol. 73, pp. 883-895.

Pelkola A., Nonlinear Multivariable Predictive Controls with Laguerre-based Wiener Neural Network Models and Partial Least Squares Model Reduction, Doctoral Dissertation 2016, Aalto University, School of Electrical Engineering, Department of Electrical Engineering and Automation, Espoo, Finland.

Prett D.M., Garcia C. E. (1988), Fundamental Process Control, Butterworths Series in Chemical Engineering, 51-121.

Schetzen M. (1080), The Volterra and Wiener Theories of Nonlinear Systems, John Wilay & Sons, 531 p.

Wiener N. (1958), Nonlinear Problems in Random Theory, The Technology Press, MIT and John Wilay & Sons Inc., New York, 131 p.

Industrial implementation of nonlinear model predictive controllers

Jørgen K . H. Knudsen [*], **John Bagterp Jørgensen** [**]

[*] *2-control Aps, Frimodtsvej 11, DK-2900 Hellerup, Denmark*
(e-mail: JoeK@2-control.dk)
[**] *Department of Applied Mathematics and Computer Science,*
Technical University of Denmark, DK-2800 Lyngby
(e-mail: jbjo@dtu.dk)

Abstract:
This paper describes some important factors for successful implementation and maintenance of nonlinear MPC in an industrial environment. *ModelBuilder* is a simple modeling language, which uses basic mass and heat balances to describe plant dynamic. The nonlinear *ModelBuilder* model can effectively be linearized as a set of state space models around given operating points. Based on this set of state space models a linear MPC controller calculates an optimal control strategy. Subsequently the set of state space models are updated based on the predicted future plant trajectory.

Keywords: Advanced process control (APC), Nonlinear model predictive control (NMPC), Model predictive control (MPC), Models, ModelBuilder

1. INTRODUCTION

In order to be successful, an advanced process control application must be commissioned and maintained by process engineers with detailed knowhow and understanding of the process to be controlled. Normally the process engineer does not have a Ph.D degree and is not a programmer used to work in MATLAB or a high level language such as C#. We have to provide tools which can be used by the process engineer, requiring a minimum of programming skills and training, and which can be used occasionally, whenever maintenance of the control system is required.

Futhermore it is important to use simulation of the plant to make the initial tests an tuning of the controller before moving the controller to the real plant and presenting it to the plant operators. If the operators looses confidence to the advanced process control system, it will be virtually impossible to achieve a succelfull installation.

MPC controllers based on linear models are being implemented successfully in the industry today. Linear models can be defined and entered into the APC control system as state space models or transfer functions.

For MPC using nonlinear models, the situation is much more difficult. Nonlinear models can be developed using high level programming languages as MATLAB or C#. Programming the necessary Jacobians are tedious and error prone. Development of these models requires a MATLAB or a compiler.

ModelBuilder provides a solution for development of nonlinear models. *ModelBuilder* describes process dynamics at high abstraction level using the mass and energy balances familiar to process enginers. *ModelBuilder* generates the model without requing a compiler and finally
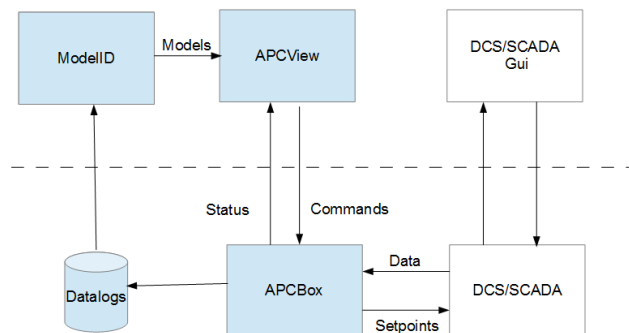

Fig. 1. *APCSuite* modules.

ModelBuilder generates Jacobians using automatically differentiation of the system equations.

ModelBuilder is a part of 2-control's *APCSuite* product, shown in Fig. 1. *APCBox* is the server running the MPC controllers 24/7. *APCBox* exchanges data and setpoints with the plant PLC system using an OPC connection. *APCView* in the client program used to configure *APCBox* and supervise the control loops.

The use of *ModelBuilder* is demonstrated on a U-Loop reactor for single cell protein production (Olsen et al. (2010)) and finally the generated model is used in a nonlinear controller.

2. THE U-LOOP REACTOR.

The U-Loop reactor consist of CSTR and an U shaped plug flow reactor as shown in the left part of Fig. 2. In the U-Loop reactor biomass (single cell protein) grows on
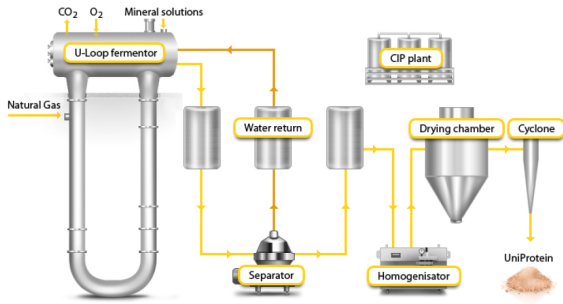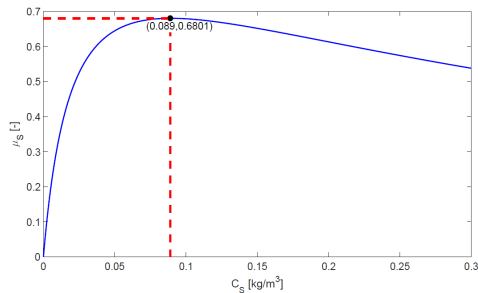
Fig. 2. U-Loop reactor.

(a) Growth rate for substrate μ_S, where the maximum growth rate, $\mu_S^* \approx 0.68$, can be obtained by a substrate concentration at $C_S^* \approx 0.089$.

Fig. 3. Biomas growth rate.

methanol and oxygen. The gases and liquids are mixed effiently in the plug flow reactor enabling the reaction. After the U-Loop reactor, separator and drying units are used to produce the final single cell protein. This part of the process is not considered in this article.

Inputs to the U-Loop reactor are the methanol, F_s, water, F_w, and oxygen, F_o flow rates. The output flow from the CSTR reactor is characterized by the concentration of biomass, C_x, the concentration of metanol, C_s, and the concentration of oxygen in the liquid phase, C_o.

The growth rate of the biomass is a highly nonlinear function of the methanol concentration, as shown in Fig. 3, making it a challenging task to control the U-Loop reactor

3. *MODELBUILDER*

ModelBuilder is used to generate ordinary differential eqations, ODE, of the form $\dot{x} = F(x, u)$ or differential algeabraic equations,DAE, of the form $F(x, \dot{x}, u) = 0$. x is a vector of states, $\dot{x}$ is the time derivative of the states and u a vector of process inputs. In both cases the process outputs are defined as $y = G(x, u)$

ModelBuilder source code consist of a declaration section followed by an equations section:

```
Model  ODE (....)

   declarations ...
```

Equations

```
   equations ....
```

End

The *Model* statement defines the model type (ODE or DAE) and defines some general information around the handling of the model. The *declarations* statements defines constants, parameters, variables, states, model inputs, and model outputs. The *equations* statements defines the relations between the entities defined under the declaration section.

Constants and parameters are defined as shown below:

```
// Yield Coefficients
Constant Yso = 0.439;
Constant Ysx = 0.732;
// Molar Weights
Constant Mws = 1.0079*4+12.011+15.9994;  // [S = CH3OH][g/mol]
Constant Mwo = 2*15.9994;                // [O = O2][g/mol]
Constant Mwx = 12.011+1.8*1.0079+0.5*15.9994+0.2*14.0067; // [X][g/mol]
// Kinetic Parameters
Parameter mumax = 0.37;  // [][1/hr]
Parameter ks = 0.021;    // [][kg/m3]
Parameter ki = 0.38;     // [][kg/m3]
Parameter ko = 6.4e-5;   // [][kg/m3]
```

Assingments can be expressions. Parameters can be changed from outside the the model.

Declaration of states and inputs:

```
// CSTR states
State Cxcstr = 10.3;    // [protein concentration][mol/m3]
State Cscstr = 0.01;    // [substrate concentration][mol/m3]
State Cocstr = 0.123;   // [oxygen concentration][mol/m3]

Input Fs = 0.00411; // [Substrate input][m3/hr]
Input Fw = 0.1736; // [Water input][m3/hr]
Input Fg = 0.7034; // [gas input][m3/hr]
```

The positions in the x and u vectors follows the declaration sequence. The states and inputs can be assigned inital values.

Declaration of variables:

```
// Mixer
Var Fliq;    // [Liquid flow][[m3/hr]
Var Ftot;    // [Total flow][[m3/hr]
Var epsilon; // [gas/liquid ratio][]
Var v;       //    [PFR flux][m/hr];
```

The values of the variables must be a function of the states and inputs, as described in the equation section.

Finally the outputs y can be defined as:

```
Output Cxcstr; // [protein concentration][mol/m3]
Output Cscstr; // [substrate concentration][mol/m3]
Output Cocstr; // [oxygen concentration][mol/m3]
```

The positions in the y vector follows the declaration sequence.

The equation section is used to specify the relations between inputs, variables and states

```
Equations

F = Fs + Fw;  // Total flow
// Mixer
// Inlet boundary conditions for the PFR
Fliq = F + FR;
Ftot = Fliq + Fg;
epsilon = Fg / Ftot;
v = Ftot /Apfr;

Cxpfrin = (Fs * Cxin + FR * Cxcstr) / Fliq;
Cspfrin = (Fs * Cmet + FR * Cscstr) / Fliq;
Copfrin = (Fs * Coin + FR * Cocstr) / Fliq;
Cgopfrin = Cgoin;
.

.
// Differential equations for CSTR
rx[N] = Cxcstr * Mu(Cscstr,Cocstr);
time * der(Cxcstr) = (Fliq / Vcstr) * (Cx[N - 1] - Cxcstr) + rx[N];
time * der(Cscstr) = (Fliq / Vcstr) * (Cs[N - 1] - Cscstr)
 - gammaS * rx[N];
time * der(Cocstr) = (Fliq / Vcstr) * (Co[N - 1] - Cocstr)
- gammaO * rx[N];
```

where the operator $der(Cxcstr)$ indicates the time derivative of a state variable $Cxcstr$. *ModelBuilder* automaticly sorts the equations in the correct sequence. The equations are of the type $expression = expression$, not just simple assignments. The number of equations must be equal to the number of states and variables.

ModelBuilder supports the standard mathematical functios as $Exp, Ln, Log, Sin, Cos, Tan, Sqrt$ and Pow. New functions, as the reaction rate, can defined in the declaration section, and subsequently be used in the equation section

```
// Kinetic Parameters
Parameter mumax = 0.37;  // [][1/hr]
Parameter ks = 0.021;    // [][kg/m3]
Parameter ki = 0.38;     // [][kg/m3]
Parameter ko = 6.4e-5;   // [][kg/m3]

// Kinectics

Function Mu(Cs,Co) = mumax * (Cs /(ks + Cs
        +Pow(Cs/ki,2)) * (Co/(ko + Co)));
.
Equations
.
rx = Cxcstr * Mu(Cscstr,Cocstr);
.
End
```

The plugflow reactor section of the U-Loop reactor is discretized into N sections of equal size. In the declaration section the states and variables for these sections can be defined as:

```
// Plug Flow reactor states
Constant N = 15;        // Number of cells in plug flow reactor
State Cx[N] = 10.3;  // [protein concentration][mol/m3]
State Cs[N] = 0.01;  // [substrate concentration][mol/m3]
State Co[N] = 0.123;  // [oxygen concentration][mol/m3]
State Cgo[N]= 10.0; // [oxygen concentration gas phase][mol/m3]
// Flux
Var Nx[N+1];  // [protein flux][mol/m]
Var Ns[N+1];  // [substrate flux][mol/m]
Var No[N+1];  // [oxygen flux][mol/m]
Var Ngo[N+1]; // [oxygen gas phase flux][mol/m]
// Reaction rates
Var rx[N+1]; // [recation rates][mol/m3];
Var Jglo[N];
```

The declaration $State\ Cx[N] = 10.3$ is equivalent to 15 statements

```
State Cx[0] = 10.3;  // [protein concentration][mol/m3]
State Cx[1] = 10.3;  // [protein concentration][mol/m3]
State Cx[2] = 10.3;  // [protein concentration][mol/m3]
State Cx[3] = 10.3;  // [protein concentration][mol/m3]
.
State Cx[14] = 10.3;  // [protein concentration][mol/m3]
```

In the equations section, the equations can be repeated using the Repeat statement

```
// Plug Flow reactor flux
Nx[0]  = v * Cxpfrin;
Ns[0]  = v * Cspfrin;
No[0]  = v * Copfrin;
Ngo[0] = v * Cgopfrin;
Repeat(1 : N -1)
{
Nx[ix]  = v * Cx[ix - 1]  - (Dx  / dz) * (Cx[ix]  - Cx[ix - 1]);
Ns[ix]  = v * Cs[ix - 1]  - (Ds  / dz) * (Cs[ix]  - Cs[ix - 1]);
No[ix]  = v * Co[ix - 1]  - (Do  / dz) * (Co[ix]  - Co[ix - 1]);
Ngo[ix] = v * Cgo[ix - 1] - (Dgo / dz) * (Cgo[ix] - Cgo[ix - 1]);
}

Nx[N]  = v * Cx[N - 1];
Ns[N]  = v * Cs[N - 1];
No[N]  = v * Co[N - 1];
Ngo[N] = v * Cgo[N - 1];
Repeat(0 : N - 1)
{
// Gas-Liquid Transport
Jglo[ix] = klaO * (RTdivMwoHo * Cgo[ix] - Co[ix]);
rx[ix] = Cx[ix] * Mu( Cs[ix], Co[ix] ) ;
time * der(Cx[ix]) = -(Nx[ix + 1] - Nx[ix]) / dz + rx[ix];
time * der(Cs[ix]) = -(Ns[ix + 1] - Ns[ix]) / dz - gammaS * rx[ix];
time * der(Co[ix]) = -(No[ix + 1] - No[ix]) / dz - gammaO * rx[ix]
+ Jglo[ix] / (1.0 - epsilon);
time * der(Cgo[ix]) = -(Ngo[ix + 1] - Ngo[ix]) / dz - Jglo[ix] / epsilon;
}
```

The $Repeat(0 : N - 1)\{......\}$ repeats the statements in { ...... } with the index variable ix set to values from 0 to 14. The Repeat statement can handle up to 3 dimensions, with index variables ix, iy, iz.

ModelBuilder models can be used as ordinary differential equations,ODE, or differential algebraic equation,DAE. The ODE are computationally more efficient than DAE models, but it put some restrictions the equation system. For that reason we standardized the *APCSuite* system to use the DAE formulation. This choice is not presented to the user.
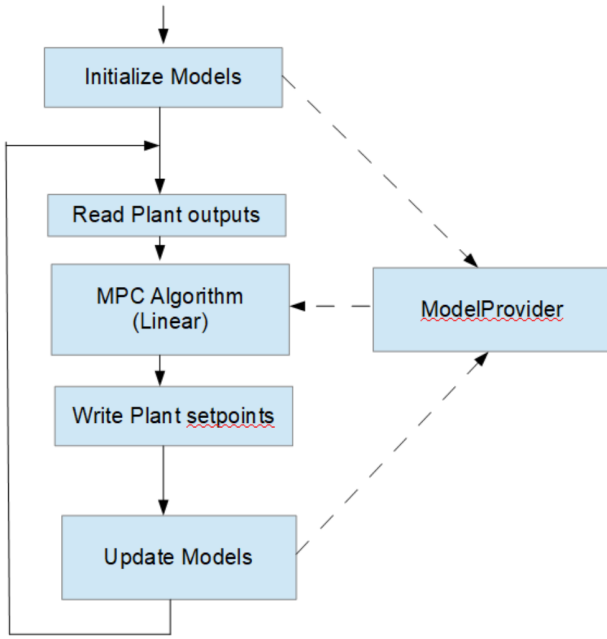
Fig. 4. Control cycle

4. THE MPC CONTROLLER

The resulting *ModelBuilder* model can be used by *APCSuite*'s MPC controllers. Here the MPC is defined declaring inputs, outputs, targets, limits e.t.c. as shown in Fig. 5.

The default option is to linearize the *ModelBuilder* model as a state space model around the operations point specified in the *ModelBuilder* source code, resulting i a conventional linear MPC controller.

Alternatively the MPC can use the *ModelBuilder* model to calculate a collection of linear linear state space models along future trajectory predicted by the MPC controller resulting in a nonlinear MPC controller, as shown in Fig. 4. The state space models are collected i a ModelProvider, which is initiailized with state space models corresponding to the operating point given in the *ModelBuilder* source code.

The plant outputs are read via the OPC connection to the plant PLC, and the current state of the plant is estimated with a Kalmann filter.

The MPC algorithm runs as a conventional linear MPC using state space models from the ModelProvider, and calculates setpoints for plant inputs together with the anticipated future trajectory of the plant.

Setpoints are written to the plant PLC.

Finally the idle time until next sample time is used to update the models in the ModelProvider according to the new future trajectory calculated by the MPC controller.

The updating of the state space models around the predicted future states can result in cyclic iterations, which can be eliminated by filtering the predicted response. The UpdateFilter, α, filters the predicted plant trajectory and plant input:
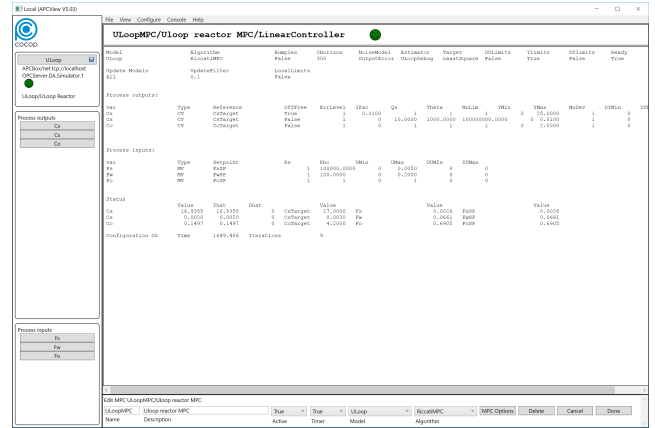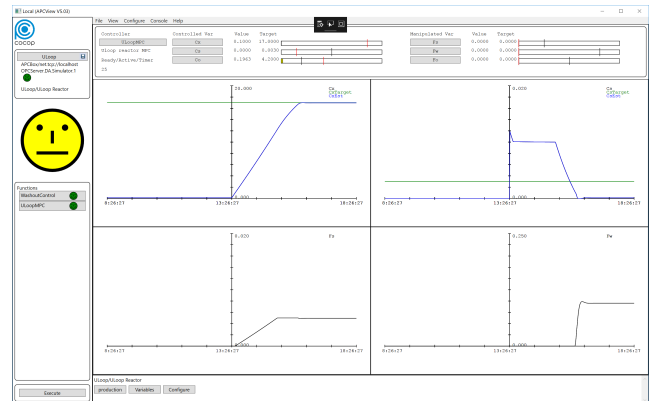

Fig. 5. MPC configuration.

Fig. 6. U-Loop initial trajectory.

$$x_f(t) = \alpha x(t) + (1 - \alpha)x_f(t) \qquad (1)$$
$$u_f(t) = \alpha u(t) + (1 - \alpha)u_f(t) \qquad (2)$$
$$0 < \alpha \le 1 \qquad (3)$$

where $x(t)$ and $u(t)$ are the predicted trajectories and process inputs calculated by the MPC algorithm. $x_f(t)$ and $u_f(t)$ are the filtered trajectory and process inputs used to calculate next set of state space models.

5. SIMULATION RESULTS

The proposed control cycle scheme was tried on the U-Loop reactor.

Fig. 6 shown the very first prediction by the MPC algorithm, using the initial state space model derived from the operation point given in the *ModelBuilder* source code. After a number of control cycles the MPC controller approaches the nonlinear predictions an shown in Fig. 7. After a while, the predicted trajectory is stable as shown in Fig.8. Finally Fig. 9 shown the state after many control cycles just before reaching the final steady state of the process.

In Fig. 10 the MPC controler was started without updating the models. This resulted in an unacceptable oscillatory response, which disappered after re-starting updating of the models as shown in Fig. 11. This is the type of results, which should be studied with a simulator and not in front of a group af sceptical process operators.
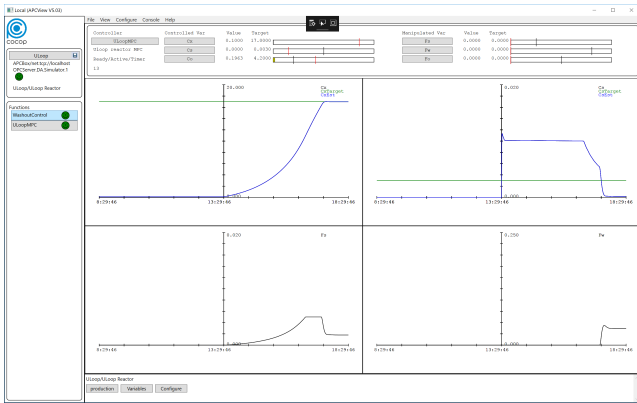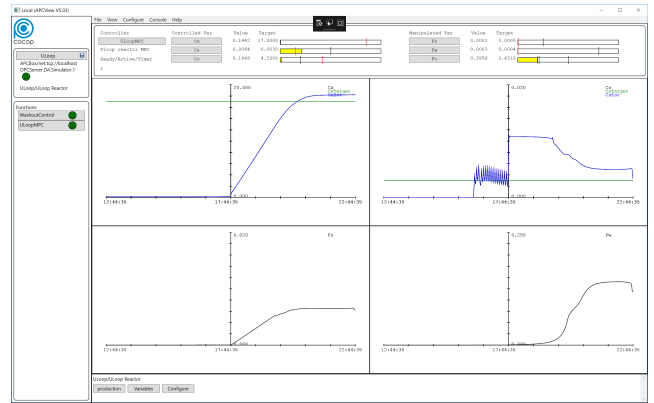
Fig. 7. U-Loop after 10 control cycles.

Fig. 8. U-Loop converged.

Fig. 9. U-Loop reaching final stationary state.

6. CONCLUSION

The *ModelBuilder* language and the proposed control cycle with a ModelProvider enables process engineers to develop and maintain advanced process controllers for nonlinear processes without having to use MATLAB or compilers.

The relatively simple strategy by using the linear algorithms combined with subsequent updating of the models, provides a fast immediate response to the process and it works for difficult cases as the U-Loop reactor. For unstable systems more complicated strategy based on "multiple-shooting" might be required.

Fig. 10. Linear MPC performance (unacceptable !).

Fig. 11. MPC after re-starting model update.

REFERENCES

Olsen, D.F., Jørgensen, J.B., Villadsen, J., and Jørgensen, S.B. (2010). Modeling and simulation of single cell protein production. In *Procedings of the 11th Intertional Symposium on Computer Applications in Biotechnology (CAB 2010)*.

A novel approach to steady-state gradient estimation using transient measurements

Dinesh Krishnamoorthy, Esmaeil Jahanshahi, Sigurd Skogestad

Department of Chemical Engineering, Norwegian University of Science and Technology, 7491,

Trondheim, Norway

Real-time optimization deals with the optimal economic operation of a process. There are several different approaches to real-time optimization in the process control literature. Recently, there has been a surge of interest in the so-called "direct-input adaptation" approaches, where the optimization problem is converted into a feedback control problem. Optimal operation is thus achieved by directly manipulating the inputs based on feedback measurements instead of solving a numerical optimization problem. Self-optimizing control, extremum seeking control and NCO-tracking belong to this category of RTO methods. In this paper, we propose a novel approach to such a direct-input adaptation strategy, where the estimated steady-state gradients are controlled using transient measurements.

In this paper, we propose a novel approach to such a direct-input adaptation based RTO scheme, where the steady-state gradient is controlled to zero using transient measurements. The proposed approach can be seen as an online variant of self-optimizing control, where the self-optimizing variable is the steady-state gradient. To control the gradient, the proposed scheme uses a dynamic model online to estimate the steady-state gradient using transient measurement data. This is done by means of a combined state and parameter estimator. With the use of the estimated states and the cost function model, a local linear dynamic model (1) can be obtain by linearization of the nonlinear model.

$$
\begin{aligned}
\dot{x} &= Ax + Bu \\
J &= Cx + Du
\end{aligned}
\tag{1}
$$

The steady state gradient of the cost function can then be obtained using the system matrices.

$$
\mathbf{J_u} = -CA^{-1}B + D
\tag{2}
$$

For driving the gradients to a setpoint of zero, any feedback controller such as PID or MPC can be used.

When compared to self-optimizing control, the model is used online instead of offline and the proposed method is based on local linearization around the current operating point, as opposed to local linearization around the nominal optimal point in self-optimizing control. By doing so, we reduce the steady-state losses associated with the standard self-optimizing control and reach the true optimum following a disturbance. Similar, to the self-optimizing control, the proposed method provides fast reaction to disturbances and converges to the new optimal point, without the need to solve computationally intensive numerical optimization problems.

1
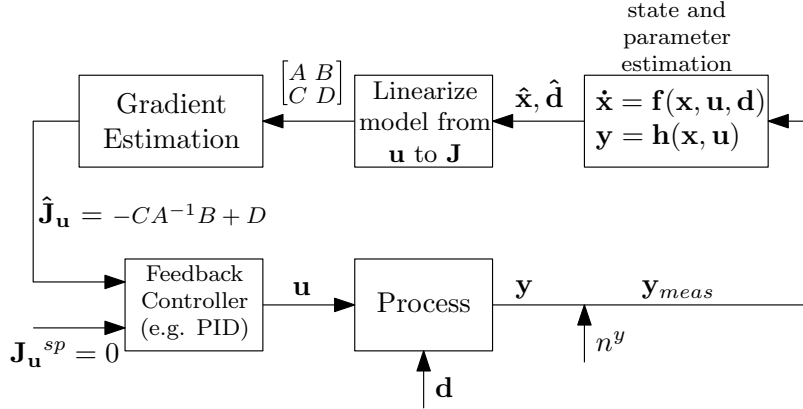
Figure 1: Block diagram of the proposed Model based extremum seeking control

The idea of controlling the steady-state gradient to a constant setpoint of zero is similar to extremum seeking control and NCO-tracking. However, extremum seeking control and NCO tracking are model-free approaches and requires the system to reach steady-state before the data can be used to estimate the steady-state gradient. Using transient measurements leads to inaccurate gradient estimation. This leads to very slow convergence to the optimum point. Model-free approaches also require the cost to be measured and requires additional perturbations for accurate gradient estimation. In the proposed method, the steady-state gradient can be estimated using transient measurements, hence providing fast reaction to disturbances. In addition, it also does not require any additional perturbations or cost measurements. However, since the proposed approach is model-based, unmodelled disturbances may not be handled as effectively as the model-free approaches.

In contrast with nonlinear Economic Model Predictive Control (EMPC), optimization is done by feedback control. Hence, the computation time of the proposed method is significantly smaller which allows for faster sampling interval of the overall control loop. As a result, problems associated with computational delay are alleviated.

The proposed method was compared to self-optimizing control (SOC), extremum seeking control and economic NMPC in simulations. The proposed method was able to drive the process to the optimal operating point without the need to re-optimize.

2

Steady-state optimization using phase-lag information

Olle Trollberg[1][2] *and Elling W. Jacobsen*[1]

Steady-state output optimization is a key problem in the process industry. Due to the presence of uncertainty and lack of sufficiently accurate models, data-driven methods are frequently used to solve this problem. The most common data-driven methods are gradient based, e.g., necessary conditions for optimality (NCO) tracking [2] and extremum seeking control (ESC) [1]. Since the gradient typically cannot be measured directly, it is estimated and then the input is adapted to move this estimate towards zero. Recently we showed [3] that extremum points in the steady-state input-output mapping are not only characterized by a zero gradient. In general, there will also exist a transmission zero at the origin at such points. This has implications for the phase lag of the process at the optimum, and herein we make use of this fact to design a method for steady-state optimization based solely on estimation and regulation of the system phase-lag.

In [3], we show that a plant linearized at an operating point corresponding to an extremum point in the steady-state input-output map, i.e., at a steady-state optimum, in general will have a transmission zero at the origin, and that this zero locally will cross between the RHP and LHP as the operating point is moved past the optimum. This implies that the local phase-lag φ will equal $\pm\pi/2$ at the optimum, and that the phase-lag will vary by π rad in a neighborhood centered about the optimum. This is exact for the frequency zero, but holds approximately also for a range of nonzero frequencies. This implies that a steady-state optimum may be found by considering the phase-lag only, in particular by adapting the input until the local phase-lag φ of the plant equals $\pi/2 + n\pi$, $n \in \mathbf{Z}$.

Here we note that this problem is similar to the problem addressed by phase-locked loops (PLL), and

design a simple controller based on elements commonly found in a PLL. In particular, we perturb the plant by adding a sinusoidal to the input and use a Kalman-Bucy filter to estimate the local phase-lag φ at the current operating point. We then use an integral controller to move the system towards a point where $\varphi = \pm\pi/2$. The controller equations are given by

$$
\begin{aligned}
\dot{x}_K &= PH^TR^{-1}(y - Hx_K) \\
\dot{P} &= Q - PH^TR^{-1}HP \\
H &= [1 \ \sin(\omega t) \ \cos(\omega t) \ \sin(2\omega t) \ \cos(2\omega t)] \quad (1) \\
\dot{\hat{u}} &= k(\text{arctan2}(x_{K,3}, x_{K,2}) + (\pi/2)) \\
u &= \hat{u} + a\sin(\omega t).
\end{aligned}
$$

Here the filter is based on the assumption that the output is periodic with the same fundamental period as the perturbation. The elements of the filters state-vector x_K then serve as estimates of the first coefficients of the Fourier series of the output, and the local phase-lag may be computed from the coefficients for the first harmonic as $\varphi = \text{arctan2}(x_{K,3}, x_{K,2})$. The matrices Q and R may be considered as tuning parameters along with the perturbation amplitude a, the perturbation frequency ω, and the gain of the integral controller k.

Assuming that we do not have a model available, we apply this controller in order to optimize an isothermal perfectly mixed tank reactor with the reactions $A \rightarrow B$, and $2B \rightarrow C$ where $y = B$ is the output and C is an unwanted byproduct. For simulations, we use standard mass action kinetics and represent the dynamics by

$$
\begin{aligned}
V\dot{c}_A &= F(c_{Af} - c_A) - Vk_1c_A \\
V\dot{c}_B &= -Fc_B + Vk_1c_A - Vk_2c_B^2
\end{aligned} \quad (2)
$$

where c_A and c_B are concentrations of A and B, respectively, $V = 1.0$ is the volume, $c_{Af} = 1.0$ is the concentration of A in the inflow, and the kinetic constants are $k_1 = 2.0, k_2 = 0.1$. The process is controlled via the total flow $u = F$ which determines the retention time in the reactor. The production of B has a unique maximum for $F = 0.375$ with $B = 0.71$.

[1]KTH Royal Institute of Technology, School of Electrical Engineering, Department of Automatic Control.
[2]Corresponding author: olletr@kth.se

1

We use the controller-parameters,

$$R = 0.01, \quad Q = 10I, \tag{3}$$
$$a = 0.01, \quad \omega = \pi/50, \quad k = 0.0001, \tag{4}$$

and initialize the search from $c_A = 0.1$, $c_B = 0.1$, $u = 0.012$. Fig. 1 shows the closed-loop trajectories of the simulation. The top and middle parts
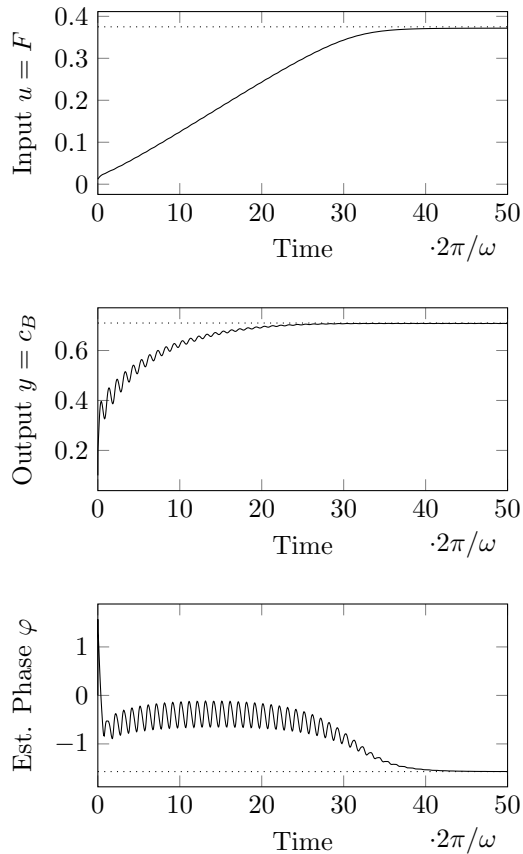
Figure 1: Optimization of the CSTR described by (2) using estimation and regulation of the plant phase-lag.

of Fig. 1 show the convergence of the input u and output y to the optimal solutions marked by dotted lines. For the input we show the The bottom part shows how the estimated phase converges to $-\pi/2$ rad, also marked by a dotted line.

References

[1] Kartick B. Ariyur and Miroslav Krstić. *Real-time optimization by extremum-seeking control*. Wiley-interscience publication. Wiley-Interscience, 2003.

[2] Johannes Jäschke and Sigurd Skogestad. "NCO tracking and self-optimizing control in the context of real-time optimization". In: *Journal of Process Control* 21.10 (2011), pp. 1407–1416.

[3] Olle Trollberg and Elling W Jacobsen. "On Bifurcations of the Zero Dynamics-Connecting Steady-State Optimality to Process Dynamics". In: *IFAC-PapersOnLine* 48.8 (2015), pp. 170–175.

State of the art of integration of scheduling and control – remaining challenges

Iiro Harjunkoski

Aalto University, School of Chemical Technology, Kemistintie 1, 02150 Espoo, Finland
ABB AG, Corporate Research Germany, Wallstadter Str. 59, 68526 Ladenburg, Germany
(Tel: +49(0)6203-716014; e-mail: iiro.harjunkoski@de.abb.com)

Abstract: Integration of scheduling and control is a relatively new field of research that gains attention especially owing to Internet of things (IoT), which enables seamless and easier communication channels between the various functions in automation. Whereas scheduling and control have separately advanced especially in the area of optimization, their interplay is still not fully clarified. It is, nonetheless, clear that optimization can be seen as the main criteria or measure to evaluate how well the integration aspects are fulfilled. There are a number of potential approaches, each of which have their own merits, but very little industrial implementations to prove the value in real-life production have been reported. In this presentation we will review some of the main methods and discuss challenges that must be solved before a wider deployment is possible.

Keywords: Scheduling, control, optimization, integration, industrial implementation

The topic of integrating scheduling and control has been discussed at least during three decades (Shobrys and Baker, 1986) and above all in the last decade many contributions especially towards optimization solutions have been reported. Recent reviews give an overview of the state-of-the art from the operations perspective (Engell and Harjunkoski, 2012), methodological overview (Baldea and Harjunkoski, 2014) summarizing the research directions, uncertainty (Dias and Ierapetritou, 2016) and framework perspective (Pistikopoulos and Diangelakis, 2016) introducing a PAROC system bringing many central aspects together. Looking at the integration problem we are basically dealing with a mixed integer dynamic optimization (MIDO) problem (Allgor and Barton, 1999), which is nontrivial to solve for larger problem instances. The key towards solving the problem more efficiently lies in the selected modeling strategy. A natural approach would be to deploy advanced process control methods, e.g. through the use of economic-MPC type of approach (Subramanian et al., 2012; Touretzky and Baldea, 2014), or to handle the process dynamics as pre-determined parameters in the scheduling models that can be updated regularly (Chu and You, 2012). Multi-parametric MPC approaches have also been deployed in Zhuge and Ierapetritou (2014) and a time scale-bridging approach in Du et al. (2015), enabling a low-order representation of the process dynamics in the scheduling framework. Design aspects and uncertainty in the demand have been studied in Patil et al. (2015) and to reduce the computational complexity Lagrangean heuristics is deployed in Terrazas-Moreno et al. (2008).

While significant progress has been achieved over the years, it is fair to say that at the moment there is not a generally accepted methodology and/or "protocol" for such an integration – it is also interesting to note that currently, there is not a commercially available software system to fully support such an activity (Pistikopoulos and Diangelakis,

2016). The most successful use cases have been mainly applied to continuous processes where the scheduling challenge limits to the sequencing of changeovers taking into account optimal trajectories e.g. in polymer production. Also batch processes with either relatively uncomplicated dynamics or low number of binary decisions have provided a good fundament for theoretical studies. In practice, it is very difficult to prove both the expectations and the outcoming value and so far operations and control are still hierarchically separated in most industrial landscapes. The mental and organizational barriers are well analyzed in Shobrys and White (2000) and in order to overcome them the value of integration must be well evaluated.

The current discussion is moving away from strict integration of "silos" but more towards collaboration concepts such as online scheduling (Gupta et al., 2016), often also with both academic and industrial contributions. This is a promising direction as the industrial Internet of Things will enable better data communication and exchange bringing "physically" solutions closer together (Harjunkoski, 2016; Isaksson et al., 2017), taking the first steps towards synergistic process control. Thus, the main challenges are

- Breaking the formal silos between scheduling and control and enable full data exchange
- Finding the best methodological approaches and understanding their pros and cons
- Proving the value of integration in practice – a challenge even on the theoretical level
- Ensuring that the right people are working together towards a common and well understood goal

Consequently, integration of scheduling and control will affect both the control and scheduling communities. The optimization aspects are central – both in enabling the collaboration as well as in proving the value of the integration.

REFERENCES

Allgor R.J, Barton P.I. (1999). Mixed-integer dynamic optimization I: problem formulation, Computers & Chemical Engineering, 23, 567–584.

Baldea, M., & Harjunkoski, I. (2014). Integrated production scheduling and process control: A systematic review. Computers and Chemical Engineering, 71, 377-390.

Chu, Y., & You, F. (2012). Integration of scheduling and control with online closed-loop implementation: Fast computational strategy and large-scale global optimization algorithm. Computers and Chemical Engineering, 47, 248-268.

Dias, L. S., & Ierapetritou, M. G. (2016). Integration of scheduling and control under uncertainties: Review and challenges. Chemical Engineering Research and Design, 116, 98-113.

Du, J., Park, J., Harjunkoski, I., & Baldea, M. (2015). A time scale-bridging approach for integrating production scheduling and process control. Computers and Chemical Engineering, 79, 59-69.

Gupta, D., Maravelias, C. T., & Wassick, J. M. (2016). From rescheduling to online scheduling. Chemical Engineering Research and Design, 116, 83-97.

Engell, S., & Harjunkoski, I. (2012). Optimal operation: Scheduling, advanced control and their integration. Computers and Chemical Engineering, 47, 121-133.

Harjunkoski, I. (2016). Deploying scheduling solutions in an industrial environment. Computers and Chemical Engineering, 91, 127-135.

Isaksson, A.J., Harjunkoski, I., & Sand, G. (2017). The Impact of Digitalization on the Future of Control and Operations. Computers and Chemical Engineering (in print).

Shobrys, D. E., & Baker, T. E. (1986). Experience with The Integration of Planning, Scheduling, And Control. Advances in Instrumentation, 41(2), 575-586.

Shobrys, D.E. & White, D.C. (2000). Planning, scheduling and control systems: why can they not work together. Computers & Chemical Engineering, 24, 163–173.

Patil, B. P., Maia, E., & Ricardez-Sandoval, L. A. (2015). Integration of scheduling, design, and control of multiproduct chemical processes under uncertainty. AIChE Journal, 61(8), 2456-2470.

Pistikopoulos, E. N., & Diangelakis, N. A. (2016). Towards the integration of process design, control and scheduling: Are we getting closer? Computers and Chemical Engineering, 91, 85-92.

Subramanian K., Maravelias C.T. and Rawlings J.B. (2012). A state-space model for chemical production scheduling. Computers & Chemical Engineering, 47, pp. 97–110.

Terrazas-Moreno, S., Flores-Tlacuahuac, A., & Grossmann, I. E. (2008). Lagrangean heuristic for the scheduling and control of polymerization reactors. AIChE Journal, 54(1), 163-182.

Touretzky, C. R., & Baldea, M. (2014). Integrating scheduling and control for economic MPC of buildings with energy storage. Journal of Process Control, 24(8), 1292-1300.

Zhuge, J., & Ierapetritou, M. G. (2014). Integration of scheduling and control for batch processes using multi-parametric model predictive control. AIChE Journal, 60(9), 3169-3183.

Intelligent Vessels

Ilkka Rytkölä and Fredrik Östman, Wärtsilä Finland Oy

The traditionally so conservative marine industry is today facing a change that is picking up pace. IoT, analytics and connectivity is promising the introduction of new business models are new value creation beyond the reach of traditional thinking. Novel sensor technologies and increased computational power enables already today technologies for intelligent and autonomous operation of vessels, which wasn't even conceivable just some years back. In this presentation, the concepts of autonomous and intelligent vessels will be presented along with a discussion around the main challenges. Concrete examples developed within Wärtsilä will, moreover, be shown related to engine control and diagnostics, to highlight what will be required in the future.

Analysis of Indirect Fire System Effectiveness Using Simulation and Data Farming

Miika Haataja [a]**, Esa Lappi** [b]**, Bernt Åkesson** [a]

[a]Finnish Defence Research Agency
[b]National Defence University, Finland
Email: bernt.akesson@mil.fi

Abstract:

Indirect fire (gun artillery, rocket launchers, mortars) is one on the most important casualty producing agents on the battlefield, with fragments from high explosive ammunition being the principal cause of casualties in modern conflicts [5].

Indirect fire can be considered a system consisting of five elements: surveillance and target acquisition, C4 (command, control, communication and computation), munitions, weapon platforms and logistics [10]. Using simulation models, the effectiveness of indirect fire systems can be studied. Possible cases include technological development influencing the subsystems, changes in use and organization of indirect fire assets, as well as protection against indirect fire.

The data farming process, introduced by [7] and codified in [1], applies a simulation-based approach to analyze complex systems. Data farming combines simulation modelling, rapid prototyping, experimental design, high-performance computing and analysis and visualization for conducting large-scale simulation experiments. Multiple simulation runs are performed using different parameter values for each run.

A numerical model for simulating the effects of indirect fire has been developed in the Finnish Defence Forces. The model is based on physical properties of the ammunition and has been validated using field experiments [3]. The simulation model has been used in a number of studies over the years [9, 2, 4], and is also integrated in the combat modelling software Sandis [8].

This paper discusses findings from simulation studies on indirect fire, where only open source data has been used as input and the data farming approach has been applied to generate and analyze data. In particular, we discuss a recently presented case study on the effectiveness of 120 mm mortar ammunition against prone infantry [6]. Two questions were analyzed, concerning more powerful explosives and improved metallurgical properties of the casing. First, what is the optimal fragment mass distribution parameter for a given target and initial fragment velocity? Second, how will increasing the initial fragment velocity change the number of projectiles needed to achieve a desired effect?

Keywords: modelling and simulation, data generation, data analysis and visualization

REFERENCES

[1] Data farming in support of NATO: Final report of task group MSG-088. STO Technical Report TR-MSG-088, NATO Science and Technology Organization, March 2014.

[2] Bernt Åkesson, Esa Lappi, Risto Bruun, and Jussi Sainio. Team 5: Artillery warfare in urban terrain. In Ted Meyer and Gary Horne, editors, *Scythe: Proceedings and Bulletin of the International Data Farming Community, Issue 13, Workshop 25*, pages 17–20. 2013.

[3] Bernt M. Åkesson, Esa Lappi, Ville H. Pettersson, Eric Malmi, Sampo Syrjänen, Marko Vulli, and Kari Stenius. Validating indirect fire models with field experiments. *Journal of Defense Modeling and Simulation: Applications, Methodology, Technology*, 10(4):425–434, October 2013.

[4] Aleksi Borén, Petri Mikkola, Ilmari Kangasniemi, Esa Lappi, Petri Reijonen, Jan Solanti, and Bernt Åkesson. Team 5: Protection of high-value targets from indirect fire using temporary constructions. In

Ted Meyer and Gary Horne, editors, *Scythe: Proceedings and Bulletin of the International Data Farming Community, Issue 17, Workshop 29*, pages 22–26. 2015.

[5] P. R. Courtney-Green. *Ammunition for the Land Battle*. Brassey's Ltd., London, England, 1991.

[6] Miika Haataja, Esa Lappi, and Bernt Åkesson. Mortar system effectiveness analysis. Paper presented at Nordic Military Operational Analysis Conference 2017, Kista, Sweden, September 2017.

[7] Gary Horne. Data farming: A meta-technique for research in the 21st century, 1997.

[8] Esa Lappi and Bernt Åkesson. Tactical size unit as distribution in a data farming environment. *Axioms*, 5(1), 2016.

[9] Esa Lappi, Mikko Sysikaski, Bernt Åkesson, and Uğur Z. Yildirim. Effects of terrain in computational methods for indirect fire. In C. Laroque, J. Himmelspach, R. Pasupathy, O. Rose, and A. M. Uhrmacher, editors, *Proceedings of the 2012 Winter Simulation Conference*, 2012.

[10] M. P. Manson. *Guns, Mortars and Rockets*. Brassey's Ltd., London, England, 1997.

Assessment of the control performance of combustion-thermal power plants

István Selek[1], Jenő Kovács[2]

[1] Systems Engineering Research Group, University of Oulu, Finland
POB 4300, 90014 Oulu University, istvan.selek@oulu.fi
[2*] Sumitomo SHI FW,
POB 201, FI-78201 Varkaus, Finland, tel: +358403522795, jeno.kovacs@shi-g.com

Abstract

Current trends indicate that renewable energy is going to have a significant share in the production portfolio, as it is forecasted (IHS Market) that approx. 50% of global capacity additions (1400GW until 2025) will be RES (solar, wind). The widespread of renewable energy reconfigures the role of conventional power production, simultaneously triggering tightening emission and safety regulations and demanding performance requirements. For example, due to the intermittent nature of variable RES (vRES) power, the role of conventional combustion plants is drifting from base power production to load flexible power generation which requires high flexibility in operation, i.e. capability for frequent start-ups, decreasing the minimum load, performing rapid load changes within well-defined load range and participating in frequency control duties. The usual load ramps are in the range of 2-5 %MCR/min (percentage of the maximum continuous rate per time), and typically in the range of 50%-90% load level. Additionally, there is a clear trend requiring smaller (5-10%) load change but in a much quicker manner.

In order to address the aforementioned challenges, the dynamic response of power plants has to be improved. The improvement can be achieved by (a) application of advanced control/automation solutions for a given construction or (b) evaluation of the dynamic characteristics during the design phase. For existing plants the most cost–effective manner to improve the operation flexibility is to (re)design the unit master control since these may inherently have great potential for flexibility currently not utilized by the applied control approach which is typically built on boiler- or turbine-follow arrangements.

This paper addresses the control performance evaluation of combustion-thermal power plants. The core problem is described as follows: given a nonlinear (mathematical) plant model, what is the best possible performance (regarding reference tracking) which can be achieved by means of feedback control subject to system constraints, assuming full state information. Consequently, the related problem to be considered is the derivation of the feedback law which actually achieves the best possible performance. Given the outlined problems, an approach is developed to provide a (lower) bound estimate on closed loop control performance for nonlinear combustion-thermal power plant models regarding reference tracking criteria. The approach assumes full state information and considers hard (process input and state) constraints. Using this, a best possible operation strategy (by means of feedback control) is proposed for the plant given a load rejection reference. Finally an application of the proposed approach is considered.

Detection and characterization of oscillations in control loops using multivariate empirical mode decomposition : An Overview

Muhammad Faisal Aftab [*1] and Morten Hovd[†1]

[1]*Department of Engineeirng Cybernetics, Norwegian University of Science and Technology (NTNU), Trondheim, Norway*

Oscillations are one of the major performance issues in industrial control systems. The presence of oscillation can lead to equipment wear and product variability, thereby effecting the profitability of the plant. Moreover, oscillations originating in one of the loops can propagate to different parts due to underlying interactions and process flows, giving rise to plant-wide oscillations. In order to reduce the adverse impacts of the oscillatory control loops a robust oscillation detection and diagnosis mechanism is required to reduce the shut down and maintenance time.

The increased level of complexity and automation in industry necessitates the provision of adaptive and data driven tools for the diagnosis and detection of oscillations. The data driven approaches are preferred over the traditional model based analysis as the accurate physical mathematical models are not easily available. Multivariate empirical mode decomposition (MEMD) has the ability to process multivariate data and to sift out different oscillatory components from the data without any model and any assumption about the underlying process itself. The MEMD is applicable to both non-stationary and non-linear time series data and is quite helpful in detection and diagnosis of the oscillations in control loops.

MEMD owing to its peculiar dyadic filter bank and mode alignment property can be applied to the variety of issues ranging from oscillations in individual loops to the plant wide oscillations. The method not only detects the oscillation in the loops but also checks for the presence of the harmonics to ascertain the existence of non-linearity as the source of oscillations in an automated manner. Presence of multiple sources of oscillations can also be handled accordingly. Moreover, the MEMD can be used for the case of plant wide oscillation detection where the loops oscillating with common cause and hence common frequency are grouped for further analysis.

---

[*]muhammad.faisal.aftab@ntnu.no
[†]morten.hovd@ntnu.no

1

The effectiveness of the MEMD based methods both for the detection of oscillations in individual control loops and plant-wide oscillations are demonstrated using simulation and industrial case studies.

2

Using Multilevel Flow Modeling for Fault Diagnosis of Produced Water Treatment

Emil K. Nielsen[a], Jerome Frutiger[b], Gürkan Sin[b], Ole Ravn[a], Morten Lind[a]

[a] Department of Electrical Engineering, Technical University of Denmark, Elektrovej 326, Kgs. Lyngby, 2800.
[b] Department of Chemical Engineering, Technical University of Denmark, Søltofts Plads 227, Kgs. Lyngby, 2800.

Decision support systems are crucial in order to improve the efficiency and safety of control systems. With an increase in system complexity and autonomy, the tasks for operators to analyse situations, of behaviours deviating from nominal system operation, becomes increasingly complicated.

Automated fault diagnosis is a method which can potentially decrease the reaction time, and increase the probability of a correct response to faults. The focus of online fault diagnosis has primarily been on component level. Multilevel Flow Modeling (MFM), is a method for modelling the functionality of complex mass and energy flow systems[1]. Models of nuclear power systems, electric power grids and oil production systems have been used for online fault diagnosis[2]. The method is used for modelling how high level functionality is supported by lower levels, commonly referred to as means-end models. MFM has numerous different applications of which one is fault diagnosis. Online fault diagnosis with MFM is limited in application[2,3,4,5,6,7], whereas offline root cause analysis has been applied diversely[8,9,10].

Faults are problems that pose a risk to the quality of a product or the safety of the environment, equipment or staff. It is impossible to foresee every possible fault on a plant. For this reason, MFM becomes beneficial, as models are general and high level descriptions of the plant functionality, at a qualitative and discrete level. This means, that models are capable of predicting a wide range of causes and consequences of faults. MFM is however intended as a tool for decision support, providing information on the type of fault and its origin, requiring a final analysis of an operator, based on the provided information. MFM is different from conventional fault diagnostic methods[11,12], as MFM does not require that one classifies faults in groups such as: broken bearing, broken shaft, broken propeller and no faults. Instead, MFM provides causal consequence/cause pathways, e.g. the flow of water has decreased into a separator, due to an imbalance between incoming and outgoing mass flows, caused by either a) a low flow at a pump, b) a valve failing to open/close, etc. MFM thus has the potential to distinguish between a considerably large amount of different faults with low modelling effort. Currently there is no method for selection amongst multiple candidate diagnoses, however this is currently a topic of investigation.

In this project, a pilot plant of an offshore water treatment process is modelled with MFM. A set of faults have been defined based on a HAZOP study and simulated on the pilot plant. The model is then used for predicting causes and consequences of triggered alarms. This projects aims to produce robust predictions of causes and consequences from MFM models, by synthesizing a method and framework for validating and testing MFM models. The framework will provide a means for comparison of different models or model versions on a specified set of faults. It will also enable comparison with other fault diagnostic methods, or different versions of the MFM methodology rule base[13].

Based on the work carried out by Wu[14] we are investigating how to validate the model, based on expert knowledge and a HAZOP for high risk and rare faults. And also on dynamic process simulations and on-line experiments. We seek to validate models by combining qualitative statements with dynamic process simulations and on-line experiments, to produce a large set of faults with variations, to determine the model robustness to fault variations.

References

1. Lind M. An introduction to multilevel flow modeling. *Nucl Saf Simul*. 2011;2(1):22-32.
2. Larsson JE. Real-Time Root Cause Analysis with Multilevel Flow Models. In: *International Workshop on Principles of Diagnosis*. Stockholm, Sweden; 2009:3-8.
3. Thunem HP-J. The development of the MFM Editor and its applicability for supervision , diagnosis and prognosis. In: *Safety, Reliability and Risk Analysis: Beyond the Horizon*. ; 2014:1807-1814.
4. Larsson JE, Öhman B, Calzada A. Real-Time Root Cause Analysis for Power Grids. In: *SECURITY AND RELIABILITY OF ELECTRIC POWER SYSTEMS*. Tallinn, Estonia; 2007:1-7. http://www.goalart.com/publications/2007-CIGRE.pdf.
5. Larsson JE. On-Line Root Cause Analysis For Nuclear Power Plant Control Rooms. In: *Proceedings of the International Symposium on Symbiotic Nuclear Power Systems for the 21st Century*. Fukui, Japan; 2007.
6. Larsson JE, DeBor J. Real-time root cause analysis for complex technical systems. *IEEE 8th Hum Factors Power Plants HPRCT 13th Annu Meet*. 2007:156-163. doi:10.1109/HFPP.2007.4413199.
7. Larsson JE. On-line Root Cause Analysis for Large Control Centers. 2005.
8. Akio G, Takahisa I. Functional information in operator support systems. *Nucl Saf Simul*. 2016;7(1):35-41.
9. Lind M, Zhang X. Functional Modelling for Fault Diagnosis and its Applications for NPP. *Nucl Eng Technol*. 2014;46(6):753-772. doi:10.5516/NET.04.2014.721.
10. Wu J, Zhang L, Lind M, et al. Hazard Identification of the Offshore Three-Phase Separation Process Based on Multilevel Flow Modeling and HAZOP. In: *International Conference on Industrial, Engineering & Other Applications of Applied Intelligent Systems*. Amsterdam, Holland; 2013:421-430. doi:10.1007/978-3-642-38577-3_43.
11. Venkatasubramanian V, Rengaswamy R, Yin K, Kavuri SN. A review of process fault detection and diagnosis part I: Quantitative model-based methods. *Comput Chem Eng*. 2003;27(3):293-311. doi:10.1016/S0098-1354(02)00160-6.
12. Venkatasubramanian V, Rengaswamy R, Ka SN. A review of process fault detection and diagnosis Part II : Qualitative models and search strategies. *Comput Chem Eng*. 2003;27:313-326.
13. Nielsen EK, Bram MV, Frutiger J, Lind M. Modelling and Validating a Deoiling Hydrocylone for Fault Diagnosis using Multilevel Flow Modeling. In: *International Symposium on Future I&C for Nuclear Power Plants (ISOFIC) 2017*. Gyeongju, Korea; 2017:1-9.
14. Wu J, Zhang L, Hu J, et al. An Integrated Qualitative and Quantitative Modeling Framework for Computer-Assisted HAZOP Studies. *Am Inst Chem Eng*. 2014;60(12):4150-4173. doi:DOI 10.1002/aic.14593.

Fault-Tolerant Control of Actuators

Mats Friman

Metso Flow Control

P.O.Box 306, FI-33101 Tampere, Finland

Extended Abstract

In the process industry, final control elements are used to implement control actions of PID control loops, such as flow, pressure, level, temperature, and quality controls. The most common controls are liquid and gas flows in pipelines, which are usually implemented by pneumatically powered servo actuating systems. They have a key position ensuring safe and economical operation of the plant, and in the case of failures, such as faulty sensors, it is important to retain control over the actuator.

Today's servo actuating systems utilize auxiliary sensors (e.g. pressure sensors) for position control, but the most important sensor is for position. Most servo actuator controllers can operate in a mode where only the position sensor is utilized for control, so a fault in any other sensor does not cause major problems for control. However, if we lose the position measurement, some indirect control must be used.

In this presentation, we introduce a new idea for fault-tolerant control targeted for failures in the position sensor. The key idea is to replace the faulty position opening measurement with a corresponding simulated value, and to use the simulated measurement for ordinary feedback control.

Analysis of Influence of Sensor Degradation on Flowrate Estimates by Virtual Flow Metering Systems

Timur Bikmukhametov, Johannes Jäschke

Department of Chemical Engineering, Norwegian University of Science and Technology, 7491, Trondheim, Norway

Abstract

Accurate flowrate measurements in petroleum production is important for optimization, fiscal metering and allocation purposes. Currently, multiphase flow meters are widely used in the industry as the most reliable source for online monitoring of oil and gas production rates. However, such meters are expensive and may give inaccurate flowrate predictions for a flow with high gas-oil ratio (GOR) and water cut (WC).

As an alternative, Virtual Flow Meters (VFM) may be used. These meters estimate the flowrates based on a computational fluid flow model in a combination with an optimization routine.

In this work, a Virtual Flow Meter is created based on OLGA-MATLAB interaction via a Matrikon OPC server. This VFM system is used together with Monte Carlo simulations in order to investigate the influence of sensor degradation on the flowrate estimates.

In addition, the influence of heat transfer modeling on the flowrate estimates is discussed. More specifically, a segmented modeling approach of the well heat transfer is compared with a non-segmented approach. Applicability of both approaches for VFM systems is discussed.

In the results it is obtained that the sensor degradation may have a noticeable impact on the flowrate estimates using VFM. In addition, it is obtained that the failure of the temperature sensors may lead to a bias in the flowrate estimates.

In the heat transfer modeling part, it is obtained that the segmented approach does not give any advantage if the wellhead pressure is known. However, under some circumstances, this approach may produce better results than the non-segmented approach.

Model-based process development and monitoring of lactic acid bacteria fermentations

Robert Spann[1], Anna Eliasson Lantz[2], Christophe Roca[3], Krist V. Gernaey[1], Gürkan Sin[1]

Gürkan Sin: gsi@kt.dtu.dk

[1] Process and Systems Engineering Center (PROSYS), Department of Chemical and Biochemical Engineering, Technical University of Denmark, Søltofts Plads Building 229, 2800 Kgs. Lyngby, Denmark

[2] PILOT PLANT, Department of Chemical and Biochemical Engineering, Technical University of Denmark, Søltofts Plads Building 229, 2800 Kgs. Lyngby, Denmark

[3] Chr. Hansen, Boege Allé 10-12, 2970 Hoersholm, Denmark

Keywords: lactic acid bacteria (LAB) fermentation, modelling, soft sensor, optimization, uncertainty analysis

<u>Abstract</u>

A mechanistic process model describing a lactic acid bacteria (LAB) fermentation was applied to both optimize a continuous fermentation process and to monitor a 700 L batch fermentation of *Streptococcus thermophilus* considering model and measurement uncertainties. The mechanistic model for a *Streptococcus thermophilus* fermentation comprised biological and chemical mechanisms. It included a description of the biomass growth rate as a function of the pH and inhibition effects of metabolites, and predicted biological state variables, such as the biomass, substrate (lactose), and lactic acid concentrations. In addition, the model predicted the pH of the fermentation broth by solving the dissociation reactions of the charged components, as lactate, ammonia, carbonate, and phosphate. (i) The dynamic model was applied to optimize a continuous fermentation in a 50 m^3 bioreactor considering the feasibility for the downstream units. The optimal substrate concentration in the feed and dilution rate were estimated in order to maximize the cell yield (biomass concentration) and to minimize the waste of substrate owing to raw material costs. Producing LAB in a continuous fermentation would reduce production costs compared to traditional batch fermentations. (ii) The model was used in a soft sensor framework to monitor a 700 L *Streptococcus thermophilus* fermentation. The soft sensor was based on a data reconciliation module and the dynamic model. The data reconciliation module used a general process stoichiometry model to update some of the model parameters with 5 minutes intervals using the very limited available on-line measurements, which were pH and amount of ammonia addition. The updated parameters were used as input to the dynamic model. The model predicted then unmeasured, important process parameters, such as biomass, lactic acid, lactose (substrate), and the measured pH. Uncertainties in model parameters, initial conditions, and measurements were accounted for by performing Monte Carlo simulations of 100 input samples leading to a probability distribution of the state variables in the monitoring system. The presented applications were implemented and solved in MATLAB® (The MathWorks®, Natick, MA) using the built in solver, ode15s, and the nonlinear least-squares solver, lsqnonlin.

Acknowledgement

Comparative study of Kalman Filter-based observers with simplified tuning procedures

Christoph Josef Backi [*] **Sigurd Skogestad** [*]

[*] *Department of Chemical Engineering, Norwegian University of Science and Technology (NTNU), NO-7491 Trondheim, Norway (e-mail: christoph.backi@ntnu.no, sigurd.skogestad@ntnu.no)*

Abstract: In the oil- and gas industry, gravity separators are used for bulk separation of hydrocarbons (oil and condensate), gas and water. Further purification happens in downstream equipment, such as hydrocyclones, gas flotation units or membranes. The composition of the multiphase inlet stream to the gravity separator is often not known, since multiphase metering is expensive or sometimes not applicable at all. However, knowledge of the amounts of gas and liquid entering the separator and in consequence also the downstream equipment is beneficial for optimal operation or to launch countermeasures in the event of severe slugging.

We use a first-principles model for a gravity separator [1] to design observers for estimation of the liquid and gas inflows to the separator, which constitute disturbance variables. Furthermore, we estimate the effective split ratio between the respective water and oil phases. The observers are based on an Extended Kalman Filter (EKF) in its continuous-time implementation. The first observer design is a standard EKF, whereas the second is a Kalman-like Filter, or more precise a least-squares observer with forgetting factor [2], since the Kalman Filter in its deterministic sense is in fact a least-squares observer. Hence, the second observer (KF-like LSO) is closely related to the EKF design. The only difference is found in the way the differential Matrix-Riccati-Equation (DMRE) is solved and consequently how the Kalman feedback gain is calculated.

For the EKF, the following well-known DMRE is solved

$$\frac{d\mathbf{P}_1(t)}{dt} = \mathbf{A}(t)\mathbf{P}_1(t) + \mathbf{P}_1(t)\mathbf{A}^T(t) - \mathbf{K}_1(t)\mathbf{C}\mathbf{P}_1(t) + \mathbf{Q}_1,$$
$$\mathbf{K}_1(t) = \mathbf{P}_1(t)\mathbf{C}^T\mathbf{R}_1^{-1}, \tag{1}$$

where $\mathbf{A}(t) = \dfrac{\partial \hat{\mathbf{f}}(\hat{\mathbf{x}}, \mathbf{u})}{\partial \hat{\mathbf{x}}}$ denotes the time-varying Jacobian of the extended system dynamics $\dot{\hat{\mathbf{x}}} = \hat{\mathbf{f}}(\hat{\mathbf{x}}, \mathbf{u})$, $\mathbf{C}$ is the output matrix in $\mathbf{y} = \mathbf{C}\hat{\mathbf{x}}$, $\mathbf{Q}_1$ and $\mathbf{R}_1$ are the covariance matrices of process and measurement noises, respectively, and $\mathbf{K}_1(t)$ is the time-varying Kalman feedback gain.

For the KF-like LSO, the DRME is slightly modified [3, Section 2.3]

$$\frac{d\mathbf{P}_2(t)}{dt} = \mathbf{A}(t)\mathbf{P}_2(t) + \mathbf{P}_2(t)\mathbf{A}^T(t) - \mathbf{K}_2(t)\mathbf{C}\mathbf{P}_2(t) + \lambda\mathbf{P}_2(t),$$
$$\mathbf{K}_2(t) = \lambda\mathbf{P}_2(t)\mathbf{C}^T\mathbf{R}_2^{-1}, \tag{2}$$

where $\mathbf{A}(t)$ and $\mathbf{C}$ have been defined before, $\mathbf{R}_2$ is the measurement covariance noise matrix, $\mathbf{K}_2(t)$ denotes the Kalman feedback gain and λ is the forgetting factor.

The advantage in using (2) instead of (1) for multivariable systems can be found in the simpler tuning procedure, which implies defining the matrix $\mathbf{R}$ and the scalar λ. Hence, tuning via the process noise covariance matrix $\mathbf{Q}$ is skipped, which is often not known anyhow and in many cases offers too many degrees of freedom.

In addition, the model structure of the gravity separator allows for the design of a cascaded observer due to the fact that decoupling for some state variables is possible. This leads to further simplification of the tuning procedure since each of the observers in the cascade can be tuned independently.

In simulation studies we demonstrate that, despite the simpler tuning procedure, the KF-like LSO performs at least equally well, if not better, compared to the EKF. The advantages of simpler tuning procedures (KF-like LSO and cascaded design) become apparent, especially for cases with added process and measurement noises.

[1]   C.J. Backi and S. Skogestad – A simple dynamic gravity separator model for separation efficiency evaluation incorporating level and pressure control. *2017 American Control Conference*, Seattle, USA, May 24–26, 2017.

[2]   R.M. Johnstone, C.R. Johnson Jr., R.R. Bitmead and B.D.O. Anderson – Exponential convergence of recursive least squares with exponential forgetting factor. *21st IEEE Conference on Decision and Control*, Orlando, USA, December 8–10, 1982.

[3]   M.A.M. Haring – Extremum-seeking control: convergence improvements and asymptotic stability. PhD Thesis, Norwegian University of Science and Technology, 2016.

State and parameter estimation for a Gas-Liquid Cylindrical Cyclone

Torstein Thode Kristoffersen [*] Christian Holden [*]

[*] *Department of Mechanical and Industrial Engineering, Norwegian University of Science and Technology (NTNU) (e-mail: torstein.t.k@gmail.com, christian.holden@ntnu.no).*

Abstract: The gas-liquid cylindrical cyclone (GLCC) is a compact separator recently considered for subsea separation of oil and gas in deep waters in remote areas (Kristiansen et al., 2016) where large, traditional separators can't be used. Several challenges need to be resolved before placing this separator at the seabed. The small operational volume reduces the separation performance and leads to high sensitivity to changes in inlet conditions. Measurements of several critical variables are therefore necessary for both operators and controllers to efficiently control the separator (Kristoffersen and Holden, 2017).

Available measurements are often limited due to a lack of suitable sensor technology, i.e., too expensive sensors, unreliable measurements or simply non-existing sensors. Soft sensors are a cost-efficient approach for estimating unmeasured states and parameters, using a prediction model and the available measurements in place of expensive sensor hardware. Previous results on estimation for GLCC separators are limited to use of the Extended Kalman Filter (EKF) for parameter estimation assuming full state knowledge (Kristoffersen and Holden, 2017). The EKF showed low robustness to measurement errors and was only able to handling approximately 1% measurement noise in this case.

Therefore, in this work, we develop an Unscented Kalman Filter (UKF) and a linear Moving Horizon Estimator (MHE) for improved robustness and state and parameter estimation of a GLCC separator having limited state knowledge. The estimators apply the same estimation model as the previously proposed EKF, but calculate the unmeasured states using an algebraic transformation. The estimation performance are evaluated by considering the statistical properties of the state estimation error. A block diagram of the closed-loop system with the estimator providing state feedback to a controller is shown in Fig. 1.

Keywords: Nonlinear estimation, Kalman filtering, MHE, UKF, EKF

Fig. 1. Block diagram showing the closed-loop system.
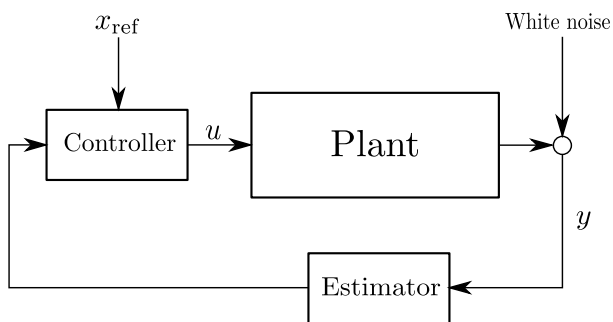
REFERENCES

Kristiansen, O., Sørensen, Ø., and Nilssen, O.R. (2016). Compactsep– compact subsea gas-liquid separator for high-pressure wellstream boosting. In *Offshore Technology Conference.*

Kristoffersen, T.T. and Holden, C. (2017). Model predictive control and extended Kalman filter for a gas-liquid cylindrical cyclone. In *Proceedings of the 1st IEEE Conference on Control Technology and Applications.*

A new efficient ratio control structure

Tore Hägglund

Department of Automatic Control, Lund University
Box 118, SE 221 00 Lund, Sweden
email:tore.hagglund@control.lth.se

In ratio control, the control objective is to keep the ratio between two signals, normally flow measurements, at a desired value. There is no problem to achieve this in a steady-state situation, but an efficient ratio control structure should be able to take care of setpoint variations, load disturbances, and control signal saturations. It is also desirable to have a structure that manages to keep the ratio also when one of the controllers is switched to manual mode.

The flow setpoint is normally varying to follow demands on combustion or production rate. There are various reasons for load variations, e.g. pressure variations in the tubes, and the control signals are often reaching their saturation limits when the control is aggressive and the actuators are not oversized.

So far, there has not been any approach that manages to track the ratio during all possible transients caused by setpoint changes, load disturbances and control signal saturations. This presentation describes the Tracking Ratio Station (TRS) that manages to take all these disturbances into account. It is also able to keep the ratio when one of the controllers takes a local setpoint or is switched to manual control.

The Tracking Ratio Station determines the setpoints of the two flow loops so that the one with the largest control error follows the external setpoint, whereas the one with the smallest control error follows the process output of the opposite control loop.

The Tracking Ratio Station has been implemented in an industrial DCS system at a paper mill, and the field tests showed that the TRS worked as desired even in this industrial environment in the presence of disturbances and sticky valves. Results from the field tests will be given at the presentation.
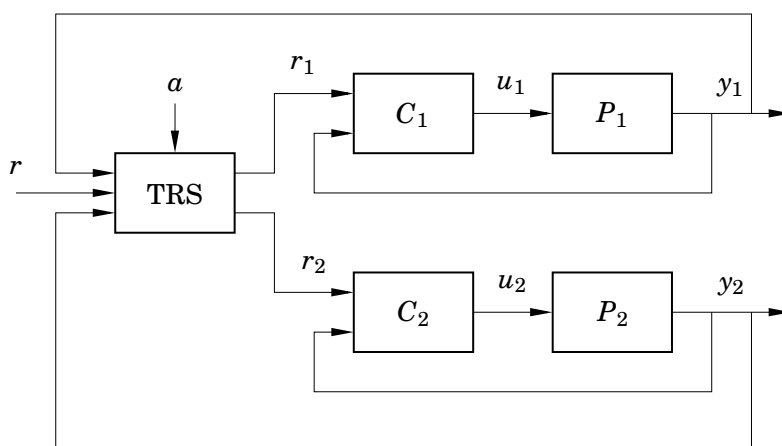
Discrete PI Controller Design for Linear Measurement Combinations in Self-Optimizing Control

Jonatan Klemets * **Morten Hovd** **

*Department of Engineering Cybernetics, Norwegian University of
Science and Technology, Trondheim, Norway
(e-mail: jonatan.klemets@itk.ntnu.no).
** Department of Engineering Cybernetics, Norwegian University of
Science and Technology, Trondheim, Norway
(e-mail: morten.hovd@itk.ntnu.no)*

Abstract: Self-optimizing control focuses on minimizing loss for processes in the presence of disturbances by holding selected controlled variables **c** at constant set-points. The loss can further be reduced by selecting **c** as linear combinations **H** of the available measurements **y** such that the controlled variables become **c** = **Hy**. Two methods for finding locally optimal measurement combinations are the Null-space and the Exact local method. Both approaches offer sets, with an infinite number of possibilities for selecting the measurement combinations that all give the same loss. Since self-optimizing control mainly focuses on the steady-state operation, little attention has been put on the dynamic performance when selecting measurement combinations. In this work, PI controllers and measurement combinations are simultaneously obtained with the aim to improve the transient response while maintaining the self-optimizing control properties. A solution can be found by solving a bilinear matrix inequality (BMI), which becomes a linear matrix inequality (LMI) by specifying a stabilizing state feedback gain. Since the resulting PI controllers and measurement combination requires solving a BMI, a globally optimal solution can't be guaranteed. However, the proposed method often seems to give good results. This is illustrated on a binary distillation column case study which shows an improved dynamic response when the process is facing disturbances.

Keywords: Self-optimizing control, Static output feedback, Linear Matrix Inequality

Risk-based health-aware control of a subsea system

- Adriaen Verheyleweghen & Johannes Jäschke, Department of Chemical Engineering, NTNU

Subsea oil and gas production and processing plays an important role in satisfying the worlds growing energy demands, despite the recent decline in oil price. Easy reserves have been largely exhausted, so new fields pose many challenges, such as large water depth, long tie-back distances or even seasonal inaccessibility. Subsea oil and gas processing can be an enabling technology in such cases, but it comes with challenges of its own. One of the biggest challenges is the large cost associated with maintenance interventions. For this reason, operation is often conservative, to prevent unplanned breakdown. Unfortunately, high system reliability is usually in conflict with the economic objective of the plant. In order to avoid sub-optimal operation, it is therefore important to devise a systematic approach to ensure optimal economic operation without compromising the system integrity.

Health-aware control has been proposed to deal with problems where there is a trade-off between reliability and economic performance (Escobet, Puig, & Nejjari, 2012). They propose a reconfigurable control scheme that keeps the remaining useful life (RUL) of the system within predefined bounds by adjusting the throughput of the plant. Model predictive control may also be used to achieve health-aware operation, by putting constraints on the maximum allowable system degradation, as shown e.g. by (Pereira, Galvão, & Yoneyama, 2010) and (Salazar, Weber, Nejjari, Theilliol, & Sarrate, 2016).

We further develop the framework presented in (Verheyleweghen & Jäschke, 2017) of health-aware operation by looking at how the problem of optimal operation should be defined in a meaningful way. Rather than constraining the maximum allowable deterioration of certain critical health-indicators, we propose to limit the overall risk of unavailability during operation, as this directly relates back to the economics of the plant. To be able to evaluate the risk of unavailability, we need to know the joint density function of the individual sub-components. This requires detailed knowledge of the RUL distribution, of which the shape maybe known, but the parametrization of which might be uncertain. This problem can be partially mitigated by using stochastic or robust optimization methods. In this work, we assume that the RUL is Weibull-distributed. The parameters of the Weibull distribution are assumed to be known to lie within upper and lower bounds. To ensure feasibility and optimality of the solution regardless of the true realization of the parameters, we use scenario-based stochastic optimization.

We demonstrate our approach on a subsea case study, where the production rate is adjusted such that the survival of the production system is guaranteed with a given probability. We also show that our approach results in more meaningful operation strategies than previously described approaches.

References

Escobet, T., Puig, V., & Nejjari, F. (2012). Health Aware Control and model-based Prognosis. *Mediterranean Conference on Control & Automation (MED)* (págs. 691-696). Barcelona: IEEE.

Pereira, E. B., Galvão, R. K., & Yoneyama, T. (2010). Model Predictive Control using Prognosis and Health Monitoring of actuators. *International Symposium on Industrial Electronics* (págs. 237-243). Bari: IEEE.

Salazar, J. C., Weber, P., Nejjari, F., Theilliol, D., & Sarrate, R. (2016). MPC framework for system reliability optimization. En Z. (. Kowalczuk, *Advanced and Intelligent Computations in Diagnosis and Control* (págs. 161-177). Springer.

Verheyleweghen, A., & Jäschke, J. (2017). Framework for Combined Diagnostics, Prognostics and Optimal Operation of a Subsea Gas Compression System. *Proceedings of the IFAC world congress*.

Resolving issues of scaling for gramian based input-output pairing methods

Fredrik Bengtsson[*], Torsten Wik[*], and Elin Svensson[†]

A common issue in many industries is that interaction between different parts of the plant gives rise to a multiple input multiple output (MIMO) system, where the same input may affect multiple outputs, or conversely, the same output is affected by multiple inputs. This is the core of the input-output pairing problem; which inputs should be used to control which outputs. While one often solves this by matching one input to one output by a decentralized configuration, at times it can be necessary to add additional feed-forward between the inputs, or even implementing a full MIMO controller for parts of the system.

There are numerous proposed input-output pairing methods, many of which are discussed in [6]. The most prominent one is probably still the Relative Gain Array (RGA), and modifications of it, such as the dynamic RGA and the Relative Interaction Array (RIA)[8]. Relatively recently a new group of input-output pairing methods have been introduced, namely the gramian based methods. This group includes the Σ_2 method [2], the participation matrix (PM) [3] and the Hankel interaction index array (HIIA) [7]. These methods use the controllability and observability gramians to create an interaction matrix which gives a gauge of how much each input affects each output. An attractive property of these interaction matrices is that they can be used to determine both a decentralized controller structure and a sparse structure (a structure which includes feed-forward or MIMO blocks). Moreover, the gramian based measures take into account system dynamics and not only the steady state properties.

The gramian based methods however differ from the RGA and its variants in that they suffer from issues of scaling in the sense that the results of the methods vary depending on input and output scaling. While some methods are suggested to solve this problem in for example [4], we will show by an example of a heat exchanger network how these methods are in some situations insufficient. A method to scale the Σ_2 interaction matrix by normalizing either its columns or rows was presented in [1] and here we will examine this method in more detail and also apply it to the PM and the HIIA. Furthermore, we will examine a new scaling scheme which uses the Sinkhorn-Knopp algorithm [5] to normalize both the rows and columns of the interaction matrix.

To demonstrate the benefit of the new scaling schemes we have developed a MIMO-generator to generate a large number of systems. The scaling method for the gramian, with either columns or rows normalized, or both using the Sinkhorn-Knopp algorithm was then compared to the gramian based methods without any additional scaling on each of the generated systems. This is done by determining the control configuration of each method and evaluating their responses to reference changes and load disturbances. It is shown that using the Sinkhorn-Knopp algorithm to scale the interaction matrices generally gives the control configuration which handled both references and disturbances the best.

References

[1] Miguel Castano Arranz and Wolfgang Birk. New methods for structural and functional analysis of complex processes. In *Control Applications,(CCA) & Intelligent Control,(ISIC), 2009 IEEE*, pages 487–494. IEEE, 2009.

[2] Wolfgang Birk and Alexander Medvedev. A note on gramian-based interaction measures. In *Proc. of the European Control Conference*, 2003.

[3] Arthur Conley and Mario E Salgado. Gramian based interaction measure. In *Proceedings of the 39th IEEE Conference on Decision and Control*, volume 5, pages 5020–5022. Citeseer, 2000.

[4] Mario E Salgado and Arthur Conley. Mimo interaction measure and controller structure selection. *International Journal of Control*, 77(4):367–383, 2004.

[5] Richard Sinkhorn and Paul Knopp. Concerning nonnegative matrices and doubly stochastic matrices. *Pacific Journal of Mathematics*, 21(2):343–348, 1967.

[*]F. Bengtsson and T. Wik are with Department of Signals and Systems, Chalmers University of Technology, SE 412 96 Göteborg, Sweden, fredben@chalmers.se, tw@chalmers.se

[†]E. Svensson is with CIT Industriell Energi AB, Chalmers Teknikpark, Sven Hultins gata 9D, SE 412 58 Göteborg, Sweden, elin.svensson@cit.chalmers.se

[6] Marc van de Wal and Bram de Jager. A review of methods for input/output selection. *Automatica*, 37(4):487 – 510, 2001.

[7] Björn Wittenmark and Mario E Salgado. Hankel-norm based interaction measure for input-output pairing. In *Proc. of the 2002 IFAC World Congress*, 2002.

[8] Zhong-Xiang Zhu. Variable pairing selection based on individual and overall interaction measures. *Industrial & engineering chemistry research*, 35(11):4091–4099, 1996.

On the Modified Hankel Interaction Index Array for Control Configuration Selection

Bijan Moaveni[1], Wolfgang Birk[2]

[1]Iran University of Science and Engineering, Tehran, Iran

[2]Control Engineering Group, Luleå University of Technology, Luleå, Sweden

Control configuration selection (CCS) is an important step in multivaraible control systems design, especially for decentralized control systems where an appropriate input-output pairing has to be selected. There are numerous methods available for evaluating the interactions between subsystems and solving the input-output pairing problem, initiated with the introduction of the Relative Gain Array (RGA). In general, input-output pairing methodologies for linear multivariable plants can be classified in two categories, transfer function based relative gain related methods and Gramian based methodologies for state space realizations. The main benefit of transfer function based approach, like the RGA, is that these methods take the closed loop properties into account, while those are usually not ideal when dealing with large scale plants. On the other hand, Gramian-based methodologies are efficient for large scale plants while these methods until now cannot consider the closed loop properties in the pairing analysis. In other words, Gramian-based methodologies are not really interaction measures, since these methodologies just consider the open loop properties of the multivariable plant. Consequently, the main critic on Gramian-based methodologies is that the methods do not provide any insight on closed loop properties like stability and integrity, as well as that they are scaling dependent.

In this presentation, we are introducing and discussing the modified HIIA (mHIIA), which tries to combine the benefits of the RGA-based and Gramian-based input-output pairing approaches. The mHIIA is defined as the element-wise ratio of the open loop Hankel norm with the Hankel norm of the closed loop.

$$\delta_{ij} = \frac{\sigma_{H,o,ij}}{\sigma_{H,T,ij}}$$

In the derivation of the mHIIA, an interpretation of the perfect control requirement for state space realisations is used and subsequently, the ratio between open-loop and closed-loop Hankel norms is calculated. It is shown that mHIA has the following interesting properties

- mHIIA is input-output scaling independent, while HIIA is not.
- mHIIA and HIIA consider the dynamics of the process in input-output pairing analysis.
- mHIIA can consider the effect of internal time delays on input-output pairing, while HIIA has problem with internal time delayed subsystems.

A number of typical benchmark cases will be used to evaluate the mHIIA and some of the shortcomings of this approach will be discussed. It is important to note that the mHIIA in its current form, does not yet provide insights on stability and integrity. Latest achievements in mHIIA approach will also be presented.

Surrogate Model Generation Using the Concepts of Self-Optimizing Control

Julian Straus, Sigurd Skogestad

Department of Chemical Engineering

Norwegian University of Science and Technology

Trondheim, Norway

Email: {julian.straus, sigurd.skogestad}@ntnu.no

Abstract—This paper presents the application of self-optimizing control in the concept of surrogate model generation. Surrogate model generation generally has problems with a large number of independent variables resulting in a large sampling case. Utilizing the concept of self-optimizing control and keeping measurements constant, it is on the one hand possible to reduce the number of independent variables resulting in a reduced sample space. On the other hand, this allows to map a close-to-optimal response surface. As the surrogate model is subsequently used for optimization, this is as well advantageous; regions in which the system is suboptimal are not mapped this way. The proposed method is studied using an ammonia reactor which for disturbances experiences limit-cycle behaviour and/or reactor extinction. Using SOC, it is possible to reduce the number of manipulated variables by three and map the optimal response surface.

I. INTRODUCTION

Surrogate models are an emerging field and may be utilized for the optimization of integrated flowsheets [1]. Using a sequential-modular software like Aspen Plus®, Aspen Hysys®, SimSci PRO/II, or UniSim Design Suite, problems may arise in the convergence, whereas equation-orientated solver may be difficult for complicated models. It is possible to simplify the optimization through the incorporation of recycles within the surrogate models. The calculation of surrogate models struggles however if the number of independent variables (n_u) is high. This is generally the case, if the surrogate model i is designed for the latter combination with other surrogate models j. In this case, the connection variables $\mathbf{x}_{i,j}$ may increase n_u. This so-called "curse of dimensionality" says that the number of sampling points n_p grows exponentially with the number of independent variables n_u. This may result in an excessive number of points one has to sample. One alternative is the application of PLS regression to define new latent variables $\mathbf{u}'$ with $\dim(\mathbf{u}') < \dim(\mathbf{u})$ [2]. As a second alternative, we proposed to use the concepts of self-optimizing control [3] to reduce n_u [1]. This allows the mapping of the region we are actually interested in and will hence be further investigated in this paper.

This paper is structured as follows; Section II introduces the problem in the context of surrogate model generation for a submodels. Section III explains how self-optimizing control is applied in this context and the properties of self-optimizing control. Section IV first introduces the utilized case study

and then shows results from the application of self-optimizing control in surrogate model generation. Section V discusses the applicability of the proposed procedure and addresses limitations and problems if self-optimizing control is utilized.

II. PROBLEM STATEMENT

Consider a large scale process to be optimized. This is generally difficult and the process is hence split into several submodels. Each of these submodels should be reformulated as a surrogate model to simplify the optimization. An optimization problem as shown below can then be defined for some of the submodels i

$$\min_{\mathbf{x}_i,\mathbf{u}_i} \quad J_i(\mathbf{x}_i,\mathbf{u}_i,\mathbf{d}_i)$$
$$\text{s.t.} \quad 0 = \mathbf{g}_i(\mathbf{x}_i,\mathbf{u}_i,\mathbf{d}_i) \tag{1}$$
$$0 \geq \mathbf{h}_i(\mathbf{x}_i,\mathbf{u}_i,\mathbf{d}_i)$$

where $J_i : \mathbb{R}^{n_x} \times \mathbb{R}^{n_u} \times \mathbb{R}^{n_d} \to \mathbb{R}$ describes the economic objective of the system, $\mathbf{g}_i : \mathbb{R}^{n_x} \times \mathbb{R}^{n_u} \times \mathbb{R}^{n_d} \to \mathbb{R}^{n_x}$ the plant model and $\mathbf{h}_i : \mathbb{R}^{n_x} \times \mathbb{R}^{n_u} \times \mathbb{R}^{n_d} \to \mathbb{R}^{n_{h_i}}$ the operational inequality constraints. The inlet connection variables, $\mathbf{x}_{i,in}$, are hereby considered to be the disturbances $\mathbf{d}_i \in \mathbb{R}^{n_d}$. The manipulated variables of a submodel i, $\mathbf{u}_i \in \mathbb{R}^{n_{u,MV}}$, are the real degrees of freedom for the submodel. However, we consider the total number of independent variables, $n_u = n_{u,MV} + n_d$, for surrogate model generation. The sampling space is then given by bounds as

$$\mathbf{d}_{min} \leq \mathbf{d} \leq \mathbf{d}_{max} \tag{2}$$
$$\mathbf{u}_{min} \leq \mathbf{u} \leq \mathbf{u}_{max} \tag{3}$$

and the sampling is performed using *e.g.* Latin hypercube sampling or regular grid sampling.

III. PROCEDURE

A direct possibility to reduce the number of independent variables by $n_{u,MV}$ is given by fitting a surrogate model for the optimal response surface. If $n_{u,MV}$ is relatively large, this would reduce the number of points which one has to sample. This approach would require the solution of n_p nonlinear problems. A further advantage of this approach is that the surrogate model is sampled in the direction interesting for the subsequent optimization. An analogy to this approach is the creation of road maps. Theoretically, it is possible to include

in a map every single small road and even hiking paths. This would however make the map complicated. Hence, maps only feature the roads that are useful for the desired application.

Alternatively, self-optimizing control can be applied to the submodels and additional n_c equality constraints given by

$$0 = \mathbf{c}_i - \mathbf{H}_i \mathbf{y}_i \tag{4}$$

with $\mathbf{c}_i \in \mathbb{R}^{n_c}$ being the SOC variables and $\mathbf{y}_i \in \mathbb{R}^{n_y}$ being chosen measurements of the system are added to the nonlinear system given by $\mathbf{g}_i$ in Eq. (1) [4]. The matrix $\mathbf{H}_i$ is the optimal selection matrix and can be calculated in different ways [5].

The advantage of using self-optimizing control in this context can be seen in the reduced number of optimization problems one has to solve compared to mapping the optimal response surface. These correspond to $n_d + 1$ nonlinear problems with additional n_u systems of nonlinear equations in the definition of the SOC selection matrix according to Eq. (4). The sampling then consists of solving n_p nonlinear systems of equations.

A. Calculation of the selection matrix $\mathbf{H}$

The optimal selection matrix $\mathbf{H}$ can be calculated using the nullspace method [6] or the exact-local method [7]. It is given by the solution to the following optimization problem

$$\min_{\mathbf{H}} \quad \|\mathbf{H}\mathbf{Y}\|_F$$
$$\text{s.t.} \quad \mathbf{H}\mathbf{G}^y = \mathbf{J}_{uu}^{1/2} \tag{5}$$

with $\mathbf{G}^y \in \mathbb{R}^{n_y \times n_{u,MV}}$ representing the measurement gain matrix with respect to the input $\mathbf{u}$. $\mathbf{Y}$ is given by

$$\mathbf{Y} = \begin{bmatrix} \mathbf{F}\mathbf{W}_d & \mathbf{W}_{n^y} \end{bmatrix} \tag{6}$$

The optimal sensitivity matrix $\mathbf{F} = \frac{\partial \mathbf{y}_{opt}}{\partial \mathbf{d}}$ can be calculated as

$$\mathbf{F} = -\left(\mathbf{G}^y \mathbf{J}_{uu}^{-1} \mathbf{J}_{ud} - \mathbf{G}_d^y\right) \tag{7}$$

using the disturbance gain $\mathbf{G}_d^y \in \mathbb{R}^{n_y \times n_d}$, the hessian of the cost function $\mathbf{J}_{uu} \in \mathbb{R}^{n_{u,MV} \times n_{u,MV}}$, and $\mathbf{J}_{uu} \in \mathbb{R}^{n_{u,MV} \times n_d}$ the second order derivative of J with respect $\mathbf{u}$ and $\mathbf{d}$. $\mathbf{W}_d$ and $\mathbf{W}_n$ are the disturbance and measurement scaling matrices given by

$$\Delta \mathbf{d} = \mathbf{W}_d \mathbf{d}'; \qquad \mathbf{n}^y = \mathbf{W}_{n^y} \mathbf{n}^{y'} \tag{8}$$

in which the vectors $\mathbf{d}'$ and $\mathbf{n}^{y'}$ are assumed to satisfy

$$\left\| \begin{bmatrix} \mathbf{d}' \\ \mathbf{n}^{y'} \end{bmatrix} \right\|_2 \leq 1 \tag{9}$$

This scaling is necessary as this allows us to define selection matrices which minimizes the loss if disturbances occur. It is important to note for the scaling matrices that the 2-norm is used in the scaling in Eq. (9). This implies, that all disturbances and measurements may not be at their upper or lower limit simultaneously. In the case of control, this seems reasonable and a detailed discussion for using the $2-$norm is given by Halvorsen et al. [4]. However, this is not the case, if we want to use the self-optimizing control variables for variable reduction in surrogate model definition. We actually

want to sample these so-called corner points to avoid extrapolation. This could be circumvented by multiplying the $\mathbf{W}_d$ by $\sqrt{n_d}$ and would make a difference, if measurement noise is considered. We propose to set the disturbance scaling matrix $\mathbf{W}_d$ in the case of surrogate model generation to

$$\mathbf{W}_d = \text{diag}\left(\max\left(\mathbf{d} - \mathbf{d}_{min}, \mathbf{d}_{max} - \mathbf{d}\right)\right) \tag{10}$$

and the measurement noise scaling matrix to

$$\mathbf{W}_{n^y} = 1^{-k_{exp}} \text{diag}\left(\mathbf{1}\right) \tag{11}$$

with $\mathbf{1}$ being a vector of ones with length n_y. The parameter k_{exp} can be chosen arbitrarily as the measurements will not have any noise in the case of surrogate model sampling. However, two necessities arise for the parameter k_{exp}

- k_{exp} is large enough so that $\mathbf{YY}^\mathsf{T}$ is nonsingular;
- k_{exp} should be small compared to the entries of $\mathbf{W}_d$ to reduce the effect of measurement noise in the calculation of the selection matrix $\mathbf{H}$;

The solution to this problem in its simplified version is given by [8]:

$$\mathbf{H}^\mathsf{T} = \left(\mathbf{YY}^\mathsf{T}\right)^{-1} \mathbf{G}^y \tag{12}$$

One could argue that the nullspace method [6] can be used as an alternative as measurement noise is not existing and the number of measurement is not important. Hence, the dynamic properties of this specific control structure do not play a role and it is possible to increase the number of measurements This results in a reduced loss as shown in [8]. Furthermore, it is possible to extent the measurements to states, which are generally not considered as they are hard to measure, *e.g.* concentrations. The application of the nullspace method would require that

$$n_y \geq n_d + n_{u,MV} \tag{13}$$

which may not be possible to satisfy for submodels with a lot of manipulated variables and connection variables. Additionally, problems may arose in the solving of the flowsheet, if a sequential-modular flowsheet solver is used. In this situation, the setpoints to the original manipulated variables $\mathbf{u}$ is obtained in an iterative manner which may slow down the solution of each sampling point. This may lead to problems especially in the case of interacting manipulated variables u. Hence, it is generally advisable to choose only a limited number of measurements.

B. Measurement Selection

In order to select the an optimal subset of measurements $n_{y,sel}$, Yelchuru and Skogestad [8] developed a mixed integer quadratic programming approach. It requires the reformulation of the problem given in Eq. (5) in vectorized form:

$$\min_{\mathbf{h}_\delta \sigma_\delta} \quad \mathbf{h}_\delta^\mathsf{T} \mathbf{F}_\delta \mathbf{h}_\delta$$
$$\text{s.t.} \quad \mathbf{G}_\delta^{y\ \mathsf{T}} \mathbf{h}_\delta = \mathbf{j}_\delta$$
$$\sum_{j=1}^{n_y} \sigma_{\delta,j} = n_{y,sel} \tag{14}$$

where $\sigma_j \in \{0,1\}$ with $j = 1 \cdots n_y$ are binary variables to indicate, whether measurements are used in the selection matrix and the optimization matrix. The quadratic cost term is given by

$$\mathbf{F}_\delta = \mathbf{Y}_\delta \mathbf{Y}_\delta^\mathsf{T} \tag{15}$$

and is block diagonal. The same holds true for $\mathbf{G}_\delta^{y\,\mathsf{T}}$ whereas $\mathbf{h}_\delta$ and $\mathbf{j}_\delta$ are a vectorized form of $\mathbf{H}$ and $\mathbf{J}_{uu}$ respectively. Further constraints have to be imposed on $\mathbf{h}_\delta$ to guarantee that $h_{jk} = 0$ for $\sigma_k = 0$ and input u_j and measurement y_k. In this problem, the big-m approach is chosen. This results in bounds for the entries in the selection matrix $\mathbf{H}$ given by

$$-\begin{bmatrix} m \\ m \\ \vdots \\ m \end{bmatrix} \sigma_k \leq \begin{bmatrix} h_{1k} \\ h_{2k} \\ \vdots \\ h_{n_u k} \end{bmatrix} \leq \begin{bmatrix} m \\ m \\ \vdots \\ m \end{bmatrix} \sigma_k \leq \sigma_k, \quad \forall k \in 1,2,\ldots,n_y \tag{16}$$

For a detailed description and derivation, the reader is referred to [8].

Unfortunately, this approach does not handle structural zeros in the selection matrix $\mathbf{H}$. That is, certain measurements should be candidates for certain manipulated variables and would lead to *e.g.* block diagonal selection matrices. This may then lead to complicated adjustments in the flowsheet solver. Hence, we propose to calculated optimal selection matrices $\mathbf{H}_i \in \mathbb{R}^{1 \times n_{y_k}}$ for input u_k using close measurements and not the overall measurement set. This does guarantee the optimal measurement combinations and may lead to cases, where problems may arise. However, it is not possible to generalize when problems may occur and when not. Unfortunately, there are no simple methods for solving this problem in a convincing way [5].

IV. CASE STUDY - AMMONIA REACTOR

The case study for the investigation of this procedure is given by a heat-integrated ammonia reactor. The investigated reactor submodel is shown in Figure 1. This reactor was previously used in stability analysis [9] as well as the feasibility of the application of economic NMPC [10] for the given system. A detailed model description can be found in [10]. The subscript i is dropped for this submodel in the following to improve the understanding. At the optimal operation point, small disturbances lead to limit-cycle behaviour and/or reactor extinction [10]. Hence, varying the manipulated variables $\mathbf{u}$ individually results on the one hand in creating a response surface including regions, in which reactor extinction is present. In regions where limit cycle behaviour occurs, it is on the other hand not possible to define a steady state for the system. Hence, the response surface is complicated and it is necessary to sample a lot of points to achieve a decent surrogate model.

A. Model Adaptation

In order to increase the applicability of the resulting surrogate model, the hydrogen to nitrogen molar ratio is not
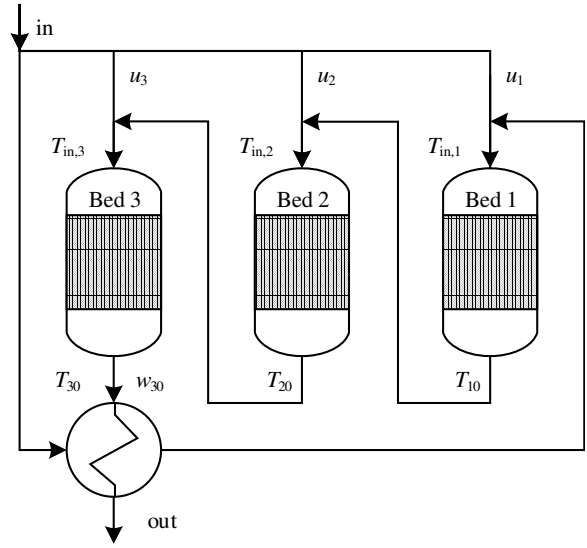

Fig. 1. Heat-integrated 3 bed reactor system of the ammonia synthesis gas loop.

considered to be fixed anymore. Instead, the ratio of hydrogen to nitrogen given by

$$R_{\mathrm{H_2/N_2},j} = \frac{\dot{n}_{\mathrm{H_2},j}}{\dot{n}_{\mathrm{N_2},j}} \tag{17}$$

in each reaction section j is introduced. This results in $3n$ additional algebraic constraints given by

$$0 = R_{\mathrm{H_2/N_2},j} - \frac{\dot{n}_{\mathrm{H_2},j-1} + r_{\mathrm{H_2},j} m_{cat,j}/M_{\mathrm{H_2}}}{\dot{n}_{\mathrm{N_2},j-1} + r_{\mathrm{N_2},j} m_{cat,j}/M_{\mathrm{N_2}}} \tag{18}$$

in which M_i is the respective molar mass and $r_{i,j}$ the reaction rate in [kg i/kg$_{cat}$ h]. Alternatively, it is possible to use the respective mass balance of hydrogen or nitrogen. It seems however useful, to use a fifth inlet variable, whose influence is directly known to process operators and which offers a direct relation to the processes before the reactor. The cost function for the optimization problem shown in Eq. (1) is given by the (mass) extent of reaction ξ

$$\xi = \dot{m}_{in} (w_{\mathrm{NH_3},30} - w_{\mathrm{NH_3},in}) \tag{19}$$

whereas the equality constraints are given by the ammonia mass balance and the temperature balance described in [10] with addition of Eq. (18) for each CSTR j in the CSTR cascade.

For this system, the independent variables are given by the three split ratios

$$\mathbf{u} = \begin{bmatrix} u_1 & u_2 & u_3 \end{bmatrix}^\mathsf{T} \tag{20}$$

as well as the inlet to the system

$$\mathbf{d} = \begin{bmatrix} \dot{m}_{in} & p_{in} & T_{in} & w_{\mathrm{NH_3},in} & R_{\mathrm{H_2/N_2},in} \end{bmatrix}^\mathsf{T} \tag{21}$$

This implies that n_u for this submodel corresponds to 8 of which 3 are real manipulated variables. The other 5 variables are input connection variables. Their respective bounds are

TABLE I
BOUNDS AND UNITS FOR THE CONNECTION VARIABLES.

	$\dot{m}_{in}$ [kg/s]	p_{in} [bar]	T_{in} [°C]	$w_{NH_3,in}$ [wt.%]	$R_{H_2/N_2,in}$ [-]
Lower Bound	59.5	185	235	7	2.8
Nominal Point	70.0	200	250	8	3.0
Upper Bound	80.5	215	265	9	3.2

given in Table I. Two output variables have to be fitted due to the assumption of constant pressure and a single outlet stream. These correspond to the outlet temperature T_{out} and the (mass) extent of reaction ξ. The outlet ratio $R_{H_2/N_2,out}$ can hereby be calculated through the respective outlet molar flows $\dot{n}_{i,out}$ which in turn are calculated using ξ. This furthermore guarantees mass conservation in the resulting surrogate model. The system was modelled using CasADi [11] and optimized using IPOPT [12]. The number of CSTRs in each bed is given by $n = 10$.

B. Application of SOC

As $n_{u,MV} = 3$, three SOC variables have to be calculated. According to Skogestad [3], a self-optimizing control variable has to satisfy among other requirements

1) the optimal value of the controlled variable should be insensitive to disturbances, which is equivalent to the entries in the scaled sensitivity matrix for the respective measurement is small;
2) the gain from the input i to the controlled variable c_i should be large. This corresponds to a flat optimum with respect to c_i;
3) the controlled variables $\mathbf{c}$ should not be closely related;

The chosen measurements are give by a local analysis for each reactor bed to reduce the correlation in-between the measurements. This does not imply that the measurements and their combination are as well optimal considering the overall process. The MIQP approach as proposed by Yelchuru and Skogestad [8] is applied hence individually for each bed resulting in a block diagonal matrix given by

$$\mathbf{H} = \begin{bmatrix} \mathbf{H}_1 & 0 & 0 \\ 0 & \mathbf{H}_2 & 0 \\ 0 & 0 & \mathbf{H}_2 \end{bmatrix} \qquad (22)$$

In order to have a small number of measurements, $n_{y,sel} = 1$ and $n_{y,sel} = 2$ are used and compared to the intuitive control structure, where the input and output temperatures of the respective beds are used. The investigated measurements for the MIQP approach are given by

$$\begin{aligned}
\mathbf{y}_1 &= \begin{bmatrix} T_{in,1} & \mathbf{T}_{1:10}^{\mathsf{T}} \end{bmatrix}^{\mathsf{T}} && \text{for Bed 1, } u_1 \\
\mathbf{y}_2 &= \begin{bmatrix} T_{in,2} & \mathbf{T}_{11:20}^{\mathsf{T}} \end{bmatrix}^{\mathsf{T}} && \text{for Bed 2, } u_2 \\
\mathbf{y}_3 &= \begin{bmatrix} T_{in,3} & \mathbf{T}_{21:30}^{\mathsf{T}} \end{bmatrix}^{\mathsf{T}} && \text{for Bed 3, } u_3
\end{aligned} \qquad (23)$$

The scaling matrix $\mathbf{W}_d$ according to Eq. (10) and Table I is given by

$$\mathbf{W}_d = \text{diag}\left(\begin{bmatrix} 10.5 & 15 & 15 & 1 & 0.2 \end{bmatrix}\right) \qquad (24)$$
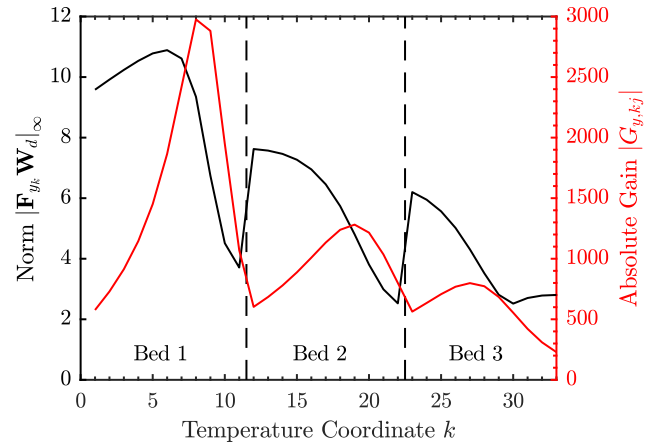

Fig. 2. Infinity norm for the row k of the scaled sensitivity matrix $\mathbf{FW}_d$ and gain $G_{y,kj}$ as a function of the measurement $y_{comb,k}$ in the system and input u_j.

whereas the parameter k_{exp} in the calculation of $\mathbf{W}_{n^y}$ is given by $k_{exp} = 3$.

Based on the requirements for SOC variables, it may be interesting to look at the sensitivity of single measurements with respect to disturbances as well as the gain. The infinity norm of the rows in the scaled sensitivity matrix $\left|\mathbf{FW}_d\right|_{\infty}$ as well as the gain $G_{y,jk}$ of each temperature k with respect to the corresponding input u_j are given in Figure 2. The temperature coordinate k is given by entry k in the vector $\mathbf{y}_{comb} = \begin{bmatrix} \mathbf{y}_1^{\mathsf{T}} & \mathbf{y}_2^{\mathsf{T}} & \mathbf{y}_3^{\mathsf{T}} \end{bmatrix}^{\mathsf{T}}$. The application of the infinity norm instead of the l_1 or l_2 norm can be reasoned by the fact, that we are interested in the worst case scenario. From this Figure, it would make sense to use as a single measurement a temperature close to the end of each bed. This would correspond to a maximized gain and minimized scaled sensitivity matrix and is indeed the solution of the optimization problem (14) with $n_{y,sel} = 1$

$$H_{QP_1,1} = T_9 \qquad H_{QP_1,2} = T_{18} \qquad H_{QP_1,3} = T_{25} \qquad (25)$$

with $m = 100$ in the big-m approach of Eq. (16). The solution to the optimization problem (14) with $n_{y,sel} = 2$ is given in Table II and unfortunately cannot be explained by Figure 2. Similar to the results reported by Yelchuru and Skogestad [8], the chosen measurements change depending on the chosen number of measurements $n_{y,sel}$.

C. Fitting of the Surrogate Model

The surrogate models are cubic B-splines fitted through the application of the SPLINTER library [13] which requires a regular grid. The regular grid is given by four points for each of the varied variable $\mathbf{d}$ resulting in $n_p = 1024$ sampling points. The advantage of using B-splines of order two or higher is given by the continuity of the first derivative of the surrogate model. This gives advantages for the subsequent optimization in which the surrogate model should be used. If self-optimizing control is not used for variable reduction,

		Chosen Variables	Selection Matrix
MIQP	$\mathbf{H}_{QP_2,1}$	T_4, T_6	$[0.952 \quad -1.000]$
	$\mathbf{H}_{QP_2,2}$	$T_{in,2}$, T_{11}	$[0.982 \quad -1.000]$
	$\mathbf{H}_{QP_2,3}$	T_{28}, T_{30}	$[1.000 \quad -0.994]$
In-Out	$\mathbf{H}_{IO,1}$	$T_{in,1}$, T_{10}	$[0.067 \quad -1.000]$
	$\mathbf{H}_{IO,2}$	$T_{in,2}$, T_{20}	$[0.098 \quad 1.000]$
	$\mathbf{H}_{IO,3}$	$T_{in,3}$, T_{30}	$[1.000 \quad 0.721]$

this would correspond to $4^8 = 65536$ sampling points. Alternatively, other surrogate model structures like Kriging [14] or the Alamo approach [15] could be used.

D. Results

The resulting surrogate models for the outlet temperature T_{out} and ξ were evaluated using 5000 randomly sampled validation points. These validation points are the optimal response surface for this model. This implies, that the surrogate model may theoretically give perfect fit for self-optimizing control model structure and it would not be seen in the results. However, this is only of minor interest as the aim of the surrogate model is to utilize it in further optimization. The relative error ε for the dependent variable is subsequently calculated with the optimal response surface. In order to compare the different methods, the maximum absolute relative error $\max |\varepsilon|$ and the mean absolute relative error $\overline{|\varepsilon|}$ are calculated. The results of the three different combination matrices can be found in Table III. Based on the presented results, we can see that arbitrarily chosen measurements do not necessarily result in a good surrogate model fit. Through application of the MIQP approach in selecting the optimal measurement variables, it is possible to reduce the maximum and mean error with respect to the optimal response surface by more than a factor of two for both the outlet temperature and the extent of reaction. Increasing the number of measurements in the MIQP approach to 2 results in a decrease of one order of magnitude with respect to 1 measurement.

Varying the inlet variables and the manipulated variables as an alternative to utilizing self-optimizing control is for this case study not advisable. This leads in the case of all inlet variables being at their lower bound (see Table I) and the manipulated variables at their nominal optimum to reactor extinction. Contrary, if all inlet and manipulated variables are at their nominal value, the reactor is at its optimum. Hence,

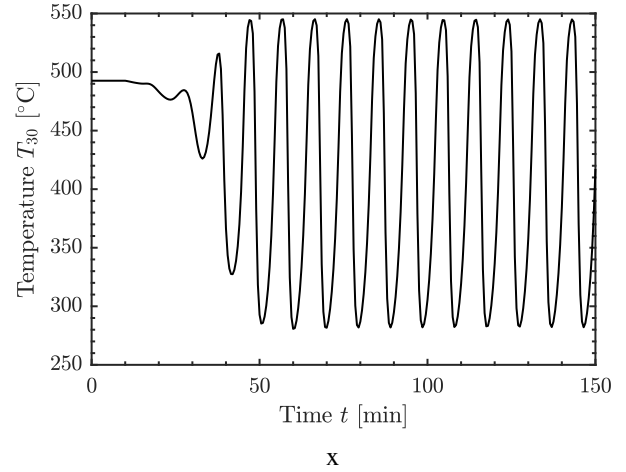| $\mathbf{H}$ definition	Extent of Reaction ξ		Outlet Temperature T_{out}	
	$\max |\varepsilon|$	$\overline{|\varepsilon|}$	$\max |\varepsilon|$	$\overline{|\varepsilon|}$
In-Out	0.540 %	0.092 %	0.232 %	0.041 %
MIQP$_1$	0.211 %	0.027 %	0.095 %	0.012 %
MIQP$_2$	0.022 %	0.003 %	0.009 %	0.001 %

Fig. 3. Outlet temperature of Bed 3 with a pressure drop of $\Delta p_{in} = -15$ bar at $t = 10$ min with a constant input $\mathbf{u}$ at the optimal point.

including the split ratios in the independent variable space would require the mapping of regions in which the reactor is extinct as well as crossing the limit-cycle region in which no upper steady-state solution exists. This region is exemplified in Figure 3 where the inlet pressure is at its lower bound and the other disturbances at their nominal value. We can directly see, that the system is in limit-cycle behaviour and it is not possible to define a steady-state value for this operating point. These regions are not important for the subsequent optimization, and hence, should not be sampled.

V. DISCUSSION

The proposed utilization self-optimizing control to map the optimal response surface can be a promising new method in the generation of surrogate models. The main advantages are given by

1) a reduced number of sampling points compared to sampling the total number of independent variables;
2) a response surface which is close to the optimal response surface with a reduced number of optimization problems to be solved;

The reduced number of sampling points is directly visible through the definition of setpoints of controlled variables. The latter allows as well to sample only regions which we are interested in and neglect regions, which will not be approached in the practical application. In the proposed case study, it is in fact not possible to use the splitratios as independent variables and a variable transformation would be required independently of the application of self-optimizing control. This is similar to the variable transformation utilizing the existing control structure as proposed by Straus and Skogestad [1]. An alternative can be seen in sampling the optimal response surface which is limited by the computational demand of this approach; it would require the solution to n_p nonlinear problems whereas in the application of the proposes method, only $n_d + 1$ have to be solved in the calculation of the optimal sensitivity matrix $\mathbf{F}$.

If it is necessary to have surrogate models for other variables, it is possible to calculate them as well, *e.g.* for the actual split ratios **u** or for additional potential measurements.

However, certain limitations can be identified and need to be addressed as well:

Number of Manipulated Variables

The number of manipulated variables is important in considering the applicability of the approach. If $n_{u,MV} = 1$, the reduction in sampling points can be negligible in cases where other sampling methods than regular grid sampling are used. Hence, there may not be a clear advantage in applying self-optimizing control for variable reduction. However, the simpler response surface through application of self-optimizing control may still hold. If $n_{u,MV} > 1$, measurement selection may result in problems associated with the non-convexity of the MIQP approach if structural zeros are defined in the selection matrix. The approach of treating each input independently can work and give good results as it is the case for the presented ammonia reactor. It is also advantageous to use a structured selection matrix **H** if one is using a sequential-modular flowsheet software. Here, the manipulated variables are adjusted iteratively, and hence, it is beneficial if there is a reduced coupling between the SOC variables **c**. However, it cannot be generalized for all problems, if the application of a structured selection matrix improves the performance. Furthermore, it cannot be said how the solution to a non-convex optimization problem (14) for a structured selection matrix would differ to the one calculated through treating the reactor beds independently.

Application in Flowsheeting Software

One may argue that the application in flowsheeting software is difficult, mostly due to the iterative procedure in which variables are adjusted in sequential-modular software. This can be especially problematic in the investigated case study, where each change in one of the manipulated variables affects the value of all controlled variables directly. As a result, the calculation time for each sampled point is higher than in the case of not applying the proposed method. This can be negated, if the measurement variables are localized close to the respective manipulated variable. As a results, a structured selection matrix **H** will be calculated. The problem is however less pronounced in equation-orientated flowsheeting solver. There, the application of surrogate model-based optimization results in smaller models, and hence, a simpler initialization of the models. Then, the only change is an increase in the number of nonlinear equality constraints and potentially a slightly more complex system of equations.

VI. CONCLUSION

Combining principles from control and surrogate modelling, a new method was derived to reduce the number of independent variables of surrogate models. In addition, the corresponding response surface may be simpler. This is caused by omitting regions in which the submodel is for example

in reactor extinction. Furthermore, the method is independent of the structure of the surrogate model. Hence, it is possible to combine it with other approaches in the literature for the calculation of surrogate models.

VII. ACKNOWLEDGMENT

REFERENCES

[1] J. Straus and S. Skogestad, "Minimizing the complexity of surrogate models for optimization," in *26th European Symposium on Computer Aided Process Engineering*, ser. Computer Aided Chemical Engineering, Z. Kravanja and M. Bogataj, Eds. Elsevier, 2016, vol. 38, pp. 289 – 294.

[2] J. Straus and S. Skogestad, "Variable reduction for surrogate modelling," in *Proceedings of Foundations of Computer-Aided Process Operations 2017, Tucson, AZ, USA*, Jan 2017.

[3] S. Skogestad, "Plantwide control: the search for the self-optimizing control structure," *Journal of Process Control*, vol. 10, no. 5, pp. 487 – 507, 2000.

[4] I. J. Halvorsen, S. Skogestad, J. C. Morud, and V. Alstad, "Optimal selection of controlled variables," *Industrial & Engineering Chemistry Research*, vol. 42, no. 14, pp. 3273–3284, 2003.

[5] J. Jäschke, Y. Cao, and V. Kariwala, "Self-optimizing control a survey," *Annual Reviews in Control*, vol. 43, no. Supplement C, pp. 199 – 223, 2017.

[6] V. Alstad and S. Skogestad, "Null space method for selecting optimal measurement combinations as controlled variables," *Industrial & engineering chemistry research*, vol. 46, no. 3, pp. 846–853, 2007.

[7] V. Alstad, S. Skogestad, and E. S. Hori, "Optimal measurement combinations as controlled variables," *Journal of Process Control*, vol. 19, no. 1, pp. 138 – 148, 2009.

[8] R. Yelchuru and S. Skogestad, "Convex formulations for optimal selection of controlled variables and measurements using mixed integer quadratic programming," *Journal of Process Control*, vol. 22, no. 6, pp. 995 – 1007, 2012.

[9] J. C. Morud and S. Skogestad, "Analysis of instability in an industrial ammonia reactor," *AIChE Journal*, vol. 44, no. 4, pp. 888–895, 1998.

[10] J. Straus and S. Skogestad, "Economic NMPC for heat-integrated chemical reactors," in *2017 21st International Conference on Process Control (PC)*, June 2017, pp. 309–314.

[11] J. Andersson, "A General-Purpose Software Framework for Dynamic Optimization," PhD thesis, Arenberg Doctoral School, KU Leuven, Department of Electrical Engineering (ESAT/SCD) and Optimization in Engineering Center, Kasteelpark Arenberg 10, 3001-Heverlee, Belgium, October 2013.

[12] A. Wächter and L. T. Biegler, "On the implementation of an interior-point filter line-search algorithm for large-scale nonlinear programming," *Mathematical Programming*, vol. 106, no. 1, pp. 25–57, 2006.

[13] B. Grimstad *et al.*, "SPLINTER: a library for multivariate function approximation with splines," http://github.com/bgrimstad/splinter, 2015, accessed: 2017-11-26.

[14] J. A. Caballero and I. E. Grossmann, "An algorithm for the use of surrogate models in modular flowsheet optimization," *AIChE Journal*, vol. 54, no. 10, pp. 2633–2650, 2008.

[15] A. Cozad, N. V. Sahinidis, and D. C. Miller, "Learning surrogate models for simulation-based optimization," *AIChE Journal*, vol. 60, no. 6, pp. 2211–2227, 2014.

Scale-up Modeling of a Pharmaceutical Crystallization Process via Compartmentalization Approach

Merve Öner[1], Getachew S. Molla[1], Michael F. Freitag[2], Stuart M. Stocks[2], Jens Abildskov[1], Gürkan Sin[1]

[1] Process and Systems Engineering Center (PROSYS), Department of Chemical and Biochemical Engineering, Technical University of Denmark, Building 229, 2800 Kgs. Lyngby, Denmark
[2] LEO Pharma A/S, Industriparken 55, 2750 Ballerup, Denmark

Abstract

Crystallization is a prevalently applied technique in many industries including food, bulk and fine chemicals as well as manufacturing of active pharmaceutical ingredients (APIs). In the pharmaceutical industry, crystallization processes are employed mainly for separation, purification as well as for formulation of APIs. Moreover, the process should guarantee that the performance of the delivered APIs is suitable for downstream processing, handling and drug efficacy. The performance of an API crystal is strongly affected by the product quality attributes such as crystal size distribution, morphology, shape and purity, which are the main targets of the process output to be achieved within specific range. Prediction of the influence of the crystallizer scale on the process behavior and process performance is one of the major challenges in the design of industrial crystallization processes. Fluid dynamic conditions of industrial scale crystallizers are far from well-mixed behavior. This leads to spatial variations of critical process variables such as temperature, super-saturation, particle concentration within crystallizer geometry. Consequently, crystallization process models based on the assumption of well-mixed behavior are not representative for a scaled-up process, and therefore not credible for the use in supporting optimal design and control of industrial crystallizers. Therefore, a more detailed insight into mixing conditions and its consequences for local crystallization phenomena – such as a spatially distributed parameter model - must be taken into account in order to achieve reliable process design, scale-up and process control.

The main objective of this work is to develop a predictive scale-up model of a pharmaceutical crystallization process based on compartmentalization approach. Compartmental modeling is a trade-off approach to overcome the limitations of well-mixed models, by considering local mixing, heat transfer and fluid dynamics separately from crystallization kinetics within a crystallizer in comparison with fully developed computational fluidic dynamics (CFD) models. Application of compartmental modeling requires the division of the crystallizer into a finite number of compartmental volumes. Minimized or negligible gradients in *e.g.* temperature, crystal distribution, super-saturation and energy dissipation should exist within individual compartmental volumes. To determine the compartmental zones within the volume of industrial-scale crystallizer equipment, primarily the fluid dynamics, mixing and heat transfer are studied by means of CFD simulations. The compartmental volumes, location and flux connections are extracted from CFD data analysis to define the interconnected compartment network. The crystallization process modeling based on compartmentalization approach is implemented in MATLAB/Simulink. The same set of model equations and model parameters are defined in order to solve the conservation balance equations for crystallization process system (population, mass, etc.) for every compartment. However, spatial variations in the crystallizer modelled by different profiles/gradients result in different rates of crystallization kinetics (nucleation, growth, dissolution, etc.) between the individual compartments, which represents the deviation from the ideal case.

The process behavior of the pharmaceutical batch cooling is analyzed with respect to crystallizer scale, process variables and operation conditions. The multi-compartment model is compared with a single-compartment well-mixed model to examine the influence of the non-uniformly distribution of the related process variables on process performance in terms of crystal size distribution.

Acknowledgment

Nonsmooth modelling methods in chemical engineering

Marius Reed, Marlene Lund and Johannes Jäschke

Department of Chemical Engineering
Norwegian University of Science and Technology (NTNU)
Trondheim, Norway

In this work, we present a set of nonsmooth modelling methods for use in chemical engineering problems. Further, a case study on modelling of a steady-state oil and gas production network is given to illustrate how nonsmooth equations allow for different directions of flow through the system.

Nonsmooth formulations such as min, max and absolute values are not widely used in modelling, because it is difficult to obtain derivatives and sensitivities in the nonsmooth points of these functions. Instead, it is common to apply hybrid models where logic is applied to switch between different modes in the model, or to make smooth approximations of the nonsmooth functions. In general, using nonsmooth equations in models relies on the ability to compute derivative-like elements that can act as derivative information in equation solvers for nonsmooth equations. For instance, the LP-Newton method presented by Facchinei et. al [1] has convergence properties comparable to Newton methods for smooth equations, if provided an element of the B-subdifferential. Such elements are not possible to compute automatically, because calculus rules, such as the chain rule, hold only as inclusions for the B-subdifferential. However, new developments within nonsmooth analysis by Khan and Barton facilitate for automatic differentiation of nonsmooth model equations [2]. Khan and Barton proved that the lexicographic derivative is a subset of the B-subdifferential for piecewise differentiable functions, and that these derivative elements obey strict calculus rules.

The oil and gas production network illustrated in Figure 1 has been modelled using nonsmooth formulations. These are applied to describe the direction of flow through the manifolds depending on the wellhead pressure of the three wells, as well as the routing of flow into available paths in terms of open valves. Traditionally, varying flow directions are dealt with using hybrid models combined with logic expressions in the implementation. However, such solutions break down if the driving force in pressure is zero over a pipe segment, for instance in the case where several wells have the same wellhead pressure. Using an absolute value formulation of the valve equation opens for changes in the flow direction, dependent on the pressures in the different parts of the system. In addition, the process of mixing streams in the manifolds can be modelled using min and max functions to describe that each flow can both enter and leave the manifold. Unlike for the hybrid case, derivatives can also be obtained in the case where the flow is zero.

Figure 1: Oil and gas production network.
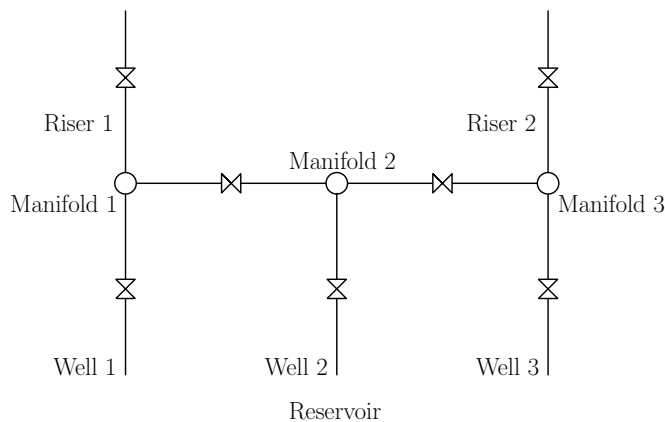
References

[1] Francisco Facchinei, Andreas Fischer, and Markus Herrich. An LP-Newton method: Nonsmooth equations, KKT systems, and nonisolated solutions. *Math. Program.*, 146(1-2):1–36, 2014.

[2] Kamil A. Khan and Paul I. Barton. A vector forward mode of automatic differentiation for generalized derivative evaluation. *Optimization Methods and Software*, 30:1185–1212, 2015.

Title: Neural network-based model reduction and sensitivity analysis of apoptosis

C. Alia Joko, Frank Pettersson & Henrik Saxén

Abstract

Apoptosis or programmed cell death ('cell suicide') is a central mechanism in many biological processes including embryonic development and cancer progression. Several mathematical models of apoptosis have been developed to shed light on the complex interactions associated with this pathway. This paper applies a neural network pruning algorithm to a large dataset from a detailed ODE-based model of apoptosis to infer input-output relations. The pruning algorithm takes advantage of the sparsity of connections in a multilayer perceptron with a single hidden layer to determine only the most important inputs. The method thus provides an approach for complexity reduction, model selection and generation of nonlinear algebraic simplifications as applied to a model of apoptosis. In addition, the method provides a tool for local sensitivity analysis. This analysis gives insights into how the dominant model inputs affect the outputs as well as the robustness of the responses. In the case study where the time to apoptosis was selected as the target output, the model identifies nine key parameters among 55 potential ones. It is also demonstrated that a reduced model with only five parameters can adequately describe the main features of the output. The progress of the pruning method and the performance of the reduced model are presented, demonstrating the effectiveness of the modelling approach.

Keywords: Nonlinear modeling, model reduction, pruning, apoptosis

A dynamic model of the response of food-borne pathogenic bacteria to high pressure processing

Bahareh Nikparvar[1], Nils Nieuwenkamp[2], Nadav Bar[1]*

[1]*Department of Chemical Engineering, Norwegian University of Science and Technology, Trondheim N7491, Norway*

[2]*University of Amsterdam, the Netherlands*

* Corresponding authors
nadi.bar@ntnu.no

Background: Minimally processed and ready-to-eat food is becoming increasingly popular, but it is susceptible to harmful human pathogenic bacteria such as *Listeria monocytogenes (LM).* Current solutions such as thermal treatment can inactivate microorganisms, but they also degrade the taste, texture, and quality of fresh food. High Pressure Processing (HPP) is a promising method with minimal adverse sensory side effects on food quality. However, it has limited success because of rapid recovery of pressure-injured bacteria.

Results: With the aim to understand and control the processes that underlie bacterial recovery after HPP, we developed a mathematical dynamic model. The model explains how high pressure stress damages the bacteria, and how they respond to such stress. It consists of a set of ordinary differential equations that comprise three main intracellular compartments: cell wall, cell membrane, and protein repair compartments. We assume that these are the primary components or processes involved in bacteria damage and response to pressure. Using rate equations and modified Hill functions, we defined the governing key metabolic pathways and transcriptional control that respond to HPP in each compartment. We used databases like STRING, KEGG, and BRENDA to estimate the model parameters. We are currently conducting a set of time-series experiments to gather data on gene expression kinetics in *LM* following HPP to increase the accuracy of the model predictions.

Conclusion: By analyzing the model, we can identify potential repair mechanisms and their weaknesses in bacteria exposed to high pressure. With the final goal of optimizing the processing conditions used in HPP, we can target those mechanisms by genome editing techniques or by natural additives that will control and limit bacterial growth in food. This has a potential to eradicate harmful microorganisms from ready-to-eat food and hereby make it safer.

Keywords: High pressure processing, Foodborne bacteria, Dynamic model.

Input PRBS design for identification of multivariable systems

Winston Garcia-Gabin*, Michael Lundh*

Abstract— **This paper presents a systematic procedure for designing the input signals to identify multivariable processes. The procedure is based on time domain specifications and can be applied to multivariable processes with m-outputs and n-inputs, which can be operating in closed-loop. The design of the input signals, which are pseudo random binary sequences, are based on the old information about the process model and the controller, together with the measures of the input and output variances of the process. The method proposes excitation in the frequency interval where the model needs to be accurate for robust feedback control. The method is illustrated using the Wood & Berry distillation column model, which is a 2-inputs-2-outputs benchmark in process control.**

I. INTRODUCTION

Empirical identification is a well-established methodology to obtain multivariable process models, often intended for control but also for other purposes. The choice of input signals for the identification has a large impact on the quality of the model [1]. However, in most cases input signals cannot be freely chosen with respect to plant performance constraints. There exist a rather extensive literature on optimal experiment design [2-8]. The problem optimal experiment design whose objective is to design the least costly identification experiment while guaranteeing a sufficiently accurate model.

The main contribution of the paper is to provide a methodology oriented to practitioners for facing the problem of input signal design for identification for cases when the current model in an MPC controller needs to be updated. The problem of the experiment design is approached with the idea of producing a procedure for designing the signals for identification of multivariable processes, minimizing the disturbance in the process, but keeping in mind that the methods for controller maintenance tools must be developed for an easy implementation for plant operators. In the proposed methodology for input signal design, first, the required increments of the output variances are defined. Then, the information relate to the process model and the controller is used for calculating the excitation signals. This paper is focused mainly in Pseudo Random Binary Sequence. However, the method provides the variance and bandwidth of the excitation signals, which can be used for characterizing other signals, e.g. multi-sine signals.

The paper is organized as follows. Introduction shows the presentation of the problem faced on the paper. Section II develops the procedure for input PRBS design for identification. A case study using Wood & Berry distillation

*ABB AB, Corporate Research, SE72178, Västerås, Sweden. e-mail: {winston.garcia-gabin, michael.lundh}@se.abb.com.

column model is presented in Section III. Finally the conclusions are summarized in Section IV.

II. INPUT PRBS DESIGN FOR IDENTIFICATION

Closed-loop identification methods requires excitation signals to be applied in the process inputs such that they produce changes in the process outputs. The resulting additional variances in the outputs are subject to a trade-off. They must be big enough to produce persistent excitation for identification, but also to disturb the normal operation of the process as little as possible. In this procedure, the nominal variances of the process outputs are taken as reference for defining the set of increment in the outputs due to the excitation signals. The excitation signals can be applied to closed-loop systems as it is shown in Fig. 1, where, $r(t)$ is the set point, $u_c(t)$ is the controller output, $u_{ex}(t)$ is the excitation signal, $u(t)$ is the manipulated variable, v(t) is the measured noise, $y(t)$ is the measured output. However, the procedure could also be also applied for designing the experiment in open-loop.
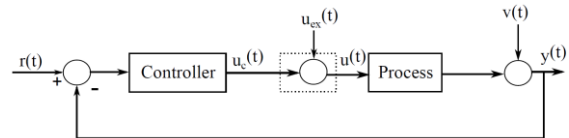

Fig. 1 Closed-loop identification diagram

Pseudo Random Binary Sequences (PRBS) are often used as excitation signals for identification propose, because it has a finite length that can be synthesized repeatedly with simple generators while presenting favorable spectra for identification propose. The spectrum at low frequencies are flat and constant, at high frequencies the spectra drop off, consequently the spectra have a specific bandwidth, which can be utilized for exciting the processes in the required frequencies.

The analytical expression for the power spectrum of a PRBS signal is given by

$$s(\omega) = \frac{A^2(N+1)T_{cl}}{N}\left[\frac{\sin(\omega t_{cl}/2)}{\omega t_{cl}/2}\right]^2 \qquad (1)$$

where A is the signal amplitude, ω is the frequency, t_{cl} is the clock period (i.e. the minimum time between changes in level

of the signal), which must be multiple of the sampling time T_s. The sequence repeats itself after $T = N \cdot t_{cl}$ units of time, where $N = 2n-1$ and n is the number of shift registers used to generate the sequence. For low frequencies, the power spectrum has the approximate value of

$$\frac{A^2(N+1)t_{cl}}{N} \quad (2)$$

At $\omega = 2.8/t_{cl}$ the power spectrum is reduced by half. Therefore, the frequency range $[\omega_{low}, \omega_{high}]$ of a PRBS signal considered to be useful for excitation here is

$$\frac{2\pi}{T} \leq \omega \leq \frac{2.8}{t_{cl}} \quad [\text{Rad/s}] \quad (3)$$

Thus, for designing a PRBS signal is necessary to determine the frequency range and the amplitude A of the signals. Some different approaches for estimation of the frequency range are discussed below.

A. Estimate the range using time domain information

The frequency specification of the PRBS is based on the ideas in [9] and [10]. They can also be used for multi-sine design as can be seen in [11]. Here, we propose the following procedure to estimate the lower frequency of interest:

1. Obtain crude estimates of the time constants and the time delays of the open loop process $(\tau_{ij}^{ol}, td_{ij}^{ol})$ for all m outputs for each n inputs using the process model that is used in the model-based controller.
2. Approximate the settling times for all the input-output pairs: $t_{ij}^{ol} = 4\tau_{ij}^{ol} + td_{ij}^{ol}$
3. Calculate the lower value of frequency as follows

$$\omega_{low} = \frac{1}{S_f \max(t_{ij}^{ol})} \quad [\text{rad/s}] \quad (4)$$

A safety factor $S_f > 1$ is introduced, with the main propose to augment the bandwidth of the excitation signal. It is carried out reducing the lower value and increasing the upper value of the frequency range. Based on simulation tests, $S_f = 1$ is enough to manage changes in the dynamic of the models around 30 % with regard to the initial model. If it is assumed that the actual model changed much more respect to the initial model, it is convenient increase the safety factor. Values in the range 1 to 4 are recommended.

The upper frequency for the range can be estimated either using open loop information or using closed loop information.

When using open loop information, estimate for each input-output pair the highest frequency content using the time constant and the time delay $(\tau_{ij}^{ol}, td_{ij}^{ol})$ as follows

$$\omega_{ij}^{cl} = \frac{\alpha S_f}{\tau_{ij}^{ol}} \text{ where } \alpha = \max\left(\left(-\frac{td_{ij}^{ol}}{\tau_{ij}^{ol}} + 2\right), 0.5\right) \quad (5)$$

The variable factor α, is a measure of how much faster the intended closed-loop speed of response will be relative to open-loop.

Then determine the upper value of frequency for the PRBS as follows

$$\omega_{high} = \max(\omega_{ij}^{cl}) \ [\text{rad/s}] \quad (6)$$

When using closed loop information, first obtain estimates of the settling time without taking into account the time delay for the closed-loop step response for all the outputs: t_i^{cl}. Then determine the upper frequency for the range using

$$\omega_{high} = \frac{4 S_f}{\min(t_i^{cl})} \ [\text{rad/s}] \quad (7)$$

where S_f is the earlier introduced safety factor and the 4 is chosen to be sure to capture the interesting frequencies in the transients.

The upper value of frequency must be lower than the Nyquist frequency thus, $\omega_{high} \leq \omega_N$.

B. Frequency response of the singular values of the closed-loop system

Another method for obtaining the bandwidth of the excitation signal is using the singular values of the output sensitivity function. This is however, only possible when a linear model and controller is available. In this case, the information regarding the controller model and process model is used to calculate the output sensitivity function. Then, the frequency response of the singular values of the output sensitivity function is drawn, as it is shown in Fig. 2.
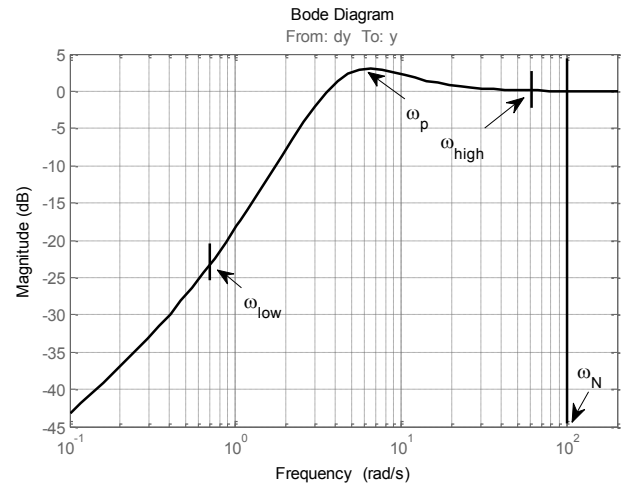

Fig. 2 Frequency response of the singular values

The idea here is to consider an interval around the peak, ω_p in the sensitivity function. The width is determined using the factor β, which in the range (4 to 10). It is selected according

to sharpness of the peak. For A narrow peak a small value of β is adequate, on the other hand, for smoother peak large value is convenient.

The upper value of the frequency range is the minimum value between β times the peak frequency and the geometric mean of peak frequency and Nyquist frequency, as it is shown below

$$\omega_{high} = \min(\beta\omega_p, \sqrt{\omega_p\omega_N}) \ [rad/s]$$

The lower value of frequency is as follows

$$\omega_{low} = \frac{1}{\beta}\omega_p \ [rad/s]$$

The lower value of frequency is of little interest in case of PRBS. However, it is useful for designing multi-sine excitation signals.

C. PRBS clock period and the number of shift registers

The clock period t_{cl} and the number of shift register n_r of the PRBS can now be determined from

$$t_{cl} \leq \frac{2.8}{\omega_{high}} \qquad N = 2^{n_r} - 1 \geq \frac{2\pi}{t_{cl}*\omega_{low}} \qquad (8)$$

D. PRBS amplitudes

Once the frequency ranges of the excitation signals are defined, the amplitudes are yet to be defined. Although several authors define methods to calculate the bandwidth of the excitation signals [1,10]. A systematic procedure is not provided for calculating the amplitude of the excitation signals. Most of the time, literature merely indicates that the amplitudes of the PRBS signals are chosen such that they will generate data with good enough signal-to-noise ratio but will not disturb the product quality. Normally, most of the information needed for determining the amplitudes of PRBS signals can be obtained by interviewing experienced operators and operation engineers [1,9,12].

Below is a systematic way proposed, how to obtain the amplitudes of the excitation signals:

A multi-sine is considered as base signal for developing this procedure. A multi-sine can be described as a weighted sum of sinusoidal signals

$$u_{ex}(t) = \sum_{k=1}^n A_k \sin(\omega_k t + \varphi_k^u) \qquad (9)$$

Where A_k is the amplitude of the k-term of the multi-sine at the frequency ω_k and φ_k^u is its phase. n is the number of terms of the multi-sine.

The signal variance of a multi-sine signal is equal to the signal power with mean removed, when the multi-sine is composed

of a sum of sine terms with different frequencies. Thus, the variance of the multi-sine (9) is

$$\sigma_{u_{ex}}^2 = \sum_{k=1}^n 2\left(\frac{A_k}{2}\right)^2. \qquad (10)$$

Considering that the amplitude A_k of all terms of the multi-sine have constant amplitude A. The variance of the multi-sine (10) is given by

$$\sigma_{u_{ex}}^2 = n\frac{A^2}{2}. \qquad (11).$$

Consider the closed loop system G from the excitation signals to the process outputs as shown in Figure 3.

Fig. 3 Linear model.

The output signal $y(t)$ is

$$y(t) = \sum_{k=1}^n G_k A_k \sin(\omega_k t + \varphi_k^y) \qquad (12)$$

where G_k is the gain of the system at the frequency ω_k and φ_k^y is phase of the output signal.

The output variance can be calculated as the power of the signal as

$$\sigma_y^2 = \sum_{k=1}^n \left(\frac{G_k A_k}{2}\right)^2 2 \ , \ \sigma_y^2 = \sum_{k=1}^n \frac{G_k^2}{2} A^2 \ \text{ for } A_k = A \quad (13)$$

Equation (13) can be rewritten for the multivariable case as

$$\begin{bmatrix} \sigma_{y_1}^2 \\ \vdots \\ \sigma_{y_p}^2 \end{bmatrix} = \frac{1}{2} \begin{bmatrix} \sum_{k=1}^n G_{11_k}^2 & \cdots & \sum_{k=1}^n G_{1q_k}^2 \\ \vdots & \ddots & \vdots \\ \sum_{k=1}^n G_{p1_k}^2 & \cdots & \sum_{k=1}^n G_{pq_k}^2 \end{bmatrix} \begin{bmatrix} A_1^2 \\ \vdots \\ A_q^2 \end{bmatrix}$$

The equation above can be written in compact form as

$$\begin{bmatrix} \lambda_1 \\ \vdots \\ \lambda_p \end{bmatrix} = \frac{1}{2} \begin{bmatrix} \psi_{11} & \cdots & \psi_{1q} \\ \vdots & \ddots & \vdots \\ \psi_{p1} & \cdots & \psi_{pq} \end{bmatrix} \begin{bmatrix} \zeta_1 \\ \vdots \\ \zeta_q \end{bmatrix} \quad \rightarrow \Lambda = \Psi Z \quad (14)$$

where Λ is a vector containing of the variances of the p outputs of the system, Ψ is a matrix where each element has the sum of the square gains of the ij-output-input pair for the sequence of frequencies ω_k, and Z is a vector with the square of the amplitude of multi-sine sequences of the q inputs.

Notice that in the multivariable case each multi-sine excitation signal must have a different frequency distribution sequences $[\omega_1, \omega_2 \dots \omega_k]$. This must be taken into account if

the multivariable system will be excited at the same time in all the inputs with multi-sine signals.

The amplitude of the inputs can be obtained as a solution of the eq. (14). This is finding a minimum of a constrained multivariable function as follows

$$J = \frac{\arg\min}{\zeta} \left(Z(\zeta) \right)^T Z(\zeta) \quad (15)$$

Subject to:

$$-\Psi Z \leq -\Lambda \quad (16)$$

Equation (15) attempts to find a constrained minimum of a scalar function given by the sum of the output powers. The solution is subject to a set of inequalities with the general form (16). This means that the variances of the p-outputs must be higher than a threshold $\Lambda = [\lambda_1 \dots \lambda_p]^T$ defined a priori, as high enough to achieve a persistence of excitation.

Inequality sets with the form

$$-\Psi \begin{bmatrix} I_1 & 0 & 0 \\ 0 & \ddots & 0 \\ 0 & 0 & I_q \end{bmatrix} Z \leq -\Lambda \quad (17)$$

can be added to guarantee that each input produces enough persistence of excitation in all the outputs. For each input i where this is required there will one constraint of the type in (17) with $I_i = 1$ and $I_j = 0 \; \forall \; j \neq i$.

Once $Z = [\zeta_1 \dots \zeta_q]^T$ is obtained as solution of (15). The amplitude A_i of the multi-sine inputs can be calculated as follows

$$A_i = \sqrt{\zeta_i}. \quad (18)$$

Finally, the variance of the excitation signals are

$$\sigma_{u_{ex_i}}^2 = n \frac{\zeta_i}{2} = n \frac{A_i^2}{2} \quad (19)$$

Thus, the input design is characterized by the variance of the excitation signals (19) and their frequency ranges. These input signals can be applied to the process as multi-sine signals or other excitation signals, for example a PRBS, which must have the variance obtained in (19). In the last case, the PRBS amplitude must switch between two levels $\pm A_{PRBS}$, this value is defined as the square root of the variance, as is shown below

$$A_{PRBS_i} = \sqrt{\sigma_{u_{ex_i}}^2} \quad (20)$$

In a case when excitation signals are applied at the same time in a multivariable process, it is important to have a low cross-correlation between the excitation signals. This can be accomplished by different initializations of the shift register

of the PRBS. This is equivalent to apply a delayed single PRBS signal in each excitation input [1,13].

III. CASE STUDY

The Wood & Berry distillation column was considered as 2-inputs-2-outputs process model for testing the procedure. The distillation column model in [14] is given by

$$G(s) = \begin{bmatrix} \frac{12.8}{16.7s+1} e^{-s} & \frac{-18.9}{21s+1} e^{-3s} \\ \frac{6.6}{10.9s+1} e^{-7s} & \frac{-19.4}{14.4s+1} e^{-3s} \end{bmatrix} \quad (21)$$

The process was controlled with a discrete time MPC (Matlab toolbox) with sampling interval $T_s = 1$ and a white noise with a variance of 0.1 was added at each output. Figure 4 shows the frequency response of the process in open loop (blue) and the output sensitivity function (red).
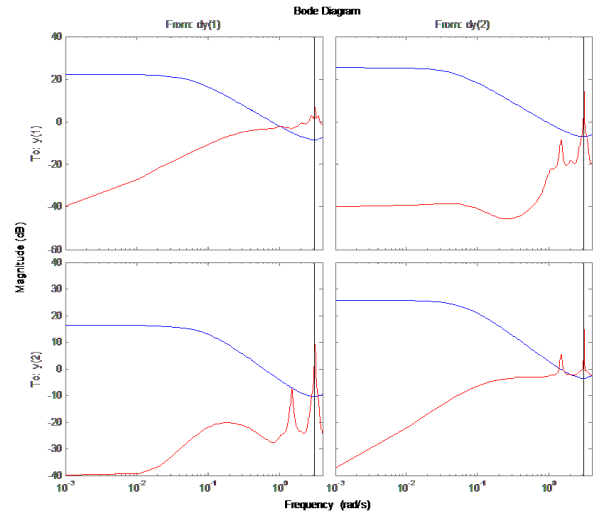

Figure 4. Frequency response of process (blue), output sensitivity function (red).

Table 1 shows the variance of the outputs in closed loop before applying the identification signals.

Table 1 Variances in the outputs and inputs in closed loop

	CV1	CV2	MV1	MV2
σ^2	0.131	0.123	0.057	0.027

Based on these output variances in closed-loop were defined as $\sigma_y^2 = 0.2$, the increment in the output variances required for the identification proposes.

A. Frequency specifications

The procedures in section II-A, were used to determine the frequency range. The time constants and the time delays for the open loop process were obtained directly from (21) here. Estimates of the closed loop rise time was obtained from simulations. The results are summarized in Table 2.

Table 2 Frequency range obtained

	ω_{low} [rad/s]	ω_{high} [rad/s]
Open- loop	0.01	0.125
Closed-loop	--	0.182

The upper frequency that will be used below is obtained using the closed-loop information (0.182 rad/s). However, the approximated upper frequency calculated using the open loop information is reasonable good compared with the closed-loop value.

B. Amplitude specifications

The procedure in section II-D, was used to determine the excitation signal amplitude. Here we used a multi-sine signal with 10 frequencies logarithmically spread from $\omega_{low} = 0.01$ to $\omega_{high} = 0.182$. The excitation was required to generate an additional output variance of $\sigma_{y1}^2 = 0.2$ and $\sigma_{y2}^2 = 0.2$. The optimization problem in (15) - (17) then gave the variances for the excitation signals $\sigma_{uex1}^2 = 0.095$ and $\sigma_{uex2}^2 = 0.055$.

C. Simulation Results

Table 3 shows the increments in the output variances when the excitation signals are applied on the closed loop simulated process. The first row shows the expected theoretical value. The second row shows the incremental variance in the outputs obtained in the simulation using a multi-sine as excitation signals. Finally, the third row shows the incremental variance when the PRBS signal is applied.

Table 3. Obtained additional variances

	$u_{ex1} \neq 0$, $u_{ex2} = 0$	$u_{ex1} = 0$, $u_{ex2} \neq 0$	$u_{ex1} \neq 0$, $u_{ex2} \neq 0$
Theoretical variance	$\sigma_{y1}^2 = 0.20$ $\sigma_{y2}^2 = 0.206$	$\sigma_{y1}^2 = 0.20$ $\sigma_{y2}^2 = 0.693$	$\sigma_{y1}^2 = 0.40$ $\sigma_{y2}^2 = 0.900$
Multi-sine	$\sigma_{y1}^2 = 0.206$ $\sigma_{y2}^2 = 0.20$ $\sigma_{MV1}^2 = 0.009$ $\sigma_{MV2}^2 = 0.001$	$\sigma_{y1}^2 = 0.204$ $\sigma_{y2}^2 = 0.845$ $\sigma_{MV1}^2 = 0.004$ $\sigma_{MV2}^2 = 0.010$	$\sigma_{y1}^2 = 0.435$ $\sigma_{y2}^2 = 1.174$ $\sigma_{MV1}^2 = 0.016$ $\sigma_{MV2}^2 = 0.028$
PRBS	$\sigma_{y1}^2 = 0.266$ $\sigma_{y2}^2 = 0.241$ $\sigma_{MV1}^2 = 0.034$ $\sigma_{MV2}^2 = 0.002$	$\sigma_{y1}^2 = 0.239$ $\sigma_{y2}^2 = 1.056$ $\sigma_{MV1}^2 = 0.008$ $\sigma_{MV2}^2 = 0.0279$	$\sigma_{y1}^2 = 0.450$ $\sigma_{y2}^2 = 1.152$ $\sigma_{MV1}^2 = 0.043$ $\sigma_{MV2}^2 = 0.027$

It can be observed in Table 3, that each output variance pass the threshold defined initially $\sigma_y^2 = 0.2$. This is because that was defined as constraint in the optimization process (15)-(17). It can also be noticed that simultaneous excitation in both inputs increases the output variance more than needed.

The generated signals have been tested for excitation in closed loop. The process inputs and outputs were used for identification using Matlab's System Identification toolbox which provided, as expected, an accurate model.

IV. CONCLUSION

This paper proposed a simple approach to determine how a multivariable model can be excited during an experiment to update the controller model. The method relies on that there exists some, no longer ideal, model for control of the process. The method is oriented for practitioners and operators using basic concepts. Also, it can be easily coded in the control system.

The method proposes a frequency range and variances of the excitation signals. This information was used in the example for designing PRBS signals, however, other signals like multi-sine functions can also be calculated. Further, this method can be straightforward applied to non-square multivariable systems. The mathematical support of the method is not limited for square systems.

REFERENCES

[1] Rivera, D. E., & Jun, K. S. (2000). An integrated identification and control design methodology for multivariable process system applications. Control Systems, IEEE, 20(3), 25-37.
[2] F. Pukelsheim, Optimal design of experiments. John Wiley, 1993.
[3] A. Atkinson and A. Doner, Optimum experiment design. Oxford: Clarendon Press, 1992.
[4] G. Goodwin and R. Payne, Dynamic System Identification: Experiment Experiment Design and Data Analysis. New York: Academic Press, 1977.
[5] T. S. Ng, G. C. Goodwin, and T. Söderström, "Optimal experiment design for linear systems with input-output constraints," Automatica, vol. 13, pp. 571–577, 1977.
[6] R. K. Mehra, "Optimal input signals for parameter estimation in dynamic systems–survey and new results," IEEE Transactions on Automatic Control, vol. AC-19, pp. 753–768, 1974.
[7] H. Hjalmarsson, "From experiment design to closed loop control," Automatica, vol. 41, no. 3, pp. 393–438, March 2005.
[8] Bombois, X., & Scorletti, G. (2012). Design of least costly identification experiments: The main philosophy accompanied by illustrative examples. Journal Européen des Systèmes Automatisés, 46(6-7), 587-610.
[9] Gaikwad, S. V., & Rivera, D. E. (1996). Control-relevant input signal design for multivariable system identification: Application to high-purity distillation. InProc. IFAC World Congress, San Francisco (Vol. 1000, pp. 349-354).
[10] Lee, H. (2006). A plant-friendly multivariable system identification framework based on identification test monitoring (Doctoral dissertation, Arizona State University).
[11] Lee, H., Rivera, D. E., & Mittelmann, H. D. (2003). Constrained Minimum Crest Factor Multisine Signals for" Plant-Friendly" Identification of Highly Interactive Systems. In In: 13th IFAC Symp. on System Identification. Rotterdam.
[12] Zhu, Y. (1998). Multivariable process identification for MPC: the asymptotic method and its applications. Journal of Process Control, 8(2), 101-115.
[13] Yao, L., Zhao, J., & Qian, J. (2006). An improved pseudo-random binary sequence design for multivariable system identification (A16-395). In Intelligent Control and Automation, 2006. WCICA 2006. The Sixth World Congress on (Vol. 1, pp. 1768-1772). IEEE.
[14] Luyben, W. L. (1992). Practical distillation control (pp. 72-84). New York: Van Nostrand Reinhold.

Experiment Designs to Obtain Uncorrelated Outputs in MIMO System Identification

Kurt-Erik Häggblom

Faculty of Science and Engineering, Åbo Akademi University, FI-20500 Åbo (Turku), Finland

A problem in open-loop identification of multiple-input multiple-output (MIMO) systems is that standard designs using uncorrelated inputs [1, 2] tend to produce correlated outputs. If the system is ill-conditioned, this correlation may be very strong. Such a correlation reduces identifiability and may even result in a model with different controllability properties than the true system.

To tackle this problem, a design method based on an estimate of the steady-state gain matrix was proposed in [3]. The idea was to explicitly excite all gain directions of the system. An overview of various aspects of the design procedure is given in [4]. Because of dynamics, the excitation goal is not necessarily achieved, however. This has motivated experiment designs, where (estimated) dynamics are explicitly considered [5, 6, 7].

A result of the above design methods, which require complicated optimizations, is nearly uncorrelated outputs. In [8], a design procedure that directly addresses the output distribution was proposed. The aim is to produce uncorrelated outputs to maximize identifiability. This is achieved by designing inputs that maximize the minimum singular value, or the determinant, of the covariance matrix of the output data with suitable constraints. The problem is formulated as a convex optimization with linear matrix inequalities (LMIs) as constraints. The user can select the type of input perturbation, e.g., random binary signal (RBS), pseudo-random binary sequence (PRBS), or multi-sinusoidal signal.

In [8], an approximate covariance model obtained from a discrete-time state-space model was used as a linear constraint in an iterative optimization. Here, two other formulations are presented: one that uses the state-space model directly, which results in a more complicated optimization problem with a bilinear constraint; one that further simplifies the covariance model to a relationship between input and output covariances (i.e., state variables are not considered), which results in a simpler iterative optimization problem. It is shown that the simplest formulation can handle the experiment design of many examples previously used in identification studies. However, there are also examples that require the approximate covariance model presented in [8], or even the full state-space formulation presented here.

[1] L. Ljung, *System Identification: Theory for the User*. Prentice Hall: Upper Saddle River, NJ, 1999.

[2] R. Isermann and M. Münchhof, *Identification of Dynamic Systems*. Springer: Berlin and Heidelberg, 2011.

[3] C.-W. Koung and J.F. MacGregor, "Design of identification experiments for robust control. A geometric approach for bivariate processes." *Ind. Eng. Chem. Res.*, vol. 32, pp. 1658–1666, Aug. 1993.

[4] K.E. Häggblom, "On experiment design for identification of ill-conditioned systems," in *Proc. 19th IFAC World Congress*, Cape Town, South Africa, pp. 1428–1433, Aug. 2014.

[5] D.E. Rivera, H. Lee, H.D. Mittelmann, and M.W. Braun, "High-purity distillation: using plant-friendly multisine signals to identify a strongly interactive process," *IEEE Control Syst. Mag.*, vol. 27, pp. 72–89, Oct. 2007.

[6] M.L. Darby and M. Nikolaou, "Identification test design for multivariable model-based control: An industrial perspective," *Control Eng. Pract.*, vol. 22, pp. 165–180, Jan. 2014.

[7] A. Kumar and S. Narasimhan, "Optimal input signal design for identification of interactive and ill-conditioned systems," *Ind. Eng. Chem. Res.*, vol. 55, pp. 4000–4010, March 2016.

[8] K.E. Häggblom, "A new optimization-based approach to experiment design for dynamic MIMO identification," in *Proc. 20th IFAC World Congress*, Toulouse, France, pp. 7582–7587, July 2017.

Data-based Testing for Nonlinearity in Dynamical Systems: Surrogate Data Compared with Nonlinear Distortion

Matias Waller

Department of Electrical Engineering,
Åland University of Applied Sciences,
Mariehamn, Åland, Finland
e-mail: matias.waller@ha.ax.

December 19, 2017

1 Introduction

The task of finding "effective data-based nonlinearity tests for dynamical systems" is recognized as a key challenge within the field of system identification Ljung [2010]. Indeed, such tests have great practical value, since nonlinear empirical modeling requires the user to choose regressors, i.e., inputs, outputs, prediction errors, etc., and the orders and delays for each regressor, in addition to a computationally demanding nonlinear optimization by, e.g., training an artificial neural network to fit the data. Finally, once a model has been developed, a data-based nonlinearity test is still needed to determine whether or not the nonlinear aspects of interest are captured by the model.

In this presentation, testing for nonlinearity in data from dynamical systems addresses the following question: Is there evidence in the data that motivates the use of nonlinear dynamical models? Applied to model validation by residual analysis, the question becomes: Is there evidence in the residuals for nonlinear predictability?

These questions are addressed by presenting two approaches that can be used for data-based detecting of nonlinearity within system identification.

1. Estimating nonlinear distortion in the frequency domain, see, e.g., Pintelon and Schoukens [2012] or Schoukens et al. [2016] for a recent survey.

2. Using Fourier-based surrogate data (FSD), developed in a recent article Waller [2017].

In the recent article, extensive simulations are used to show how Fourier based surrogate data, with modest computational efforts, can be applied to an array of

1

nonlinear systems and how it can detect some nonlinearities that the nonlinear distortion approach cannot. Some of these results are presented here. In addition, the article Waller [2017] reviewed the use of nonlinear correlation functions, see, e.g., Billings [2013], and concluded that the use of nonlinear correlations is not a reliable alternative for data-based detection of nonlinearity.

2 Surrogate data

Surrogate data is, on a very general level, data that shares some specific (but not all) properties with the original data, such as mean, variance and power spectrum. Different statistics can then be calculated for the original and the surrogate data and can possibly be used to distinguish features specific to the original data. The concept has been developed and established within the frame of nonlinear time series analysis Theiler et al. [1992], Schreiber and Schmitz [2000], Small et al. [2001], Kantz and Schreiber [2004], Kugiumtzis [2008], where surrogate data is typically used for testing for nonlinearity in the presence of noise and where determinism might be weak. Since such conditions often occur in system identification, surrogate data seems suited for use in nonlinear identification. Although some publications within the field of identification and control use surrogate data for discriminating between stochastic characteristics and nonlinear dynamics Coca et al. [2000], Barnard et al. [2001], Waller and Saxén [2003], Jemwa and Aldrich [2006], Choudhury et al. [2008], surrogate data is still rarely used in nonlinear system identification. Thus, surrogate data is not mentioned in books on (nonlinear) system identification (e.g., Nelles [2001], Isermann and Münchhof [2011]). One possible explanation for this is that even the articles mentioned discuss the time series case, i.e., there is no (manipulatable) control signal. An appropriate framework for using surrogate data within system identification is briefly summarized in this Section.

2.1 Different surrogates

Two approaches for creating surrogate data are often distinguished in the literature Theiler et al. [1992], Small et al. [2001], Kantz and Schreiber [2004], Kugiumtzis [2008]:

1. Fitting a model and simulating the model to obtain surrogate data, i.e., a Monte Carlo method also known as the *typical realisations* approach.

2. Transforming the data, retaining some aspects and randomizing others and then using an inverse transform to obtain surrogate data. Typically, such surrogates are based on the Fourier transform.

2.1.1 Typical realisations approach

The approach of typical realisations fits a model to the data and then uses "typical simulations" to create surrogate data. The fundamental question of

the present study is whether the data can be adequately described within a general linear-type model of the form Ljung [1999],

$$y(k) = G(q)u(k) + H(q)e(k) \tag{1}$$

and not only *some* model of Eq. (1), i.e., a model with *fixed* orders. Such a hypothesis is called composite. If a typical realisations approach is applied to a composite hypothesis, the statistic used for the test must be pivotal Theiler and Prichard [1996]. Although the correlation dimension has been widely used and advocated as a pivotal statistic in a variety of tests in nonlinear time series analysis (see, e.g., Small and Judd [1998a,b], Small et al. [2001]), it seems that correlation dimensions have not been expressed for dynamical systems with manipulatable inputs. Furthermore, it is not trivial to estimate a correlation dimension and there is, apparently, no consensus on a suitable pivotal statistic that is easy to estimate, reliable and robust Schreiber and Schmitz [2000], Kugiumtzis [2008]. For these reasons, the typical realisations approach is not considered in this presentation.

2.1.2 Fourier-based surrogates

In order to explain and motivate the use of Fourier-based surrogate data for nonlinearity testing, it can be noted that a general linear dynamical system of Eq. (1), where $u(k)$ is the input and $e(k)$ is white noise, can be expressed in the frequency domain by Ljung [1999]

$$\Phi_{yu}(\omega) = G(e^{i\omega})\Phi_{uu}(\omega) \tag{2}$$

where $\Phi_{uu}(\omega)$ is the power spectrum for u, $\Phi_{yu}(\omega)$ is the cross-power spectrum between y and u, and $G(e^{j\omega})$ is the frequency response function for the linear system $G(q)$. Given the existence of the Fourier transforms of u and y, denoted $U(\omega)$ and $Y(\omega)$ respectively, the power spectrum for u can be determined by[1]

$$\Phi_{uu}(\omega) = U^*(\omega)U(\omega) \tag{3}$$

where $U^*(\omega)$ denotes the complex conjugate of $U(\omega)$. Similarly, the cross-power spectrum can be determined by

$$\Phi_{yu}(\omega) = Y^*(\omega)U(\omega) \tag{4}$$

In practice, the estimate of $Y(\omega)$ and (possibly) $U(\omega)$, denoted $\hat{Y}(\omega)$ and $\hat{U}(\omega)$, will include contributions from the (filtered) noise sequence $H(q)e(k)$. However, for the method introduced in this paper, no attempt to estimate, e.g., $G(e^{i\omega})$ from $\Phi_{yu}(\omega)$ and $\Phi_{uu}(\omega)$ is made. Therefore, the influence of (linear) noise on the estimate $\hat{Y}(\omega)$ does not impose problems.

---

[1]To express the power spectrum of a stochastic signal as the Fourier transform of the autocorrelation would render the treatment more general, but not as useful for explaining the basic ideas behind FSD for input-output systems. Correspondingly, Eqs. (2)–(4) should in this paper be considered only as explanatory.

3

Instead, the general idea behind FSD is to introduce randomness in the phases of $\hat{Y}(\omega)$ and $\hat{U}(\omega)$ $\hat{U}_s(\omega) = |\hat{U}(\omega)|e^{j\angle(\hat{U}(\omega)+\eta)}$ and $\hat{Y}_s(\omega) = |\hat{Y}(\omega)|e^{j\angle(\hat{Y}(\omega)+\eta)}$ where η is the same for $\hat{U}_s(\omega)$ and $\hat{Y}_s(\omega)$. Also, η is uniformly distributed in $[0, 2\pi)$ and constrained in order to preserve the conjugate symmetry in the Fourier transform of a real signal. Clearly, this randomness will not affect any of Eqs. (2)–(4). The surrogate data thus created will have the same power spectra as the original data. Since the power spectra $\hat{\Phi}_{yy}(\omega)$ and $\hat{\Phi}_{yu}(\omega)$ also are the Fourier transform of the auto- and cross-correlation functions respectively, the original and surrogate data will share the auto- and cross-correlation functions. What is *not* defined by the auto- and cross-correlations, e.g., any correlations not linearly described is, on the other hand, lost by introducing the random phases. In other words, the original and surrogate data will exhibit the same linear characteristics and can be expressed by similar linear dynamical models, i.e., Eq. (1), while nonlinear structures are lost.

3 Fourier-based surrogates and testing for nonlinearity

Together with the original data, the collection of surrogate data is subjected to a statistical test that, for a level of significance, can reveal features in the original data that cannot be described by linear correlations and by distributions. The choice of test is central, since the test will define the discriminating features of the approach. Still, there seems to be no consensus regarding an "optimal" test, and different measures have been suggested, e.g., correlation dimensions, time reversibility, Poincaré maps, etc.

Since surrogate data is to be used in system identification, it seems motivated to apply a simple test that, in some sense, assesses the very goal of system identification. Often, a convenient measure of the purpose of the modeling can be expressed as the ability to predict the (short-term) behavior of the system: a predictive model is well suited for simulations and for supervisory as well as control purposes. Therefore, assessing the possibilities for improving predictions with nonlinear models seems like an appealing choice for a discriminative test. However, one reason to test for nonlinearities in the data is to avoid an unwarranted and cumbersome fitting of a nonlinear model to the data, and therefore a simple test is required. One such (model-free) predictor is given in Eq. (7).

A general predictive description is given by

$$\hat{y}(k) = g(\varphi(k-1)) \tag{5}$$

where $g(\cdot)$ is a mapping (the predictive model) from the regressors, $\varphi(k-1)$, to the predicted output, $\hat{y}(k)$, at sampling k. The one-step-ahead prediction error is defined by the difference between measured and predicted outputs, $\varepsilon(k) = y(k) - \hat{y}(k)$.

Although choosing appropriate regressors is a challenge in system identification, a simple test naturally requires a simple approach. Consequently, the

4

components of the regressors are chosen from the set of data, Z^N, i.e., the N observations of inputs and outputs. For a SISO system the vector of regressors can thus be expressed

$$\varphi(k-1) = (y(k-1) \quad \cdots \quad y(k-p)$$
$$u(k-L-1) \quad \cdots \quad u(k-L-m)) \quad (6)$$

where p and m are the orders with respect to the outputs and inputs respectively and L is the delay from input to output. For the SISO-case, $\varphi(k-1) \in \mathbf{R}^{p+m}$ while for a general $n_y \times n_u$ MIMO-system $\varphi(k-1) \in \mathbf{R}^{\sum_{i=1}^{n_y} p_i + \sum_{j=1}^{n_u} m_j}$.

A model-free, intuitively appealing predictive scheme is the nearest neighbor approach Lorenz [1969]. The nearest neighbor approach to prediction is based on finding the regressor $\varphi(l-1)$ closest to $\varphi(k-1)$, i.e., $\|\varphi(k-1)-\varphi(l-1)\| \leq \epsilon_{\min}$ where $\epsilon_{\min}$ is the smallest value for $\|\varphi(k-1)-\varphi(l-1)\|$ for all $l \in N$, $l \neq k$. The prediction for $y(k)$ is then given by $\hat{y}(k) = y(l)$. In order to make the method less sensitive to specific noise characteristics, a collection of nearest neighbors can be used, resulting in the prediction Kantz and Schreiber [2004]

$$\hat{y}(k) = \frac{1}{|U_\epsilon(\varphi(k-1))|} \sum_{\varphi(l-1) \in U_\epsilon(\varphi(k-1))} y(l) \quad (7)$$

which is an average of the outputs $y(l)$ corresponding to the regressors in the neighborhood $U_\epsilon(\varphi(k-1))$, i.e., the number of regressors satisfying the criteria $\|\varphi(k-1) - \varphi(l-1)\| < \epsilon$ for all $l \in N$, $l \neq k$. This integer is denoted by $|U_\epsilon(\varphi(k-1))|$. By varying ϵ, a suitable number of neighbors can be found.

The extension of the simple predictive scheme to MIMO systems is trivial. It can also be noted that the methodology is not restricted to square systems, e.g., no restrictions on the number of inputs are made. Numerical tools for generating surrogate data and predictions using the simple scheme described above are also readily available Hegger et al. [1999].

3.1 Algorithm for nonlinearity testing

The algorithm for data-based test for nonlinearity based on Fourier surrogates can be summarized as follows:

1. Choose a level of significance, $(1-\alpha)$, for the discriminative test based on the probability of a false rejection, α.

2. For an $n_y \times n_u$ MIMO system, use the set of outputs y_i $(i = 1, \ldots, n_y)$ and inputs u_j $(j = 1, \ldots, n_u)$,

$$\begin{pmatrix} y_1(1) & \ldots & y_{n_y}(1) & u_1(1) & \ldots & u_{n_u}(1) \\ \vdots & \ddots & \vdots & \vdots & \ddots & \vdots \\ y_1(N) & \ldots & y_{n_y}(N) & u_1(N) & \ldots & u_{n_u}(N) \end{pmatrix} \quad (8)$$

5

and generate a collection of surrogate data, i.e., $Q = 2/\alpha - 1$ sets for a two sided test: e.g., 39 sets for a minimal significance requirement of 95% are needed.

3. Choose orders and delays p_i, m_j and L_j so that the regressors for the simple predictor of Eq. (7) can be determined. Some arbitrary default choices are recommended, e.g., $p_i = m_j = 2$–4 for all i and j, since, e.g., optimizing p_i, m_j for the original data is an erroneous approach because this can render the statistical test biased. Rough estimates of the delays, L_j, are also needed and can be based on, e.g., prior knowledge of the system or on visual inspection of simple experiments. Alternatively, if the delays are unknown, a more exhaustive numerical exploration can be applied merely by adding shifted input vectors as columns to the data set.

4. Calculate predictions of the outputs by Eq. (7). Compare the variance of the prediction errors for the original set as well as for all surrogate sets. If the variance of the prediction error for an output y_i is either smaller or larger for the original set than for all surrogates, there is, on the chosen significance level, statistical evidence of nonlinear predictability of y_i in the original data set.

Clearly, MIMO systems are handled as easily as SISO systems, as only n_y prediction errors need to be evaluated. Also, there is no need for the systems to be square so, for example, even a large collection of unclassified data from an industrial plant could be subjected to a nonlinearity screening using the presented approach. Furthermore, the outputs y_i are simply replaced by the corresponding residuals ε_i (one-step ahead prediction errors) for the case of model validation.

4 Simulations

In order to illustrate the results of the nonlinear distortion in the frequency domain and the surrogate data approaches for nonlinearity detection, some simulated examples are used.

The first example considered is

$$
\begin{aligned}
x(k) &= \sin(x(k-1)) + u(k-1) \\
y(k) &= x(k) + e(k)
\end{aligned}
\tag{9}
$$

Results using the nonlinear distortion approach are illustrated in Fig. 1. For the figure, $u_{\mathrm{rms}} = 0.5$ was used for the multisines needed for the frequency domain identification and the standard deviation of the added Gaussian noise e was set to $u_{\mathrm{rms}}/10$. As the figure reveals, the approach provides an estimate of the best linear approximation (BLA) as well as an indication of the improvement that can be achieved by nonlinear considerations, i.e., the nonlinear distortion. For the example, the significant linear approximation is clearly seen in the figure and, interestingly, it can be noted that the nonlinear distortion is approximately
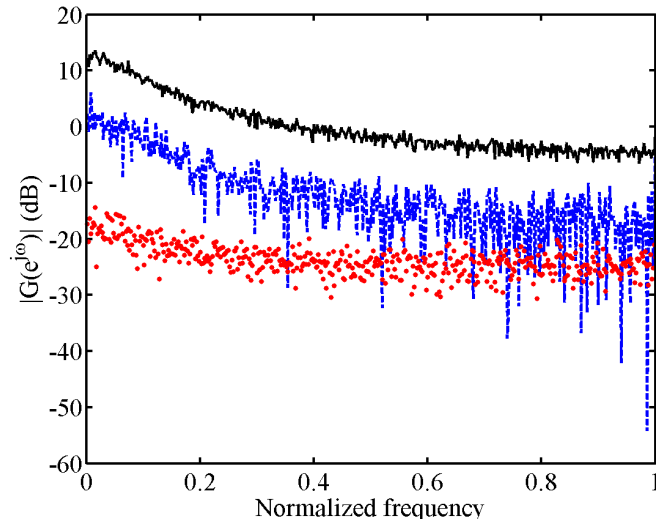
6

Figure 1: Frequency response functions for the model of Eq. (9)—BLA, (solid black), nonlinear distortion (dashed blue), noise (dotted red). The panel illustrates averaged results for 6 independent simulations of 2 consecutive periods of multisines with 1000 observations for each period, i.e., the total number of observations used to produce the results are $N = 12000$.

15dB under the BLA. This coincides very well with the model: given the first two terms in the expansion of the nonlinear function, i.e., $\sin(x) \approx x - x^3/3!$, the level of nonlinear distortion is approximately given by the ratio $\text{std}(x^3/3!)/\text{std}(x)$. The standard deviation of x^3 can be determined from the variance, $\text{E}\{(x^3 - \text{E}\{x^3\})^2\}$. For normally distributed x with zero mean and variance δ^2, $\text{E}\{(x^3 - \text{E}\{x^3\})^2\} = 15\delta^6$, thus yielding $\text{std}(x^3/3!)/\text{std}(x) = \delta^2\sqrt{15}/3!$. For the case illustrated in Fig. 1 with $u_{\text{rms}} = 0.5$, this gives $\delta \approx 0.5$ and $\text{std}(x^3/3!)/\text{std}(x) \approx -16$ dB. Fig. 1 also illustrates the fact that nonlinear distortion is typically detected by visual inspection.

Using surrogate data only provides a binary answer of whether or not an output exhibits (predictable) nonlinear features. For the model of Eq. (9), the result for the surrogate data approach is, with a 5% statistical error margin, simply a list of 40 numbers, i.e., the variance of the prediction errors using the predictive model of Eq. (7) for the original data set as well as for the 39 surrogate sets. Since the variance of the prediction errors is smaller for the original data set than for all surrogates, there is evidence of nonlinearity in the data. For this example, the two approaches are apparently qualitatively quite different but seem, with respect to data-based nonlinearity detection, similar.

The second example studied is a MIMO systems originally presented in

7

Billings and Zhu [1995] and is given by

$$
\begin{aligned}
y_1(k) ={}& 0.5y_1(k-1) + 0.1y_2(k-1)u_1(k-1) \\
&+ u_1(k-2) + 0.2y_1(k-2)e_1(k-2) \\
&+ 0.5e_1(k-1) + e_1(k) \\
y_2(k) ={}& 0.9y_2(k-2) + 0.2y_2(k-1)u_2(k-2) \\
&+ u_2(k-1) + 0.1y_2(k-1)e_1(k-2) \\
&+ 0.5e_2(k-1) + e_2(k)
\end{aligned}
\tag{10}
$$

with $\mathrm{std}(u_1) = \mathrm{std}(u_2) = 1.0$ and $\mathrm{std}(e_1) = \mathrm{std}(e_2) = \sqrt{0.04}$. The surrogate data approach needs approximately 5000 observations in order to reliably indicate that the simulated system is nonlinear. Among the large number of simulations reviewed in Waller [2017], this example is among the ones that require the greatest number of observations for the surrogate data approach to yield reliable results. For most examples studied, 500–1000 observations are sufficient.

Results for the nonlinear distortion approach for the model of Eq. (10) are provided in Fig. 2. The figure clearly shows that the approach detects the nonlinearity. Moreover, the linear dependence from u_1 to y_1 is most clearly visible (upper left panel) and to a lesser extent from u_2 to y_2 (lower right panel). The other transfer functions, from u_2 to y_1 (upper right panel) and from u_1 to y_2 (lower left panel) are mainly nonlinear as the estimated BLAs are at the level of, or lower than, the nonlinear distortion. This is also consistent with the model. As the figure reveals, the nonlinear distortion approach can be a powerful tool for detecting and quantifying nonlinearity in data.

A third example uses the well-known logistic map

$$
w(k) = \mu w(k-1)(1 - w(k-1)) \tag{11}
$$

with $\mu = 4$ to provide as a basis for determining a state variable observed through a linear filter,

$$
y(k) = ay(k-1) + w(k-1) + bu(k-1) + e(k) \tag{12}
$$

with $u_{\mathrm{rms}} = 0.5$ and the standard deviation of e set at $u_{\mathrm{rms}}/10$ for the simulations. For this model, the method for estimating nonlinear distortion classifies the input-output relationship from u to y as linear. Since the chaotic state w is not directly observable through the input-output relationship, the method cannot detect the nonlinearity, even without any added Gaussian noise e. The estimated BLA and nonlinear distortion are illustrated in Fig. 3 and the nonlinear distortion cannot be distinguished from the stochastic noise. The nonlinear distortion approach will also fail for other examples with noise-related nonlinearity, e.g.,

$$
y(k) = u(k-1) + e(k-2)e(k-5) + e(k) \tag{13}
$$

and

$$
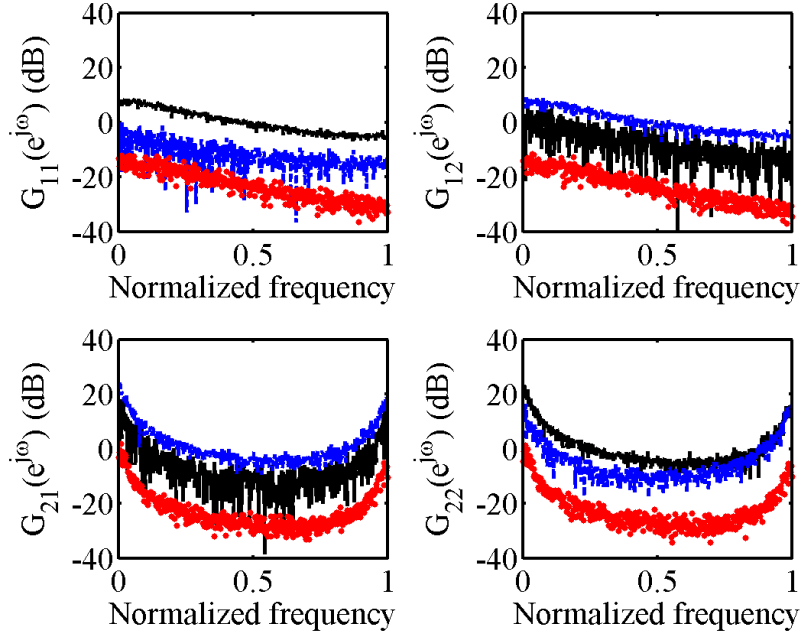y(k) = u(k-1) + u(k-2)e(k-5) + e(k) \tag{14}
$$

8

Figure 2: Frequency response functions for the model of Eq. (10): BLA, (solid black), nonlinear distortion (dashed blue), noise (dotted red). The figure illustrates averaged results for 6 independent simulations, each consisting of 2 consecutive periods with 1000 observations, i.e., the total number of observations used to produce the results are $N = 12000$. From u_1 to y_1 in the upper left panel, from u_2 to y_1 in the upper right panel, from u_1 to y_2 in the lower left panel and from u_2 to y_2 in the lower right panel.

both originally presented in Billings and Woon [1986]. For one-step-ahead prediction and related applications, this disadvantage of the frequency domain approach for detecting nonlinearity should be duly noted.

The surrogate data approach, on the other hand, reliably detects the nonlinearity in the model of Eqs. (11)–(12), already for $N = 1000$. This is also true for the models of Eqs. (13)–(14).

Given these examples, the surrogate data approach appears to be the most reliable alternative for detecting nonlinearity in data from general nonlinear dynamical systems.
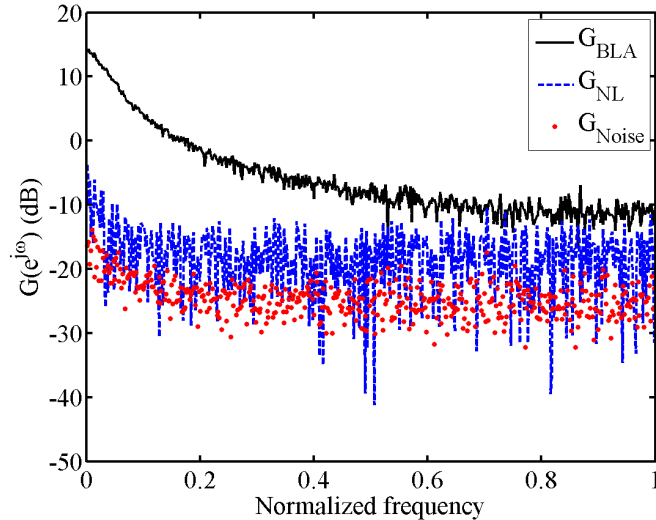
9

Figure 3: Illustrated results for the model of Eqs. (11)–(12). BLA (solid black), nonlinear distortion (dashed blue) and noise (dotted red). The figure illustrates averaged results for 6 independent simulations of 2 consecutive periods, each period consisting of 1000 observations, i.e., the total number of observations used to produce the results are $N = 12000$.

5   Conclusions

The use of Fourier-based surrogate data with a simple predictive scheme seems to be a powerful data-based nonlinearity test for dynamical systems and can thus be used to determine whether or not the data motivates nonlinear modeling. For detecting nonlinearity in data from general nonlinear systems, the presented method apparently outperforms alternative methods. As such, the method may be of significant importance within system identification.

A disadvantage of the surrogate data is that only a binary answer of whether or not an output exhibits (predictable) nonlinear features. An appealing possibility could therefore be to combine the power of the nonlinear distortion in the frequency domain approach for quantifying nonlinearity with the reliability, i.e., that no nonlinearities go undetected, of the surrogate data approach.

References

J. P. Barnard, C. Aldrich, and M. Gerber. Identification of dynamic process systems with surrogate data methods. *AIChE Journal*, 47:2064–2075, 2001.

S. A. Billings. *Nonlinear System Identification : NARMAX Methods in the*

10

Time, Frequency, and Spatio-Temporal Domains. John Wiley & Sons, Somerset, New Jersey, 2013.

S. A. Billings and W. S. F. Woon. Correlation based model validity tests for nonlinear models. *International Journal of Control*, 60:235–244, 1986.

S. A. Billings and Q. M. Zhu. Model validation test for multivariable nonlinear models including neural networks. *International Journal of Control*, 62:749–766, 1995.

M. A. A. S. Choudhury, S. L. Shah, and N. F. Thornhill. *Diagnosis of Process Nonlinearities and Valve Stiction: Data Driven Approaches*. Springer, Berlin, 2008.

D. Coca, J. E. W. Mayhew, and S. A. Billings. Nonlinear system identification and analysis of complex dynamical behavior in reflected light measurements of vasomotion. *International Journal of Bifurcation and Chaos*, 10:461–476, 2000.

R. Hegger, H. Kantz, and T. Schreiber. Practical implementation of nonlinear time series methods: The TISEAN package. *CHAOS*, 9:413–435, 1999.

R. Isermann and M. Münchhof. *Identification of Dynamic Systems: An Introduction with Applications*. Springer-Verlag, Heidelberg, 2011.

G. T. Jemwa and C. Aldrich. Classification of process dynamics with monte carlo singular spectrum analysis. *Computers & Chemical Engineering*, 30: 816–831, 2006.

H. Kantz and T. Schreiber. *Nonlinear Time Series Analysis*. Cambridge University Press, Cambridge, 2 edition, 2004.

D. Kugiumtzis. Evaluation of surrogate and bootstrap tests for nonlinearity in time series. *Studies in Nonlinear Dynamics & Econometrics*, 12, 2008.

L. Ljung. *System Identification—Theory for the User*. Prentice Hall, New Jersey, 2 edition, 1999.

Lennart Ljung. Perspectives on system identification. *Annual Reviews in Control*, 34:1–12, 2010.

E. Lorenz. Atmospheric predictability as revealed by naturally occuring analogues. *Journal of Atmospheric Sciences*, 26:636–646, 1969.

O. Nelles. *Nonlinear System Identification: From Classical Approaches to Neural Networks and Fuzzy Models*. Springer-Verlag, Berlin, 2001.

R. Pintelon and J. Schoukens. *System Identification—A Frequency Domain Approach*. John Wiley & Sons, New Jersey, 2 edition, 2012.

11

J. Schoukens, M. Vaes, and R. Pintelon. Linear system identification in a non-linear setting. *IEEE Control Systems Magazine*, 36:38–69, 2016.

T. Schreiber and A. Schmitz. Surrogate time series. *Physica D*, 142:346–382, 2000.

M. Small and K. Judd. Correlation dimension: A pivotal statistic for non-constrained realizations of composite hypotheses in surrogate data analysis. *Physica D*, 120:386–400, 1998a.

M. Small and K. Judd. Detecting nonlinearity in experimental data. *International Journal of Bifurcation and Chaos*, 8:1231–1244, 1998b.

M. Small, K. Judd, and A. Mees. Testing time series for nonlinearity. *Statistics and computing*, 11:257–268, 2001.

J. Theiler and D. Prichard. Constrained-realization monte-carlo method for hypothesis testing. *Physica D*, 94:221–235, 1996.

J. Theiler, S. Eubank, A. Longtin, B. Galdrikian, and J. D. Farmer. Testing for nonlinearity in time series: The method of surrogate data. *Physica D*, 58: 77–94, 1992.

M. Waller. Data-based testing for nonlinearity in dynamical systems: The use of surrogate data. *Accepted for publication in IEEE Transactions on Control Systems Technology*, PP:1–10, 2017. doi: 10.1109/TCST.2017.2771431.

M. Waller and H. Saxén. Time-varying event-internal trends in predictive modeling—methods with applications to ladlewise analyses of hot metal silicon content. *Industrial & Engineering Chemistry Research*, 42:85–90, 2003.

12

Identification of low order output-error models

Mikael Manngård[*], Jari M. Böling, Hannu T. Toivonen

Process Control Laboratory, Faculty of Science and Engineering, Åbo Akademi University.
Biskopsgatan 8, FIN-20500 Åbo, Finland

Abstract

We show that low order output-error models can be identified from input-output data by parametrizing the model in terms of it's impulse response, and constraining the rank of the corresponding Hankel operator. The problem is formulated as a rank constrained optimization problem, which is relaxed using the nuclear norm [1]. This formulation results in convex optimization problem which can be solved efficiently using any general purpose convex optimization software, such as CVX [2] and Mosek 7.1 [3]. Given a low-rank solution, a minimal partial state-space realization of the same order can be obtained by applying the Ho-Kalman algorithm [4]. The proposed method have been validated on benchmark datasets, and is compared to other state-of the art output-error system identification methods.

Keywords: Output-error identification, nuclear norm, impulse response models

References

[1] M. Fazel, H. Hindi, S. Boyd, Rank minimization and applications in system theory, in: Proceedings of the American Control Conference, vol. 4, 3273–3278, 2004.

[2] M. Grant, S. Boyd, CVX: Matlab Software for Disciplined Convex Programming, version 2.1, `http://cvxr.com/cvx`, 2014.

[3] MOSEK ApS, The MOSEK optimization toolbox for MATLAB manual. Version 7.1 (Revision 60)., URL `http://docs.mosek.com/7.1/toolbox/index.html`, 2015.

[4] B. Ho, R. E. Kalman, Effective construction of linear state-variable models from input/output functions, at-Automatisierungstechnik 14 (1-12) (1966) 545–548.

---

[*]Corresponding author.
Email address: `mikael.manngard@abo.fi` (Mikael Manngård)

Comparison of two classes of observers in a biochemical process

Caroço R. F.[1*], Abildskov J.[1], López-Arenas T.[2], Huusom J. K.[1]

[1] *CAPEC-PROCESS, Department of Chemical and Biochemical Engineering, Technical University of Denmark*
[2] *Departamento de Procesos y Tecnología, Universidad Autónoma Metropolitana-Cuajimalapa, Artificios 40, 01120 Mexico D.F.,Mexico*

POSTER

One of the major limitations in the biochemical industry is the multitude of disturbances that each process is subjected to. Large segments of the industry operate in a heuristic recipe-driven way, dependent on rule-of-thumb experience which results too often in batch-to-batch discrepancies. These difficulties can be mitigated by an appropriate monitoring strategy and model building comes as an integral part of such a strategy. Models supply a representation of the underlying physical/chemical phenomena, allowing for the estimation of both measured and unmeasured states, enabling subsequent control decisions.

From development to optimization of established processes, model-based monitoring and control strategies are crucial in a product/process life-cycle. They enable us to address a large number of objectives such as process understanding, troubleshooting, real-time control actions and continuous process optimization.

Our work studies the application of two distinct classes of observers (Luenberger-based and Bayesian) in a biochemical toy case, for different test-scenarios. The challenge of employing the observer structures, which update key performance indicators (KPI) forecast, as new quality data is supplied, is highlighted. This allows scenarios of real industrial value such as estimating unmeasured states or identifying parameters. Insights on the properties of the different observers in a biotech context are presented.

---

*Corresponding author; Ricardo F. Caroço, Department of Chemical and Biochemical Engineering, Technical University of Denmark, Søltofts Plads2800, Denmark. E-mail: rcar@kt.dtu.dk

Control strategy based on radial basis function for an Ibuprofen batch crystallization process under upstream uncertainty

Frederico Montes[a], Krist V. Gernaey[a], Gürkan Sin[a]

Gürkan Sin: gsi@kt.dtu.dk

[a]Process and Systems Engineering Centre (PROSYS), Technical University of Denmark, Søltofts Plads Building 229, 2800 Kgs. Lyngby, Denmark

Due to its process flexibility, crystallization is one of the most commonly used processes in the pharmaceutical industry. Although continuous crystallization is becoming more common, batch operation is still the most frequent option, as it easily allows the production of different API through different batches. However, crystallization is a highly non-linear process and therefore difficult to model and simulate. Moreover, uncertainty in process parameters and previous process outputs has an important and critical influence on the control strategy used for the same process.

In order to study the design space and overcome such uncertainties, a two dimensional population balance model of ibuprofen batch crystallization is used, with uncertainty from previous synthesis steps included [1,2] and uncertainty from process parameters as reported in the literature [3,4]. A nonlinear control strategy is then applied, comparing different radial basis functions (quadratic, cubic, Gaussian…)[5], in order to minimize the formation of off-spec API crystals by manipulating and updating the cooling profile of the same process.

The resulting three operation strategies are benchmarked with respect to key performance metrics (setpoint deviation and input variation): open-loop, open-loop strategy under process uncertainties, and closed loop operation subject to process uncertainties. The final CSD is reported as a confidence interval, in order to be used for further downstream processing.

[1] - V. Elango, M. Murphy *et al*., 1991, USA 4.981.995

[2] – F. Montes, K. Gernaey, G. Sin, ESCAPE 27, Barcelona, 2017

[3] - A. Rashid, E.T. White *et al*., Proc. Chemeca, Adelaide, 2010

[4] - A. Rashid, E.T. White *et al*., Proc. Chemeca, Perth, 2009

[5] – M. Pottman, D. E. Seborg, Comp. Chem. Eng., 1997

Acknowledgment

Modelling of the Prehydrolysis Kraft Process for Process Control

Antton Lahnalammi[*], Herbert Sixta, Sirkka-Liisa Jämsä-Jounela

Department of Chemical and Metallurgical Engineering, Aalto University, Kemistintie 1, ESPOO, 02150, FINLAND

Abstract

Prehydrolysis kraft process adds a separate prehydrolysis stage prior to traditional kraft batch cooking cycle in order to selectively remove portion of the wood hemicelluloses. The removal of hemicellulose is unavoidably accompanied by adverse reactions, most importantly partial hydrolysis amorphous alpha-cellulose and release of condensation prone acid soluble lignin. On-line monitoring of the reactions is missing, and only available signals from the digester are the temperature and pressure profiles. This paper presents a mechanistic dynamic model for the prehydrolysis stage, which approximates the progression of the unmeasured reactions based on the energy and component balances determined for individual digester sub-sections. Energy balance is determined for solids, liquid fraction and the walls inside each section, while the reaction rates are modelled for liquid and solid fractions in each section using second order kinetics. The model can be used directly for the control and optimization of the process or for the development and testing of soft sensors and novel control strategies.

Keywords: autohydrolysis, batch digester, mechanistic model, dynamic model

1. Introduction

The demand for hemicellulose lean dissolving pulp has been increasing rapidly, due to constantly growing textile market, which cotton cultivation is no longer able to saturate (Hämmerle, 2011). Removal of hemicelluloses by continued cooking cannot be accomplished without sacrificing selectivity. Therefore, a separate acidic prehydrolysis stage with mineral acid or autohydrolysis is required. Here autohydrolysis is considered, where the prehydrolysis is conducted simply with water or steam: heating of the digester up to $160 - 180$ °C results in the cleavage of native acetyl groups as acetic acid. The increased acidity and high temperature drive the hydrolysis reaction, which results in the dissolution of wood hemicelluloses. Amorphous alpha-cellulose and lignin are similarly susceptible for acid hydrolysis: the partial hydrolysis of cellulose decreased pulp viscosity and cooking yield, while the highly reactive acid soluble lignin limits the recovery of sugars from the prehydrolyzate. The main quality parameters—e.g. viscosity, alpha-cellulose content and kappa number—are measured off-line and the process is optimized on a batch-to-batch basis. No chemicals are added during the autohydrolysis stage and therefore the control problem consists of simply determining the suitable P-factor—which incorporates combination of time and temperature—that results in the desired pulp quality.

Temperature and pressure are the only monitored variables during the prehydrolysis stage, which limits the on-line estimation of the quality parameters. Reaction kinetic models can be used for determining the relationship between the acidity and temperature and the rate of the unobservable reactions. The complex and inhomogenous structure of the lignocellulose matrix limits the accessibility and reactivity of wood biopolymers

towards to hydrolysis reactions, leading to fractions with different reactivity. Conner, (1984) successfully modelled xylan removal using pseudo first order kinetics by dividing the wood xylan into fast and slow reacting fractions, with different activation energy and frequency factor. Later Borrega et al. (2011a, 2011b) showed that the same model structure can be used for simulating the degradation of lignin and cellulose fractions. A more recent model by Ahmad et al. (2016) uses second order kinetics, which requires modelling of deacetylation and mass transfer phenomena, but offers more realistic results especially in lower temperatures, where the deacetylation is slower, leading to slower development of acidity.

The aforementioned kinetic models assume even temperature profile and are normalized to isothermal conditions. As the reaction rates are depend exponentially on the temperature according to the Arrhenius equation, accurate modelling of the digester energy balance offers more realistic framework for the modelling of the wood degradation reaction kinetics and can lead to insight regarding in batch variation. Consequently, modelling of the PHK-process for process control requires a comprehensive model which captures the dynamics of the entire digester and allows estimation of control actions on the process.

This paper presents a dynamic mechanistic model for the water phase autohydrolysis inside a simple circular flow batch digester system consisting of reactor vessel, heat exchanger and the required piping. The process model is described in Chapter 2, while the conclusions are drawn in Chapter 3.

2. Dynamic model for the PHK-process in batch digester

The reactor vessel, the outflow pipe, the heat exchanger and the inflow pipe are divided into N, M1, H and M2 sections. Perfect mixing and isothermal conditions are assumed inside each subsection. The energy balances for each section (Fig. 1) are:

$$\dot{Q}_{L,n} = \dot{Q}_{F,n} - \dot{Q}_{LC,n} - \dot{Q}_{LW,n} \tag{1}$$

$$\dot{Q}_{C,n} = \dot{Q}_{LC,n} + \dot{Q}_{R,n} \tag{2}$$

$$\dot{Q}_{W,n} = \dot{Q}_{LW,n} - \dot{Q}_{CWA,n} - \dot{Q}_{RWA,n} \tag{3}$$

Where $\dot{Q}_{L,n}$, $\dot{Q}_{C,n}$ and $\dot{Q}_{W,n}$ are the n:th liquid, chip and wall fraction energy balances, consisting of the advection flux ($\dot{Q}_F$), the convection from wood to chips ($\dot{Q}_{LC}$), and walls ($\dot{Q}_{LW}$) and from walls to ambient by convection ($\dot{Q}_{CWA,n}$) and radiation ($\dot{Q}_{RWA,n}$) and the heat of reactions ($\dot{Q}_{R,n}$). Determining of the convective heat fluxes ($\dot{Q}_{LW}, \dot{Q}_{LC,} \dot{Q}_{WA} \in \dot{Q}_{conv}$) equals to finding the average overall heat transfer coefficients $\bar{h}_{conv,n}$ (Incropera et al., 2007). The flux is then linearly proportional to the temperature gradient (ΔT_{conv}). The convection term $\dot{Q}_{LW,n}$, $\dot{Q}_{LC,n}$ and $\dot{Q}_{CWA,n}$ can be approximated as internal flow inside a circular pipe, liquid flow through packed bed and as free convection of air respectively or coefficients can be determined experimentally. The radiative term ($\dot{Q}_{RWA,n}$), can be computed from Stefan-Boltzmann constant (σ), surface emissivity (ε_W), ambient wall area (A_A), ambient temperature (T_A) and wall surface temperature (T_W). The advection term ($\dot{Q}_{F,n}$) is function of the volumetric flow rate ($\dot{F}$) and the specific heat capacity (C_L), density (ρ_L) and temperature (T_L) of the adjacent liquid fractions. The heat

released by reactions $\dot{Q}_{R,n}$ is summation over the reaction rate of n_R reactants $[\dot{R}_i]$ multiplied by heat of the corresponding reaction λ_i

$$\dot{Q}_{conv,n} = \bar{h}_{conv,n}\Delta T_{conv} \tag{4}$$

$$\dot{Q}_{RWA,n} = \sigma\varepsilon_{W,n}\left(T_{W,n}^4 - T_A^4\right) \tag{5}$$

$$\dot{Q}_{F.n} = \dot{F}(C_{L,n-1}\,\rho_{L,n-1}T_{L,n-1} - C_{L,n}\rho_{L,n}T_{L,n}) \tag{6}$$

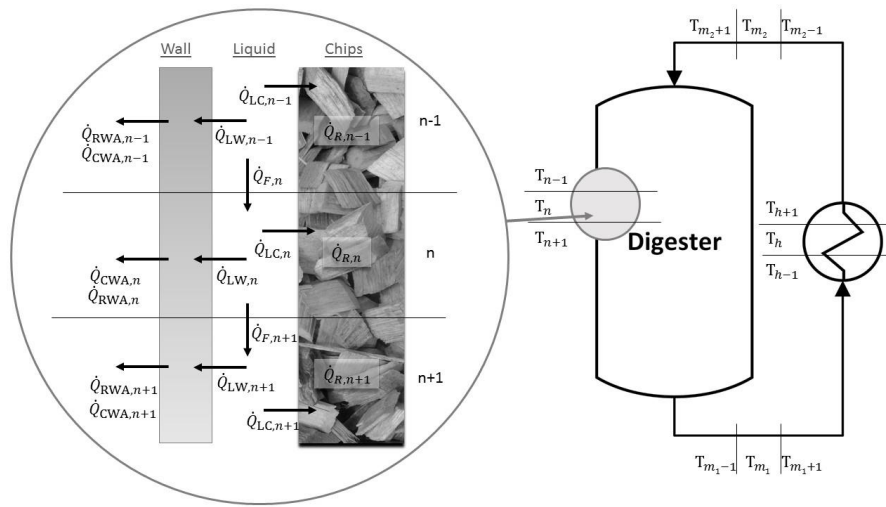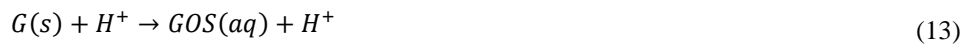$$\dot{Q}_{R,n} = \sum_{i=1}^{n_R}\lambda_i[\dot{R}_{i,n}] \tag{7}$$

Figure 1. Circulation of the liquid fraction inside the reactor system and the heat fluxes simulated in the energy balances of the dynamic model.

The component balances are determined for the cellulose $[C]$, xylan $[X]$, lignin $[L]$, glucomannan $[G]$, acetyl groups $[OAc]$ and acetic acid $[AcOH]$ using second order kinetics (Eq. 8,9).

$$H_2O \rightleftarrows H^+ + OH^- \tag{8}$$

$$ROAC + H^+ \rightarrow AcOH + H^+ \tag{9}$$

$$AcOH(aq) \rightleftarrows AcO^-(aq) + H^+(aq) \tag{10}$$

$$C(s) + H^+ \rightarrow COS(aq) + H^+ \tag{11}$$

$$X(s) + H^+ \rightarrow XOS(aq) + H^+ \tag{12}$$

$$G(s) + H^+ \rightarrow GOS(aq) + H^+ \tag{13}$$

$$L(s) + H^+ \rightarrow L(aq) + H^+ \tag{14}$$

$$L(aq) + H^+ \rightarrow LC(s) + H^+ \tag{15}$$

Water autohydrolysis and acetic acid equilibrium are calculated each step using equilibrium constants in corresponding temperature. Diffusion of acetic acid and solubilized lignin from the wood chips into the bulk liquid is approximated by Fick's law of diffusion in order to eliminate the need for rigorous modelling of multiple ionic species.

$$[\dot{R}_{i,n}] = -k_{R_i}[R_{i,n}][H_n^+] \tag{16}$$

$$[\dot{R}_{C,n}] = -D_{CL}\big([R_{C,n}] - [R_{L,n}]\big) \tag{17}$$

3. Preliminary testing

The model was tested using parameters obtained from literature: the kinetic parameters for acetyl group cleavage and lignin reactions were obtained from (Ahmad et al., 2016), while the degradation kinetics of xylan were adapted from (Borrega et al., 2011b). The diffusion of solubilized lignin and acetic acid from the entrapped liquid into the bulk liquid was modelled with diffusion coefficients obtained from (Haynes et al., 2017) multiplied with effective capillary cross sectional area of 0.1 (Inalbon et al., 2017). The heat transfer coefficients of the liquid-solid, liquid-wall and wall-ambient interfaces were approximated as 200, 500 and 37 W/(m^{2}K) respectively.

 The temperature profile of the solid fraction—where the reactions are taking place—is lagging behind the liquid fraction—where the temperature is measured—by approximately 10 ºC, and the overshoot in temperature control is much less significant. The cleavage of acetyl groups progresses gradually during the first 60 minutes: as the reaction rate depends linearly on hydrogen ion concentration, the reaction rate will be time dependent long after the reactor reaches the temperature set point. The removal of lignin is much slower in comparison with (Ahmad et al., 2016), which may be the result of large uncertainty in the parameters, while the removal of xylan closely resembles that simulated by (Borrega et al., 2011b). Therefore, further experimental work is still required for the estimation of the kinetic parameters developed here.
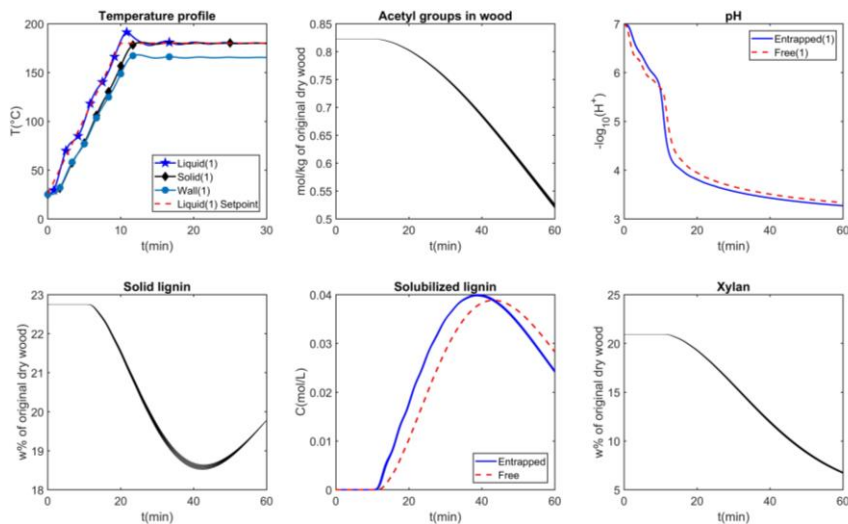

Figure 2. Temperature profile and component balances simulated by the model.

4. Conclusions

Dynamic mechanistic model was developed for the autohydrolysis stage in the prehydrolysis kraft process in a batch digester. The model—consisting of energy and component balances defined for separate reactor system sections individually—offers a more realistic framework for simulating effect of different control actions. Therefore, the model allows further development and testing of soft sensors and novel control strategies for the prehydrolysis process. However, acquisition of accurate model parameters for the heat transfer coefficients and reaction rates requires additional experimental work. The experimental data will be used for further testing and validation of the developed model in near future.

References

Ahmad, W., Kuitunen, S., Borrega, M., Alopaeus, V., 2016. Physico-chemical modeling for hot water extraction of birch wood. Ind. Eng. Chem. Res. 55, 11062–11073. doi:10.1021/acs.iecr.6b02987

Borrega, M., Nieminen, K., Sixta, H., 2011a. Effects of hot water extraction in a batch reactor on the delignification of birch wood. BioResources 6, 1890–1903.

Borrega, M., Nieminen, K., Sixta, H., 2011b. Degradation kinetics of the main carbohydrates in birch wood during hot water extraction in a batch reactor at elevated temperatures. Bioresour. Technol. 102, 10724–10732. doi:10.1016/j.biortech.2011.09.027

Conner, A., 1984. Kinetic Modeling of Hardwood Prehydrolysis. Part I. Xylan Removal by Water Prehydrolysis. Wood Fiber Sci. 16, 268–277. doi:10.1002/ejlt.200600223

Haynes, W.M., Lide, D.R., Bruno, T.J., 2017. CRC Handbook of Chemistry and Physics. CRC Press, Florida.

Hämmerle, F.M., 2011. The Cellulose Gap (the future of cellulose fibres). Lenzinger Berichte 89, 12–21.

Inalbon, M.C., Solier, Y.N., Zanuttini, M.Á., 2017. Hydrothermal treatment of Eucalyptus wood: Effects on Ion permeability and material removing. Ind. Crops Prod. 104, 195–200. doi:10.1016/j.indcrop.2017.04.042

Incropera, F.P., DeWitt, D.P., Bergman, T.L., Lavine, A.S., 2007. Fundamentals of Heat and Mass Transfer. John Wiley & Sons. doi:10.1073/pnas.0703993104

Fault propagation analysis based on a nonparametric multiplicative regression causality estimator combined with process connectivity information

R. Landman. S-L. Jämsä-Jounela

Aalto University, School of Chemical Technology, Process Control and Automation Research Group, P.O Box 16100, 00076
Finland (Tel: 358-(0)50-4382296; e-mail: rinat.landman@ aalto.fi).

Abstract:

Industrial processes are often subjected to faulty operations, which can easily propagate via the process units and elements along material or information flows. Oscillatory disturbances are one of the most common disturbances which affect the control loops of a process leading to poor control performance and excessive energy consumption. Early detection and diagnosis of abnormal events can assist in minimizing the production losses and impede fault progression. Establishing causal dependencies among process measurements has a key role in fault detection analysis due to its ability to identify the root cause of a fault and its propagation path. This study proposes a non-linear causality estimator based on Nonparametric Multiplicative Regression (NPMR) for identifying the propagation of oscillation in control loops. NPMR-based estimator offers several advantages over the traditional causality methodologies: it is nonparametric, i.e., it does not rely on estimation of any type of parametric model. It can be applied to both linear and non-linear processes and there is no restriction on the order of nonlinearity that can be estimated. Furthermore, the method can be used for both pairwise and multivariate analysis without any modifications. In order to facilitate the analysis, the process connectivity information is automatically integrated into the analysis using a unique depth-first search algorithm. The process connectivity information is extracted in the form of a connectivity matrix, which is captured from an XML scheme using AutoCAD P&ID. The search algorithm mainly serves to determine the type of directionality between two control elements. Accordingly, the bivariate NMPR-based causality estimation is calculated for all paths which are considered as direct based on the connectivity information while the conditional (multivariate) NPMR-based causality is calculated for each indirect path. This type of approach enables to tackle efficiently complex systems with a high level of connectivity and thereby enhance the quality of the results. In particular, this approach is highly beneficial when analyzing complex systems with several recycle streams or bidirectional connectivity. Moreover, the possibility for an automatic extraction of the process connectivity information and integrating it with data-based analysis generates an enhanced and powerful diagnostic tool. This methodology is exemplified using a case study of an industrial board machine with multiple oscillating control loops due to valve stiction. This highly inter-connected system serves to illustrate the effectiveness and the advantages of the proposed methodology.

1. Introduction

Recently, a new causality estimator based on Non-Parametric Multiplicative Regression (NPMR) was proposed by Nicolaou & Constandinou (2016). The concept of NPMR originates from the field of ecology and was first introduced by MacCune (2006; 2011) in the context of habitat modeling. In their thorough review of existing causality estimators, Nicolaou & Constandinou (2016) showed how NPMR-based estimator addresses the limitations of other methods. For instance, this type of estimator offers several advantages over the traditional causality methodologies: it is nonparametric, i.e., it does not rely on estimation of any type of parametric model. It can be applied to both linear and non-linear processes and there is no restriction on the order of nonlinearity that can be estimated. Furthermore, the method can be used for both pairwise and multivariate analysis without any modifications (Nicolaou & Constandinou, 2016). The inherent features of NPMR eliminate any overfitting issues, a problem which often leads to detection of spurious causalities when using many current nonlinear methods (Palus & Vejmelka, 2007). The statistical significance can be tested using surrogate data and the sensitivity measure Q can be used to evaluate the contribution of particular parameters within the model (Nicolaou & Constandinou, 2016).

In this study, we propose to combine a causality estimator based on NPMR with the information on process connectivity in order to provide a powerful diagnostic tool which can efficiently tackle complex industrial processes. A number of recent studies suggest that the results of the data-based methods should be combined with qualitative information, e.g., expert knowledge or validated by P&ID (Thambirajah, et al., 2007; Landman, et al., 2014; Duan, et al., 2014; Yang, et al., 2012). In particular, this approach is highly beneficial when analyzing complex systems with several recycle streams or bidirectional connectivity (Landman & Jämsä-Jounela, 2016). Moreover, the possibility for an automatic extraction of the process connectivity information and integrating it with data-based analysis generates an enhanced and powerful diagnostic tool (Duan, et al., 2014; Thornhill & Horch, 2007). The process connectivity information is extracted in the form of a connectivity matrix, which is captured from an XML scheme using AutoCAD P&ID (Thambirajah, et al., 2009; Landman, et al., 2014).

The combination of the connectivity information with NPMR estimator is automated by means of a unique search algorithm based on a depth-first search (Thambirajah, et al., 2009). The search algorithm mainly serves to determine the type of directionality between two control elements. Accordingly, the bivariate NMPR-based causality estimation is calculated for all paths which are considered as direct based on the connectivity information while the conditional (multivariate) NPMR-based causality is calculated for each indirect path.

This procedure offers an enhanced and efficient diagnostic tool for identifying the source of oscillation and its propagation path. This methodology is exemplified using a case study of an industrial board machine with multiple oscillating control loops due to valve stiction. This highly inter-connected system serves to illustrate the effectiveness and the advantages of the proposed methodology.

2. The NPMR-based causality analysis framework

The study aims to identify the propagation path of oscillations through control loops. The analysis consists of the following steps: first, the search algorithm searches for feasible propagation paths between two control loops. Then, if such paths exist, the search algorithm checks whether the controllers are connected directly or via other controllers. If two controllers are directly connected, the bivariate NPMR-based causality is estimated while if the controllers are connected indirectly, the conditional (multivariate) NPMR-based causality is calculated for all indirect paths and the maximum value is taken. Finally, all the estimations undergo a statistical significance test using surrogate data. The logic of the overall analysis is illustrated in Figure 1.
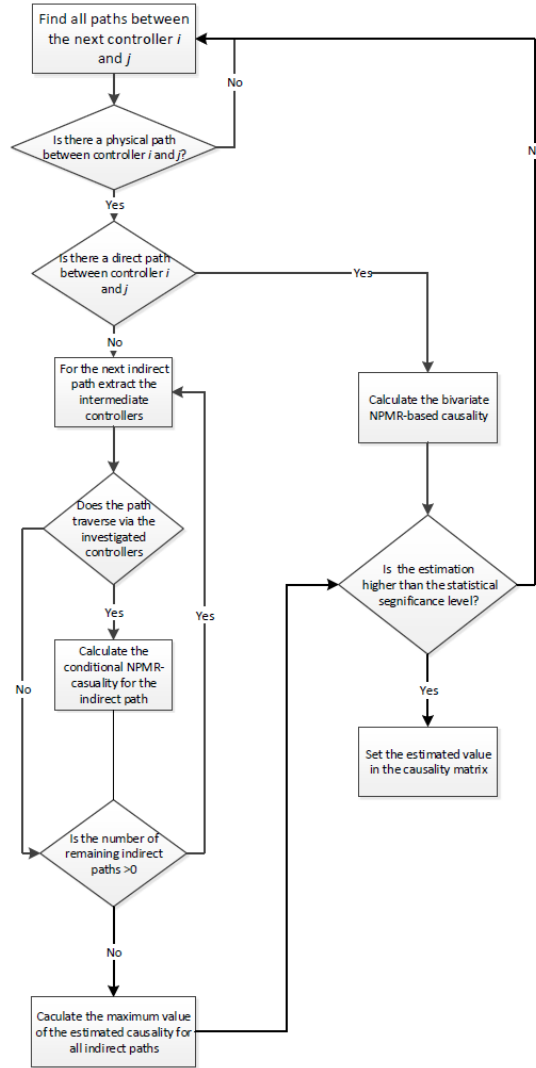
Figure 1 : The logic of the NPMR-based causality analysis

3. NPMR-based causality estimator

Consider a response variable Y with N samples $Y = [y_1, y_2, \dots y_N]$ and consider a matrix X with m predictors

$$X = \begin{pmatrix} x_{1,1} & \cdots & x_{1,m} \\ \vdots & \ddots & \vdots \\ x_{N,1} & \cdots & x_N \end{pmatrix} \qquad (1)$$

Next, a response surface of y is built from its m predictors using a multiplicative kernel smoother (McCune, 2006). This is achieved by estimating each value y_n from its local neighborhood corresponding to the predictor space $X_n = [x_{n,1}, x_{n,2,\dots,}x_{n,m}]$. The influence of each predictor X_j, $(j = 1, \dots, m)$ on the estimation is defined by its corresponding tolerance of the kernel smoother, s_j, which is a unique feature for NPMR. In this study, the local neighborhood is defined as the weighted mean and the weights are estimated using a Gaussian weighing function. The weights are the distances of each of the m predictors from a target point X_n scaled by the standard deviation (tolerance) of each predictor (Nicolaou & Constandinou, 2016).

$$w_{i,j} = e^{-1/2\left[\frac{x_{i,j} - x_{n,j}}{s_j}\right]^2} \qquad (2)$$

Thereupon, the estimation of target point n of y can be obtained as follows:

$$\hat{y}_{n=} \frac{\sum_{i=1, i\neq n}^{N} y_i (\prod_{j=1}^{m} w_{i,j})}{\sum_{i=1, i\neq n}^{N} (\prod_{j=1}^{m} w_{i,j})} \qquad (3)$$

The estimate is the mean value of the observations where each observation is weighted according to its distance from the target point in the predictor space with the weights being the product of the individual weights. By omitting the target point n from the estimation, overfitting is reduced and error estimates are more realistic (McCune, 2006). Nicolaou & Constandinou (2016) extended the basic idea of NPMR in the context of causality estimation by extending the predictor space to include past information as additional predictors. For time instance n, the embedded vector x_n is defined as $x_n = [x_{n,}, x_{n-\tau,\dots,}x_{n-(d-1)\tau}]$ where d is the embedded dimension and τ is the embedding time delay. The bivariate NPMR-based causality estimator is defined as follows:

$$C_{NPMR}(X_j \rightarrow Y) = \log\left(\frac{\sigma^2(Y, \bar{Y})}{\sigma^2\left(Y, (\bar{Y}, \bar{X}_j)\right)}\right) \qquad (4)$$

where X_j is the jth predictor and $\sigma^2(Y, \bar{Y})$ $\sigma^2\left(Y, (\bar{Y}, \bar{X}_j)\right)$ and are the error variances when past values of Y are used as predictors and when both past values of Y and X are used as predictors, respectively. Likewise, the conditional (multivariate) C_{NPMR} is defined as:

$$C_{NPMR}(X_j \rightarrow Y/Z) = \log\left(\frac{\sigma^2(Y, \bar{Y}, Z)}{\sigma^2\left(Y, (\bar{Y}, \bar{X}_j, Z)\right)}\right) \qquad (5)$$

where Z corresponds to the intermediate variables, excluding X_j. Negative C_{NPMR} values imply that including the past information on the predictors resulted in worse model fit, i.e., there is no causal dependency among the time series (Nicolaou & Constandinou, 2016).

4. Process case study

The process case study involves a large-scale board machine (BM) which produces a three-layer liquid packaging and board cups. In particular, the analysis is focused on the drying section of the machine where the remains of the excess water in the web are removed to achieve the desired moisture content. The drying section is consists of six drying groups (DGs) wherein each drying group includes a steam group (SG) containing steam filled cylinders and its corresponding condensate tank (CT) where the condensate is collected by syphons and separated into water and steam. Each DG has three types of controllers. Pressure controllers which provide steam for each SG using 5 and/or 10 bar pressurized steam headers. Pressure difference controllers which are used to manipulate the steam outlet of the CTs in order to maintain the proper pressure difference between each of the SG and its CT to allow an efficient condensate removal. In addition, level controllers are used to maintain the appropriate condensate level in the CTs by regulating their outlet flow. The entire drying section is illustrated in Figure 2. The case study involves a valve stiction in the pressure controller PC1652. The cycling nature of the stiction typically manifests as an oscillatory behavior of the control loops since the stiction delays the valves movement while the process inputs remain the same. Oscillations generated by valve stiction easily propagate among control loops and eventually deteriorate the overall control performance. (Pozo Garcia, et al., 2013) The time series used for the investigation are corresponding to the process measurement (*PVs*). 1000 samples measured with a sampling interval of 10 s were used for the analysis. Prior to the investigation, the series were normalized by removing the mean and scaling to a unit standard deviation. Due to the oscillatory behavior of the time series, the power spectra of the series was used in order to detect measurements with a similar spectral behavior. The control loops which share this common oscillation frequency are: PC1653, PC651, PC652, PC653, PC670, LC652, PC1652, PC671, LC653 and PC673. The time delay τ was estimated as the time when the auto-correlation function reaches $1/e$ (Nicolaou & Constandinou, 2016) and was chosen as 3. Next, the embedding dimension was evaluated according to the method presented by Cao (1997) and was selected as $d=4$. Finally, the kernel tolerance σ was tuned for each pair of series. Using $\tau = 3$ and $d=4$, the model fit was calculated for $\sigma = 0.2, 0.4, 0.6, \dots 2$. The tolerance which produced the best model fit (Nicolaou & Constandinou, 2016) for each pair was selected. There was a slight variation in the optimum value of σ for each pair of series ($0.2 < \sigma < 0.8$), hence, an optimum value was set individually for each pair.
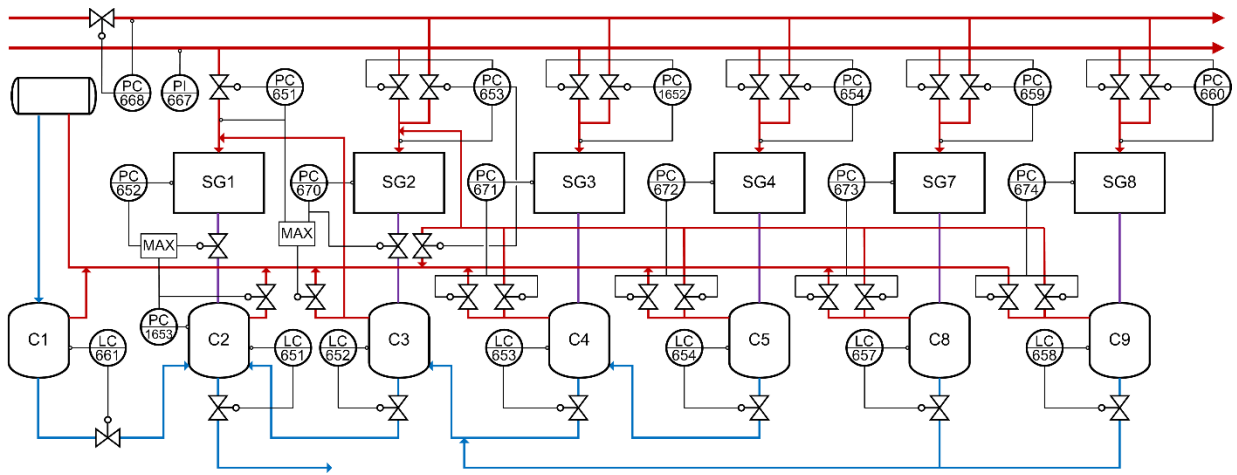
Figure 2: The drying section of the BM. PC=Pressure Controller, C=Condensate tank, LC=Level Controller, PI=Pressure Indicator

5. Results

The causality matrix with the $C_{NPMR}(X_i \rightarrow X_j)$ for each $(i,j)^{th}$ pair of controllers is shown in Table 1 (to the left) . Empty cells indicate either on lack of physical connectivity or C_{NPMR} values which are lower than their significance level. In addition, negative values of C_{NPMR} were excluded. Table 1 (to the right) presents the connectivity information according to the search algorithm: empty cells indicate on lack of physical connectivity, circles denote indirect paths

	PC1653	PC651	PC652	PC653	PC670	LC652	PC1652	PC671	LC653	PC673
PC1653										
PC651			0.053							
PC652	0.065	0.172								
PC653					0.303					
PC670		0.036	0.078	0.156		0.100				
LC652		0.102	0.058							
PC1652							0.190	0.498		
PC671				0.094	0.134		0.090	0.234		
LC653		0.108	0.249			0.135				
PC673										

	PC1653	PC651	PC652	PC653	PC670	LC652	PC1652	PC671	LC653	PC673
PC1653										
PC651	○		●							
PC652	●	●								
PC653	○	○	○		●	○				
PC670	○	●	●	●		●				
LC652	●	●	●							
PC1652	○	○	○	○	○	○		●	●	
PC671	○	○	○	●	●	○	●		●	
LC653	○	●	●	○	○	●				
PC673	○	○	○	●	●	○				

Table 1: The causality matrix to the left an circles indicating on indirect/direct connectivity to the right (empty circles denote indirect paths while filled circles denote direct paths

and filled circles denote direct paths between the row and column controllers. According to the results, all the paths which were identified as indirect by the search algorithm were also verified as indirect according to their C_{NPMR} values. The majority of the paths which were identified as direct by the search algorithm were also confirmed as direct by their C_{NPMR} values. In this study, two possible scenarios could lead to misidentification of direct causality: causality might exist but on a very low level (e.g., LC652 → PC1653) or there is a direct physical path but there is no information transfer due to closed valve. The latter scenario could be the case for PC673 → PC653 and PC673 → PC670. This exemplifies that physical connectivity does not necessarily imply on causality.

The causal mode is shown in Figure 3. The paths which are suspected as indirect are denoted as dashed arcs. The path PC1652 → LC653 is initially suspected as indirect according to the captured topology; however, according to the search algorithm the path is direct since the steam condensate from SG3 is transferred directly to C4. Moreover, the high C_{NPMR} value implies on a high level of interaction between PC1652 and LC653. The paths from LC653 to controllers PC651 and PC652 is recognized as direct, however, the search algorithm reveals that the direct path from LC653 to PC651 and PC652 is via C3 whose one of the steam outlet streams flows directly into SG1. However, since the bottom

flow outlet of C4 initially alters the level in C3, it is reasonable to assume that LC652 is primarily affected by LC653. Consequently, the C_{NPMR} values of LC653 →PC652 and LC653 →PC651 via intermediate controller LC652 are calculated. The values of C_{NPMR} (LC653→ LC652 →PC651)=0.051 (0.093) and
C_{NPMR} (LC653→LC652 → PC652)=0.138 (0.011) (The second number refers to the significance level) suggest that the causality from LC653 to PC652 is direct whereas the causality from LC653 to PC651 can be considered as indirect.
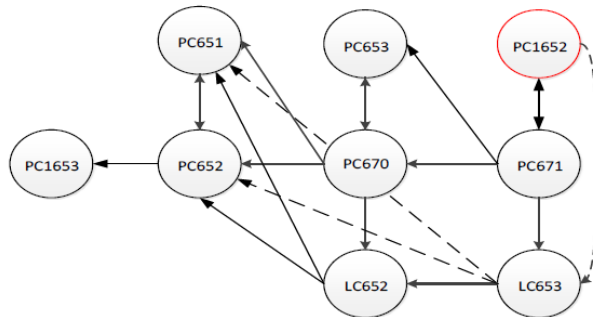
Figure 3: The causal model depicting the propagation path

6. Summary and Conclusions

This study introduced a unique methodology for retracing the propagation path of a fault using a nonlinear nonparametric causality estimator. The methodology was successfully demonstrated on industrial case study involving valve stiction in a board machine. Formerly, the NPMR-based causality estimator has been applied in habitat modeling (McCune, 2006; McCune, 2011) and on physiological data (Nicolaou & Constandinou, 2016) while this study extends its application to industrial processes. The numerous advantages of NPMR estimator make it highly efficient and practical compared with other causality estimators (Nicolaou & Constandinou, 2016).

Overall, the analysis proved to be highly efficient and accurate in identifying the propagation path. Misdetection might be attributed to the parameters selection, especially tunning the kernel tolerance. When tunning σ we observed that even a small variation in σ lead to a significant difference in the corresponding C_{NPMR} values. Moreover, σ has larger influence on C_{NPMR} than d and τ. Therefore, optimization of the tolerance remains a challenge for further investigations. On the other hand, although we found that parameters tunning is essential to obtain adequate results, several estimations with different parameters revealed that the causality pattern remains similar and only the amplitude of C_{NPMR} changes which results in more false positive results. When applying the same analysis but using fixed initial parameters ($\tau = 1$, $d = 4$, $\sigma = 1$), the results demonstrate that the causality pattern is almost unaltered, however, it is expected to obtain more false-positive results.

Bibliography
Cao, L., 1997. Practical method for determining the minimum embedding dimension of a scalar time series. *Physica D,* Volume 110, pp. 43-50.

Di Geronimo Gil, G., Alabi, D., Iyun, O. & Thornhill, N., 2011. *Merging Process Models and Plant Topology.* Thousand Islands Lake, Hangzhou, IEEE, pp. 15-21.

Duan, P., Chen, T., Shah, S. & Yang, F., 2014. Methods for root cause diagnosis of plant-wide oscillations. *AIChE Journal,* 60(6), pp. 2019-2034.

Landman, R. & Jämsä-Jounela, S.-L., 2016. Hybrid approach to casual analysis on a complex industrial system based on transfer entropy in conjunction with process connectivity information. *Control Engineering Practice,* Volume 53, pp. 14-23.

Landman, R., Kortela, J., Sun, Q. & Jämsä-Jounela, S.-L., 2014. Fault propagation analysis of oscillation in control loops using data-driven causal analysis and plant connectivity. *Computers & Chemical Engineering,* Volume 71, pp. 446-456.

McCune, B., 2006. Non-parametric habitat models with automatic interactionds. *Journal of vegetation science,* Volume 17, pp. 819-830.

McCune, B., 2011. *Nonparametric Multiplicative Regression for Habitat Modeling,* s.l.: Oregon State University.

Nicolaou, N. & Constandinou, T., 2016. A nonlinear Causality Estimator Based on Non-Parametric Multiplicative Regression. *Frontiers in Neuroinformatics,* Volume 10, pp. 1-21.

Palus, M. & Vejmelka, M., 2007. Directionality of coupling from bivariate time series: How to avoid false causalities and missed connections. *Physical Review E,* Volume 75: 056211, pp. 1-14.

Pozo Garcia, O., Tikkala, V.-M., Zakharov, A. & Jämsä-Jounela, S.-L., 2013. Integrated FDD system for valve stiction in a paperboard machine. *Control Engineering Practice,* 21(6), pp. 818-828.

Thambirajah, J., Benabbas, L., Bauer, M. & Thornhill, N., 2007. *Cause and effect analysis in chemical processes utilizing plant connectivity information.* Vancouver, Canada, s.n., pp. 1-6.

Thambirajah, J., Benabbas, L., Bauer, M. & Thornhill, N., 2009. Cause-and-effect analysis in chemical processes utilizing XML, plant connectivity and quantitative process history. *Computers and Chemical Engineering,* Volume 33, pp. 503-512.

Thambirajah, J., Benabbas, L., Bauer, M. & Thornhill, N., 2009. Cause-and-effect analysis in chemical processes utilizing XML, plant connectivity and quantitative process history. *Computers and Chemical Engineering,* Volume 33, pp. 503-512.

Thornhill, N. & Horch, A., 2007. Advances and new directions in plant-wide disturbance detection and diagnosis. *Control Engineering Practice,* Volume 15, pp. 1196-1206.

Yang, F., Shah, S. & Xiao, D., 2010. *SDG (signed directed graph) based process description and fault propagation analysis for tailings pumping process.* Cape Town, South Africa, s.n., pp. 50-55.

Yang, F., Shah, S. & Xiao, D., 2012. Signed directed graph based modeling and its validation from process knowledge and process data. *Internation Journal of Applied Mathematis and Computr Science,* 22(1), pp. 387-392.

Yang, F., Shah, S. & Xiao, D., 2012. Signed directed graph based modeling and its validation from process knowledge and process data. *International Journal of Applied Mathematis and Computr Science,* Volume 22, pp. 387-392.

Yang, F. & Xiao, D., 2012. Progress in Root Cause and Fault Propagation Analysis of Large-scale Industrial Processes. *Journal of Control Science and Engineering,* Volume 2012, pp. 1-10.

A receding horizon optimal control approach for solution purification process

Bei Sun[1], *Sirkka-Liisa Jämsä-Jounela*[1],, *Chunhua Yang*[2]

1. Aalto University, School of Chemical Engineering, P.O. Box 16100, FI-00076 Espoo, Finland, Tel: +358 50 582 6428, sirkka-liisa.jamsa-jounela@aalto.fi
2. Central South University, School of Information Science and Engineering, P.O. Box 410083, Changsha, China, Tel: +86 0731 88836876, E-mail: ychh@csu.edu.cn

ABSTRACT: This paper presents a two-layer control scheme for solution purification process. Based on the characteristics of the process, two concepts, including additive utilization efficiency (AUE) and impurity removal ratio (IRR), are designed. By using the two concepts, a gradient optimization approach is proposed. The gradient optimization approach transforms the economical optimization problem into finding an optimal decline gradient of the impurity ion concentration along the reactors. A robust adaptive controller is designed to track the optimized system states in the presence of process uncertainties. The ability of the scheme is illustrated with a simulated case study.

KEY WORDS: solution purification process, hydrometallurgy, gradient optimization

1 INTRODUCTION

A hydrometallurgy process is composed of leaching, purification and electrowinning [1,2]. The raw ore is first treated in the leaching process, in which the valuable metal in the solid state ore is extracted and converted into soluble salts in liquid solution. As leaching process is not completely selective, the leaching solution inevitably contains undesirable impurity ions. The presence of these impurity ions would decrease the current efficiency in the subsequent electrowinning process in which pure metal is recovered, resulting in energy waste and downgrade of product quality. Therefore, the leaching solution is processed in solution purification process to remove the impurity ions gradually. A solution purification process is composed of several sub-steps each of which is tailored to remove a particular type of impurity under specific reaction conditions. The control objective of an impurity removal process is to use the least amount of additives to remove the impurity ions such that after removal concentration of the impurity ions is no larger than a predefined value.

Determination of additive dosages of each reactor is an essential problem in the control of solution purification process. An excessive amount of additive is a waste of costly material, while an insufficient amount fails to remove the impurity adequately. This paper develops a control scheme for multiple reactor system based on its characteristics. The concepts of Additive Utilization Efficiency (AUE) and Impurity Removal Ratio (IRR), are proposed based on an indepth analysis. By using these two concepts, the control of multiple reactor system is decomposed into two problems, i.e., estimated additive dosage optimization and robust adaptive tracking control of the optimized operation point. Correspondingly, the proposed control scheme is composed of two layers. The upper layer works on a slow time scale. The additive dosage optimization, which has an economic objective function subject to constraints on purification performance and process stability, is transformed into finding an optimal decline gradient of impurity ion concentration along the reactors. The lower layer works on a fast time scale. A robust adaptive controller is designed to track the optimized impurity ion concentrations in the presence of model uncertainties.

2 PROBLEM ANALYSIS AND FORMULATION

An impurity removal process is composed of $N(N \geq 1, N \in \mathbb{Z})$ consecutive reactors and a thickener in which the liquid-solid separation takes place. Assume the fluid in each reactor is perfectly mixed, and the contents are uniform throughout the reactor volume. Then according to the mass balance principle, the dynamics of the process can be described by following equations:

$$\frac{dx_i}{dt} = \frac{f_{i-1}}{V} x_{i-1} - \frac{f_i}{V} x_i - k_i x_i \tag{2}$$

in which $i = 1, 2, \cdots, N$, V is the volume of the reactor, f_{i-1}, x_{i-1} and k_i are the outlet flux, outlet impurity ion concentration and reaction rate of the ith reactor respectively, while f_i and x_i are the inlet flux, inlet impurity ion concentration of the ith reactor respectively. The dynamics of reaction rate $\dot{k}_i = g(u_i, \theta_i)$ is a function of additive dosage u_i and reaction conditions θ_i. The control objective is to determine the best combination of the additive dosages of each reactor according to current inlet conditions and reaction status such that the technical index(the outlet impurity ion concentration of the N th reactor) is satisfied while the economical index(total additive consumption of the reactors in a certain period of time) is optimized:

$$\min \quad J(\mathbf{u}) = \int_{t_0}^{t_f} \sum_{i=1}^{N} u_i(\tau) d\tau \tag{3}$$

$$\text{st.} \quad 0 \leq x_N \leq x_{\text{index}}$$

where $\mathbf{u} = [u_1, u_2, \cdots, u_N]$, x_{index} is the upper limit of x_N, $[t_0, t_f]$ is the interval of interest·

3 A TWO-LAYER GRADIENT OPTIMIZATION APPROACH

Due to the absence of a unified control approach for complex industrial systems, the realization of optimization and control objective relies on a subtly designed control scheme. In this section, based on two intuitional concepts derived from the process characteristics, a two-layer gradient optimization scheme is developed. The original control problem of Eq. (3) is decomposed to two layers.

3.1 Additive utilization efficiency

A major problem in deciding the additive dosage is that not all the additive involved in reaction (1). According to the mass balance principle, the proper amount of additive to be fed into the reactor depends on its efficiency in removing the impurity[4]. Consider a certain period of time, Additive Utilization Efficiency (AUE) is the ratio of additive practically involved in impurity removal when a certain amount of additive is added into the reactor:

$$\mu = \frac{u_{real}}{u} \tag{4}$$

where u is the amount of additive added, u_{real} is the amount of additive involved in impurity removal.

Consider a block of solution with volume V, for reactor i, denote μ_i as its AUE, x_{i-1} and x_i as the impurity ion concentration before and after its retention in the reactor, assume μ_i, x_{i-1} and x_i are constant during the retention, then the required additive dosage is:

$$u_i = \mu_i^{-1} \frac{M_A}{M_B} V(x_{i-1} - x_i) \tag{5}$$

where M_A and M_B are the atomic weight of additive and impurity.

3.2 Impurity removal ratio

The retention of solution in multiple reactor system is essentially a gradually decline process of the impurity ion concentration along the reactors. For reactor i, the Impurity Removal Ratio (IRR) is the ratio of impurity ion removed in it:

$$\lambda_i = \frac{x_{i-1} - x_i}{x_0} \tag{6}$$

IRR of each reactor need to be optimized in order to achieve the required purification performance.

3.3 Optimization strategy

Using the two concepts, consider the time interval $[t_0, t_f]$, the original optimization problem could be reformulated as following:

$$\min \quad J(\mathbf{u}) = \frac{M_A}{M_B} V \sum_{i=1}^{N} \mu_i^{-1} \lambda_i$$

$$\text{st.} \quad 0 \le x_N = x_0(1 - \sum_{i=1}^{N} \lambda_i) \le x_{\text{index}} \tag{8}$$

$$\lambda_{\min i} \le \lambda_i \le \lambda_{\max i}$$

where $\lambda_{\min i}$ and $\lambda_{\max i}$ are the predefined lower and upper bounds of IRR of the i th reactor.

Solving Eq.(8), which would obtain the optimized IRR of each reactor, equals to finding the optimal setting values of the effluent impurity concentration of each reactor, or in other words, finding a best decline gradient of impurity ion concentration along the reactors (Fig. 1). However, due to the process uncertainties, a two-layer gradient optimization approach is designed. The upper layer, which works on a slow time scale, solves the estimated economical optimization problem in a receding horizon manner. The AUE estimator could be constructed by applying data-driven modeling approaches, e.g., RBFNN(Radial Basis Function Neural Network). The lower layer, which works on a fast time scale, handles the model uncertainties by using a robust adaptive controller (Fig. 2).
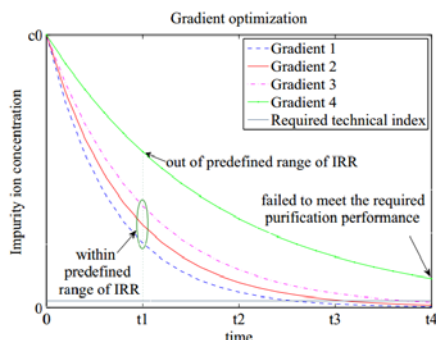

Figure. 1. Gradient optimization along reactors
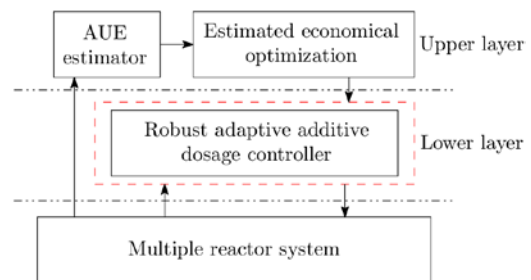

Figure. 2. Two-layer control framework

3.3   Robust adaptive system state tracking controller

Take the first reactor as an example, its dynamics could be presented and augmented as following:

$$\dot{x}_0 = g_0(\theta_{in}, t)$$

$$\dot{x}_1 = \frac{f_0}{V}x_0 - \frac{f_1}{V}x_1 - h_1 + d_1(t) \tag{9}$$

$$\dot{h}_1 = \omega$$

where θ_{in} is the inlet condition, $d_1(t)$ is the time-varying disturbance, $h_1 = x_1 k_1$, ω is an auxiliary control to be determined. The bound of $d_1(t)$ is denoted as D_1 which is not assumed to be known. If make following coordinates transformation:

$$z_1 = x_1 - x_{r1}$$

$$z_2 = h_1 - \alpha_1 \tag{10}$$

where x_{r1} is the optimized setting value of x_1, α_1 is a virtual control law to be designed. By applying Lyapunov stability theorem and backstepping technique [5,6], following theorem could be established.

Theorem 1.: For multiple reactor system described by Eq.(9), it is global asymptotically stable by applying the control law with :

$$k_1 = \frac{h_1}{x_1}$$

$$\dot{h}_1 = \omega \tag{11}$$

$$\omega = -c_2 z_2 + z_1 + (c_1 - \frac{f_1}{V})(\frac{f_0}{V}x_0 - \frac{f_1}{V}x_1 - h_1) - \text{sgn}(z_2)|c_1 - \frac{f_1}{V}|\hat{D}_1$$

$$+ \frac{f_0}{V}\text{sgn}(z_1)\hat{x}_0 - c_1\dot{x}_{r1} - x_{r1}^{(2)} + \text{sgn}(z_1)\dot{\hat{D}}_1$$

$$\dot{\hat{D}}_1 = \eta_1(|z_1| + |z_2(c_1 - \frac{f_1}{V})|)$$

Then consider the 'reaction rate-additive dosage' system:

$$\dot{k}_1 = g(u_1, \theta_1) \tag{12}$$

Design an auxiliary approximation system:

$$\dot{\hat{k}}_1 = f_v(u_1) + c_3 sgv(z_3) + \hat{D}_3 sat(z_3)$$

$$\dot{\hat{D}}_3 = \eta_3 |sgv(z_3)| \tag{13}$$

in which, $f_v(u_1) = \zeta_1(x_0 - \mu_1 u_1)$, $c_1, c_2, c_3, \eta_1, \eta_3$ are positive design parameters, $z_3 = k_1 - \hat{k}_1$ is the approximation error, $\hat{D}_1$ is the estimate of D_1, which is the bound of $d(t)$, $\hat{D}_3$ is the estimate of D_3, which is the bound of uncertainties in Eq(12), function $sgv(z_3)$ and $sat(z_3)$ are defined as:

$$sgv(z_3) = \begin{cases} z_3 - c_v & if \ z_3 \geq c_v \\ 0 & if \ |z_3| < c_v \\ z_3 + c_v & if \ z_3 \leq -c_v \end{cases}$$

$$sat(z_3) = \begin{cases} \text{sgn}(z_3) & if \ |z_3| \geq c_v \\ \dfrac{z_3}{c_v} & if \ |z_3| < c_v \end{cases} \tag{14}$$

in which, c_v is a positive design parameter.

Theorem 2.: For the 'reaction rate-additive dosage' system described by Eq.(12), by using following control policy, the tracking error converges asymptotically to $\xi = \{z_5 : |z_5| \leq c_v\}$:

$$u_1 = \frac{1}{\zeta_1 \mu_1}[\zeta_1 x_0 + c_3 sgv(z_3) + \hat{D}_3 sat(z_3) - \dot{k}_{r1} - c_4 z_4] \tag{15}$$

in which, $z_4 = \dot{k}_{r1} - \dot{\hat{k}}_1$, $z_5 = k_{r1} - k_1$, c_4 is a positive design parameter, k_{r1} is the desired value of k_1.

The proofs of Theorem 1 and Theorem 2 follow the same lines of reasoning as in the proofs of [2], Th. 1 and Th. 2. In addition, the control law for the other reactors could be deduced using the same formulation by changing the subscripts. The control result is shown in Fig. 3. It is indicated that, by using the two-layer control scheme: 1) The final impurity ion concentration always satisfies the purification requirement; 2) The impurity ion concentration of each reactor can track their reference trajectories well; 3)There is no large fluctuation and excessive increment in the additive dosage.
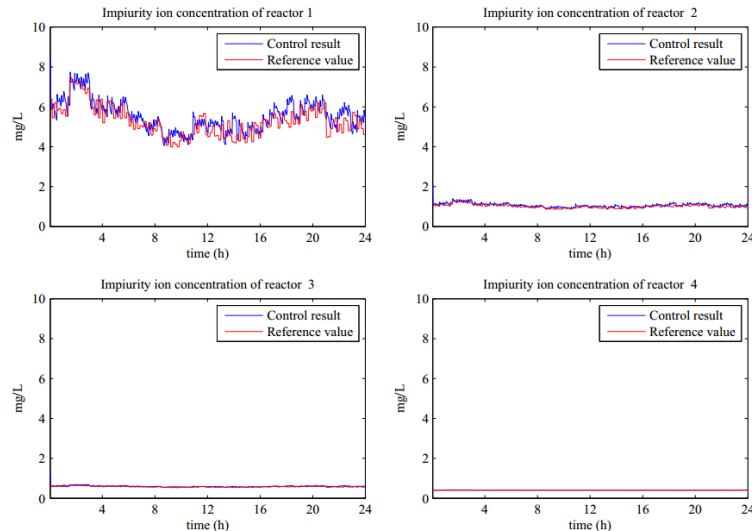
Figure. 3. Tracking performance of the impurity concentration of each reactor

4 CONCLUSION

This paper proposed a two layer control scheme for solution purification process. The idea of gradient optimization was derived based on two concepts (AUE and IRR) extracted from the common characteristics of solution purification process. The desired trajectories of effluent impurity ion concentration of each reactor were tracked by controlling the additive dosages. The feasibility of the proposed scheme was proved and illustrated through a simulation study. However, there are still some drawbacks of the proposed scheme. The performance of this scheme is affected by the accuracy of the process model and selection of the design parameters. It is suggested to determine these design parameters at the development stage. If the accuracy of the process model is not sufficient or the user is lack of experience in tuning the design parameters, the performance of the scheme may deteriorate. Thus model free controller design approach, and more precise and comprehensive process modeling method still need to be studied to increase the ability of the scheme in the future.

6 REFERENCES

1. Flett D.S.: Solution purification. *Hydrometallurgy*, 30(1992) 1, 327–344.
2. Bei Sun, Wei-Hua Gui, Ya-Lin Wang, Chun-Hua Yang, Ming-Fang He. A gradient optimization scheme for solution purification process, *Control Engineering Practice*, 2015, 44, 89-103.
3. Sędzimir J.A.: Precipitation of metals by metals (cementation)—kinetics, equilibria. *Hydrometallurgy*, 64(2002) 3, 161–167.
4. Kim S., Kim K., Park E., Song S., Jung S.: Estimation methods for efficiency of additive in removing impurity in hydrometallurgical purification process. *Hydrometallurgy*, 89(2007) 3-4, 242–252.
5. Wen C.Y., Zhou J, Liu Z., Su H.. Robust adaptive control of uncertain nonlinear systems in the presence of input saturation and external disturbance. *IEEE Transactions on Automatic Control*, 56(2011) 2, 307–323.
6. Khalil H.K.: *Nonlinear systems*, Prentice Hall, Upper Saddle River, New Jersey, United States, 2002, 111-133.

Spectroscopic method for bacterial quantification in suspension

Minh Nguyen[1], Jarmo Alander[2], and Kai Zenger[3]

[1]Aalto University, Department of Electrical Engineering and Automation, Espoo, Finland
[2]Vaasa University, Faculty of Technology, Vaasa, Finland
[3]Aalto University, Department of Electrical Engineering and Automation, Espoo, Finland

Abstract

Microbiological quantification is an important aspect in food and medical industry for quality and safety control. It is traditionally determined with standard plate count method in biology. This method, however, is laborious, time-consuming and requires at least over-night incubation to assess the bacterial contamination in the samples.

This work aims to determine the possibility of monitoring growing phases of bacteria and quantifying them in liquid samples (suspension) using spectroscopy and multivariate analyses. The spectroscopic method is based on attenuation of light owing to absorption and scattering when propagating through a mixture. Absorption refers to light being absorbed by the sample and converted to a different form of energy. Scattering explains that the incident light is redirected into different directions by the particles in its transmitting medium. These effects result in spectra similar to ones illustrated in Figure 1. Two multivariate statistical techniques, principal component analysis (PCA) and partial least square regression (PLS), are used for analysing the data. PCA plays a role of finding suitable wavelengths for spectral analysis whereas PLS identifies the relation between spectra and the concentration of analytes. Absorbance spectra are acquired at different samples corresponding to different concentrations of bacterial suspensions using a spectroscope. Then they are subjected to PLS for developing a prediction model. This model can be applied in quantifying bacteria in other suspensions with known spectra. This approach, hence, promises an on-line application for monitoring and estimating the concentration of microbes in aqueous samples.
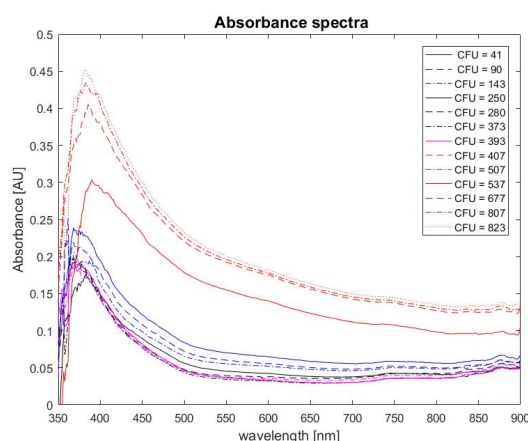
Figure 1: Absorbance spectra of bacterial suspensions with different concentrations.

Additionally, for further applicability, it would be beneficial to determine the association between the dose of indocyanine green (ICG) and near-infrared (NIR) light in photodynamic therapy (PDT) with the growth of bacteria. Indocyanine green (ICG) is a photosensitiser with low toxicity. Under decomposition effect of NIR light in PDT, ICG can excite oxygen from the environment leading to production of singlet oxygen which is acutely lethal to microbial organisms.

Estimation of the regulating power potential of the grocery store S-Market Tuira

István Selek, Enso Ikonen

Systems Engineering Research Group, University of Oulu, Finland
POB 4300, 90014 Oulu University, istvan.selek@oulu.fi, enso.ikonen@oulu.fi

Abstract

Today's electrical infrastructure is at the edge of a major change. Current trends show that the conventional thermal power based power generation is to be augmented by sustainable power production based on renewables, mostly wind and solar power. The breakthrough of renewable power introduces a major challenge for the balance control between electric power supply and demand within the power-grid, due to the volatile and intermittent nature of the renewable sources.

In case an imbalance occurs between supply and demand, regulating power up or down (depending on the frequency conditions of the grid) is used to restore the (balanced) nominal conditions. Renewables increase the production uncertainty so as the need for up/down regulating power. Regulating power can be provided by means of controlling the demand within the grid. This requires the application of demand side management which controls and/or (re)schedules the load pattern. Demand side management has a great potential focusing on industrial refrigeration systems applied in grocery stores and cold storages/warehouses due to the facts that: (1) industrial refrigeration systems have considerable regulating power potential and (2) thermal capacity of the refrigerated goods/food items can be exploited to modify the pattern of electric energy consumption, thus to provide up/down regulating power.

This paper develops a dynamic model based estimator of the regulating power potential of the grocery store S-market Tuira, located in Oulu, Finland. First, the development of the mathematical model of the vapor compression cycle of the grocery store is considered which aims to describe the dynamic–behavior of the refrigeration system and estimate the related electric power consumption. The developed model is comprised by a nonlinear Hammerstein type dynamic and (quadratic) static sub–models. The dynamic sub–model describes the thermal behavior of the refrigerator units used in the market, while the static sub–model estimates the total electric power consumption of the compressor banks located in the hydrodynamic circuit of the vapor compression cycle. Once the mathematical model is obtained, an optimization framework (using linear, quadratic programming) is introduced to estimate the regulating power potential subject to system's state, system dynamics, constraints and lookahead horizon. Simulations regarding up/down regulating power scenarios for the case store are provided.

Methods and Software for Solving Convex Mixed Integer Nonlinear Programming Problems

Jan Kronqvist
Process Systems Engineering
Åbo Akademi University

Mixed-integer nonlinear programming (MINLP) is a branch of optimization that deals with optimization problems containing both continuous and integer variables as well as linear and nonlinear functions. The combination of integer variables along with nonlinear functions gives a great flexibility in modeling, and there are a vast number of applications in areas such as engineering, computational chemistry, molecular biology and finance [1].

An MINLP instance is usually defined as convex if an integer relaxation results in a convex nonlinear programming (NLP) instance. Many methods for solving nonconvex MINLP relay on the ability to solve a sequence of convex MINLP instances. Therefore, the ability to efficiently solve convex MINLP is of utter importance for complex real world problems. Currently there are several methods available for solving convex MINLP instances, e.g. , the extended cutting plane (ECP) method, the extended supporting hyperplane (ESH) method, outer approximation (OA) and branch and bound techniques [2,3,4].

A short introduction to some of the concepts used for solving convex MINLP problems will be given here as well as a numerical comparison of the standards software for solving such problems.

References

[1] Floudas, C.A.: Deterministic Global Optimization, vol. 37 of Nonconvex Optimization and its Applications, 2000

[2] Westerlund, T., Petterson, F.: An extended cutting plane method for solving convex MINLP problems. *Computers & Chemical Engineering* 19, 131–136, 1995

[3] Kronqvist, J., Lundell, A., Westerlund, T.: The extended supporting hyperplane algorithm for convex mixed-integer nonlinear programming. Journal of Global Optimization 64 (2), 249-272, 2016

[4] Grossmann, I.E., Kravanja, Z.: Mixed-integer Nonlinear Programming: A survey of Algorithms and Applications. In: Large-scale optimization with applications. Springer, 1997

Profile based analysis for automatic feature extraction from time series data

John-Eric Saxén, Jerker Björkqvist, and Hannu T. Toivonen, Åbo Akademi, Finland

Many machinery companies are today collecting sensor data from their equipment with the objective to enable condition-based maintenance, diagnostics or operational optimization. Due to the large magnitude of raw sensor data available in modern machinery, it is desirable to detect the events from the raw data that may serve as indicators for faults, which in turn can be used as input for cloud-based deep learning methods. In order to derive compressed event and performance data, we propose a profile-based methodology, where typical time series profile segments are identified and added to a library of know time series profiles.

The proposed method extracts the events from raw data based on windowing of time series using for example peak detection. Data from windowed time series is used to collect a set of profiles, which are representing events of typical operation. In order to discern between different events, k-nearest neighbor clustering is applied to group and determine the number of profiles. The obtained raw data profiles are compared against a library of known profiles, which is updated adaptively to reflect a normal operation state of the machinery. The profiles from the library are optimally aligned with the raw data using dynamic time warping or by minimizing the sum of Euclidean distances. In order to reduce the influence of noise, signal averaging is applied over several repetitions of the time series to obtain the reconstructed profiles. The extracted profiles and the reconstruction error are used to calculate scalar and vector features, which serve as input for machine learning.

The method has been applied on real acceleration data from elevator car and doors. From the collected profile features, event and performance indicators can be derived for further use in diagnostics or condition-based maintenance.

A control oriented model for inline deoiling hydrocyclone

Tamal Das   Johannes Jäschke

Chemical Engineering Department,
Norwegian University of Science and Technology

Deoiling hydrocyclone (HC) is a separator that uses cyclonic forces for removing oil from produced water in oil and gas producing fields. HCs can be placed downstream of 1st or 2nd stage separators, such as three- or two phase gravity separators, in order to achieve high water purity with very low oil content. Discharged water from HCs is usually further processed before discarding it into the sea or injection wells. Permissible emission limits on water discharge are in the range of $20-30\ ppm$ [1].

(a) Schematic of an inline deoiling Hydrocyclone

(b) OiW control
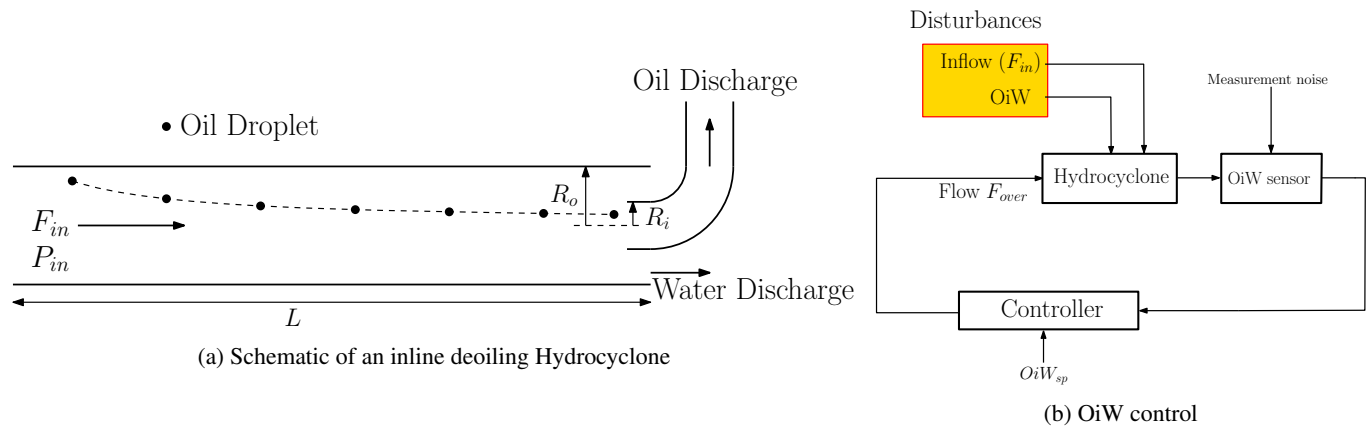
Figure 1: Hydrocyclone control structures

HC operation usually relies on automatic control in order to meet the oil emission limits, for which dynamic models are required. In the literature for HC modeling, data driven approaches have attracted a lot of focus [2]. Data driven models, though useful, fail to cover a wide range of operating conditions [3]. In the oil and gas fields in which a common separation system handles a network of wells and tie-in wells, HCs could be subjected to a wide variety of feeds and inlet water quality. In order to overcome the challenges faced by data driven models, in this work we focus on developing a control oriented mechanistic dynamic HC model. The HC we consider is an inline deoiling HC as shown in Fig. 1a, in which all the flows are co-current.

Our dynamic model is based on a balance on the oil volume as we do not consider any changes in density. The model is an extension of the previously developed steady state model [4]. The model establishes a relationship between the oily discharge flow and the oil in water at the discharge. The oil droplets have specific radial and axial velocities, which are functions of their size, their radial and axial positions inside the separator and the flow rate. The droplets quickly achieve terminal velocities in the radial and axial directions, but these velocities have a spatially local validity. We assume that based on HC design the separator volume can be segmented into two volumes. Droplets that cross the common boundary of these two volumes are going to switch from one outlet to the other. The larger the droplet, the higher the radial velocity, and therefore, the higher the possibility of them exiting in the oily discharge. Based on a spatial profile of the local oil fraction, we calculate the oil cut in the two outlets. This spatial profile will change temporally under transient conditions.

Based on our dynamic model, we propose a control loop from Oil in Water to oily discharge flow as shown in Fig. 1b. This control structure will be heavily dependent on the reliability, accuracy and the response time of the Oil in Water sensors. [5] presented some results on the evaluation of Oil in Water sensors for control, which seem promising.

References

[1] Discharges, ospar convention (2001).
    URL https://www.ospar.org/work-areas/oic/discharges

[2] P. Durdevic, S. Pedersen, M. Bram, D. Hansen, A. Hassan, Z. Yang, Control oriented modeling of a de-oiling hydrocyclone, IFAC-PapersOnLine 48 (28) (2015) 291–296.

[3] P. Durdevic, S. Pedersen, Z. Yang, Challenges in modelling and control of offshore de-oiling hydrocyclone systems, in: Journal of Physics: Conference Series, Vol. 783, IOP Publishing, 2017, p. 012048.

[4] T. Das, P. Tyvold, J. Jäschke, Modelling and optimization of compact subsea liquid-liquid separation system, Vol. 38, Elsevier, 2016.

[5] P. Durdevic, S. Pedersen, Z. Yang, Evaluation of oiw measurement technologies for deoiling hydrocyclone efficiency estimation and control, in: OCEANS 2016-Shanghai, IEEE, 2016, pp. 1–7.

SIMC-Tuned PID Feedback control strategy in fed-batch bioreactors

Pedro A. Lira-Parada, Nadav Bar*

Department of Chemical Engineering, Norwegian University of Science and Technology, Trondheim N7491, Norway

* Corresponding author
nadi.bar@ntnu.no

Abstract

Background: Control of growth and production of microorganisms under intensive culture conditions is a requisite for the production of chemicals. In particular, it is necessary in fed-batch bioreactor to have adequate feeding strategies and a control scheme to obtain a reasonable trade-off between biomass accumulation and production from the substrate. However, selection of an adequate control strategy (e.g. a PID controller) may be difficult, since the process and controller dynamics are often not well understood, or are too simplified. Moreover, there is a significant time delay between the intracellular production (expression of proteins or formation of metabolites) to the product's accumulation in the medium or downstream. Several control tuning methodologies were applied previously in industrial processes , for instance in baker's yeast production, ethanol biomass production, wastewater treatment penicillin and amino acids production. Since the control requirement varies between processes, the robust, simple and versatile PID control is often applied to control feeding and growth rates.

However, the standard commonly applied tuning methods for the PID control involve the heuristic Ziegler-Nichols method that often yields too aggressive response and poor performance in systems with considerable time delay. The flaws in performance of such heuristic methods restrict the PID control applications to simple tasks that can tolerate delays, inverse response, overshoot, steady state biases and other undesired responses. Therefore, we need an efficient PID tuning method for the wide range of (fed-) batch fermentation processes.

Results: This paper presents a tuning procedure of a PID feedback controller using SIMC rules, implemented on bioreactors for the production of chemicals. To derive general expressions to any fed-batch bioreactor, we employed dimensionless form of the model and the SIMC rules, and then analyzed the model robustness. We implemented a simple two-step SIMC procedure (Skogestad, 2003). The procedure is general and easily applicable to bioreactors, with the first-order (PI) and/or second-order (PID) plus delay model and then deriving the model-based controller strategies. Herein, we show that the SIMC tuned PID feedback control yields better performance compared to the PID control tuned with Ziegler-Nichols. The results suggest that the present methodology can be implemented in most fed-batch biochemical processes to achieve high performance (production, rates and yields).

Conclusion: A good control performance in bioreactors is a first step to a deeper, next level control of intracellular pathways of the fermenting microorganisms that will achieve high production levels of chemicals.The SIMC feedback control procedure presented here have the potential to enable an easy coupling of the micro (intracellular) and macro (feeding and process conditions) control levels for a continuous and stable production of desirable chemicals.

Keywords: fermentation process control, white biotechnology, green chemistry.

Combining Safety and Control using System Theoretic Process Analysis and Adaptive Control

Sveinung Ohrem, Hyungju Kim, Christian Holden, Mary Ann Lundteigen

Department of Mechanical and Industrial Engineering, Norwegian University of Science and Technology

Abstract

When designing a new production or processing facility, the design and choice of a control algorithm is usually not included at an early stage. Results from preliminary hazards and risk analyses provide important constraints on how the plant should be operated. However, more insight into opportunities that can be embedded in the design of control algorithms could also be important when identifying strategies for preventing and responding to onsite hazards. Unfortunately, the more traditional methods for hazards identification are not well suited for capturing hazards that stem from the intended and unintended interaction of software intensive safety-instrumented systems and control systems. Being able to identify, at an early stage, the relationship between control algorithm performance and design requirements and constraints for safety-instrumented systems, could reduce costs and improve safety.

Software-intensive systems represent both opportunities, by allowing more flexible functionality and advanced control algorithms for diagnostics and control, and challenges, by being prone to systematic faults whose triggering conditions and resulting effects can be difficult or impossible to detect. Software related faults most often contributes to accidents by giving unsafe commands, or by not issuing a correct command to a plant [2].

The main purpose of this work is to investigate the use of the new hazard analysis tool called Systems-Theoretic Process Analysis (STPA) [2] to support an early identification of design requirements for control algorithms, that stem from the analysis of the interaction of safety and control systems. In this work we propose a framework for combining safety and control, consisting of 3 steps: i) use STPA to identify safety issues that are solvable by control, ii) design a controller able to solve those safety issues, iii) use STPA on the controlled system to determine the final risk assessment of the system.

The STPA method is based on systems theory rather than reliability theory and treats safety as a control problem rather than a failure problem, i.e., it considers failures arising from unsafe interactions between non-failing components [2, Ch.8.8]. One advantage with STPA is that it can be applied early on in the process and hence drive the decisions, rather than waiting for a design, then review it and potentially change it. We argue that the choice of a control algorithm should also be implemented at an early stage, as small changes to a design may have significant effects on the controllability of a system [3, Ch.5.1].

Here, we apply our framework to a subsea gas compression system consisting of a scrubber, compressor with anti-surge line, condensate pump and several valves, see Fig. 1, where we amongst other things consider safe shut down, disturbance handling, model uncertainties and failures.

References

[1] Åsgard gas compression system. `https://www.spe.org/en/ogf/ogf-article-detail/?art=298`. Acessed 26.10.2017.

[2] Nancy Leveson. *Engineering a safer world: Systems thinking applied to safety.* MIT press, 2011.

[3] Sigurd Skogestad and Ian Postlethwaite. *Multivariable feedback control: analysis and design*, volume 2. Wiley New York, 2007.
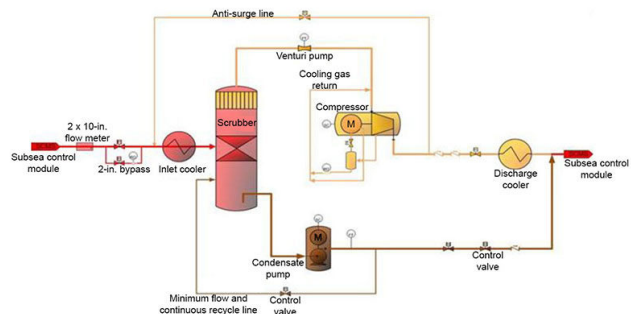
Figure 1: Subsea gas compression system. Figure from [1].

Optimal Operation using Classical Advanced Control Structures

Adriana Reyes-Lúa, Cristina Zotica, Sigurd Skogestad*

Norwegian University of Science and Technology,
Department of Chemical Engineering,
Sem Sælands vei 4, 7491 Trondheim, Norway

With "classical advanced control" we mean the control structures that are commonly used in industry for multivariable control. These structures have been in use for at least 50 years, but surprisingly there is little literature published on how to design such structures in a systematic manner to maintain optimal operation in the presence of disturbances. We suggest that it is possible to organize the available information in a systematic manner to design the regulatory layer using classical control structures so that (near)-optimal operation is maintained, also when changing the optimal operating point and active constraint region.

In this work, we present a design procedure to assure optimal operation when active constraint changes occur. When changing active constraint region, we should decide which CVs to keep controlling and which to give-up. In order to do this systematically, we propose the use of priority lists of constraints as a core step of the design procedure of the control structure. In this contribution, we also discuss how to maintain optimal operation using advanced control structures such as split range control, selectors, and valve position control (input resetting).

We present two examples. First, we consider optimal operation and a priority list of constraints for a cooler with temperature and flow control. We also analyze optimal operation of a simple refrigeration cycle. In both cases, we apply our suggested procedure and evaluate alternative classical advanced control implementations.

Robust Optimization of a Gasoline Blending System

Mandar Thombre, Johannes Jäschke

Norwegian University of Science and Technology
mandar.thombre@ntnu.no

Process plants are operated under a wide variety of operating conditions and product specifications. In practice, however, only partial information regarding these conditions and specifications is known exactly. There is significant uncertainty associated with certain parameters that needs to be accounted for.

Robust Optimization is a relatively recent approach that can be employed to deal with optimization under uncertainty. The uncertainty model in robust optimization is set-based as opposed to stochastic with a probabilistic distribution. As such, the goal is to find a solution that satisfies any realization of the data within the uncertainty set - including the so-called 'worst-case' scenario.
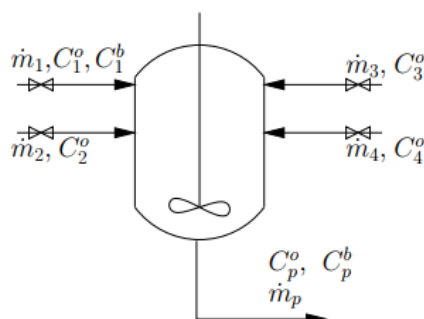
Figure 1: Process: Four gasoline feeds blended to make the product

In this work, a gasoline blending process as shown in Figure 1 is considered. The process consists of 4 gasoline feeds that are blended to make the product. Each of the feed streams has an associated octane number, benzene concentration and unit price. The aim is to minimize the operational cost i.e. the cost of the feed stream, subject to certain constraints. The objective function of this optimization problem can be formulated as:

$$\min J = \sum_{i=1}^{4} p_i \dot{m}_i$$

where p_i is the unit price of stream i and $\dot{m}_i$ is the corresponding mass flow rate. The product mass flow rate is constrained. There are specifications relating to the octane number and benzene concentration requirements in the product. Further, certain relative weight fractions of the different streams in the product are also specified.

This work considers uncertainties in octane numbers and benzene concentrations (process uncertainty) as well as the unit prices (market uncertainty) of the feed streams. The formulation of the so-called 'Robust Counterpart' depends on the shape of the uncertainty set. Robust optimization techniques for different types of uncertainty sets like the box, ellipsoidal and data-driven uncertainty sets are compared for the blending process.

References

A. Ben-Tal, L. El Ghaoui, and A. Nemirovski, *Robust Optimization*, Princeton Series in Applied Mathematics, Princeton University Press, 2009

V. Alstad, *Studies on the Selection of Controlled Variables*, Ph.D. Thesis, Norwegian University of Science and Technology, 2005

Future directions in control relevant models for granulation loop in fertilizer production

Ludmila Vesjolaja[a*], Bjørn Glemmestad[b], Bernt Lie[a]

[a]*Department of Electrical Engineering, IT and Cybernetics, University College of Southeast Norway, Kjølnes ring 56, Porsgrunn 3918, Norway*

[b]*Process Modeling and Control Department, Yara Technology Centre, Hydrovegen 67, Porsgrunn 3936, Norway*

Abstract: This paper is focused on the last stage of fertilizer production, namely the granulation process. The operation of granulation plants in an industrial scale is challenging. It is common to operate granulation loops below their maximum design capacity and periodic instability may also occur. The typical recycle ratios of granulation loops are varying from 6:1 to 4:1 (recycle/product). These operational problems lead not only to reduced product quantity, but also to reduction in product quality. In this study, discussions are made to address these problems. Particularly, the focus is placed on the importance and the necessity of developing dynamic models of the process which can be used along with model based control strategies for a stable operation of the granulation loop. Emphasis is given on population balance modelling.

Keywords: granulation loop; population balance; granulation mechanisms; dynamic model

1. INTRODUCTION

Granulation is a particle design process that finds application in a wide range of industries. Batch processes are typically used in pharmaceuticals, agricultural, chemicals and nuclear wastes industries, while continuous processes are typically used in fertilizer, inorganic salts and detergents industries. Granulation is a particle enlargement process during which fine particles and/or atomizable liquids, i.e. solutions or melts, are converted into granules via a series of complex physical processes. The main objective is to produce granules with improved properties (e.g., flow-ability, dustiness etc.) compared to their ungranulated form and to meet product quality requirements.

A number of studies have been performed to understand the underlying phenomena occurring during granulation. Among others, these include several studies conducted at University of Newcastle, Australia, e.g., Iveson (2002) and University of Queensland, e.g. Litster and Ennis (2004) and Wang et al. (2006). Despite the numerous studies that have been performed on granulation, industrial granulation processes still operate inefficiently, suffer from high rejection rates in batch processes, and from high recycle ratios of off-spec product for continuous processes (Wang et al., 2006). Periodic instabilities are not uncommon in granulation loops. An important reason for the oscillations is the process configuration and the recycle in particular. The recycle is necessary, but it also affects the dynamics significantly.

This paper focuses on a granulation loop used for manufacturing fertilizers. The granulation plant operate well below the design capacity and suffers from high recycle ratios. It is necessary to control the operation of the granulation process for reducing the high recycle ratio and thus improving the efficiency of the plant. A model based control approach can be a way to achieve improved operation of the granulation loop. The main objective of this paper is to discuss future directions in the development of dynamic models that can be used for control purposes.

2. PROCESS DESCRIPTION

A granulation loop consists of a granulator, drier, granule classifier (screens), and a crusher. A typical schematic of a granulation process with a recycle loop is shown in Figure 1. The granulator can be of different types such as a drum granulator, pan granulator, fluidized bed, and etc. The drying of the granules can be performed simultaneously inside the granulator, and/or as a separate unit in the loop. The granulator receives the fines from the external particle feed, as well as from the recycled stream. These particle feeds are sprayed with a fresh fertilizer liquid melt (slurry), and granules are formed. During this process the properties (e.g., particle size, porosity, moisture content etc.) of the produced particles (granules) are changed. Inside the granulator, particles are exposed to complex physical processes, including wetting, layering, agglomeration, and drying. A hot air is fed to the granulator to dry the granules. After the dried granules leave the granulator, they are sent to screens where the particles are separated into three different classes according to their sizes: product size, oversize, and undersize particles. The oversized particles are crushed using a roll-crusher and then added to the undersized particle stream and taken back to the granulator as a recycle stream.

* Corresponding Author:
 Tel: +47 35 57 51 67; *E-mail address:* ludmila.vesjolaja@usn.no
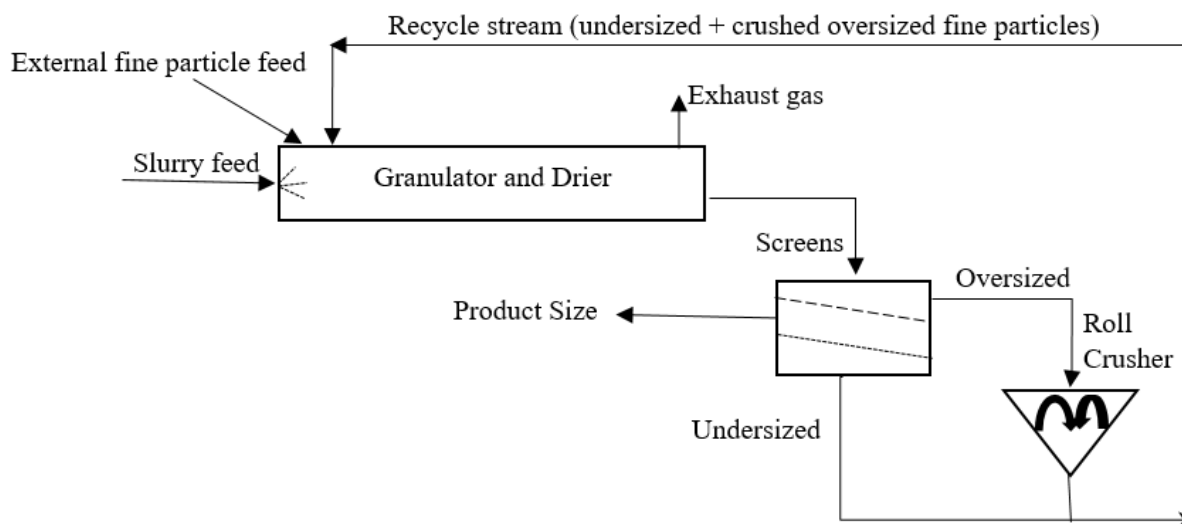
Fig. 1 Schematic diagram of granulation loop.

The recycle feed is an integral part of the granulation process. The recycle of the off-spec particles is partly needed to maintain the particle enlargement process, i.e., granulation, since granulators inevitably need seeds. The amount of recycle as well as its particle size distribution (PSD) are important for the granulation loop. Another reason to have the recycle feed is due to a wide PSD of the granules from the granulator outlet. Typically, the PSD of the granules leaving the granulator is wider compared to the required PSD of the final product (Fig. 2). The undersized and oversized granules cannot be considered as a waste material and discarded from an economic and environmental points of view. Instead, they are taken back to the granulator as a recycle stream.
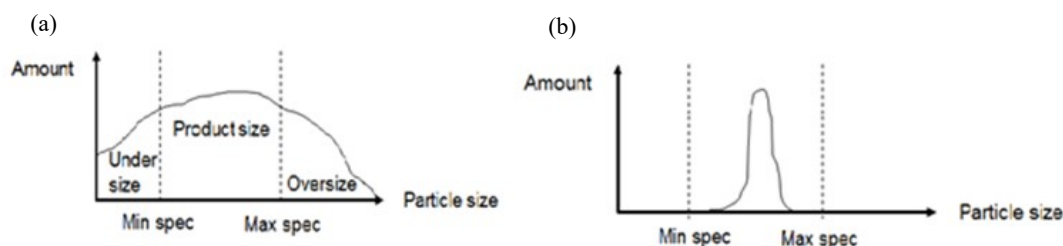
Fig. 2 Particle size distribution (a) obtained after granulation, (b) desired product PSD[†].

3. OPERATIONAL CHALLENGES

The industrial granulation plant studied in this paper is operated well below design capacity with a typical recycle ratio of 4:1. This implies a high ratio between the off-spec (undersize and oversize) particles and the required product size particles. This high recycle rate leads to instability in operation with cyclic variations in the product quality distribution (particle size and shape, bulk density, moisture content and porosity). It has been difficult to obtain a steady narrow particle size distribution from the process and the reason for this partially due to a granulation drum itself. However, the instability is linked to the entire granulation loop since the drum receives a fluctuating recycled stream input. Therefore, for a stable operation of the entire loop a good process control strategy, probably model based, is essential. This further implies that a complete granulation loop model, including crusher, that is able to exhibit the main/necessary dynamics of the granulation process should be developed.

Currently, a simple model of the granulator is used for studying the behaviour of the process. This model has considerable uncertainties in representing complex interactions of the particles. It assumes that the particle growth inside the granulator is only due to layering, while particle growth by nucleation and agglomeration is ignored. In addition, particle breakage and consolidation effects are not taken into account in the model. It is believed that the use of an advanced model that could capture these particle growth mechanisms would improve PSD at the outlet of the granulator and might improve the overall stability of the granulation loop.

In addition to the granulator itself, the particle crusher (roll-crusher) may also introduce operational instability as discussed in Radichkov et al. (2006). In their work, qualitative analysis through dynamic simulations of the granulation loop of a

---

[†] Glemmestad, B. Retrieved from internal presentation at Yara Technology Centre.

fluidized bed as the granulator was performed. The process stability was analysed by giving step changes to the mean diameter (d_m,) of the particles (Fig. 3).

For coarser particles (having a relatively larger diameter) the process reaches a stable steady state represented by the Sauter diameter d_{32} (Fig. 3a), while for finer particle fraction the process shows an oscillatory behaviour (Fig. 3b). For very fine particles, the process again shows a stable steady state (Fig. 3c). Furthermore, as can been seen from Figure 3a, for larger values of particle diameter, the process shows damped oscillatory transient behaviour with settling time of about 6 hours (Radichkov et al., 2006). Interestingly, the simple model of the granulation loop used in particular plant also exhibits a similar behaviour. Thus, the crusher gap (mill grade, i.e., particle diameter) has a significant influence on process stability and these should be taken into account when developing a model of the crusher.
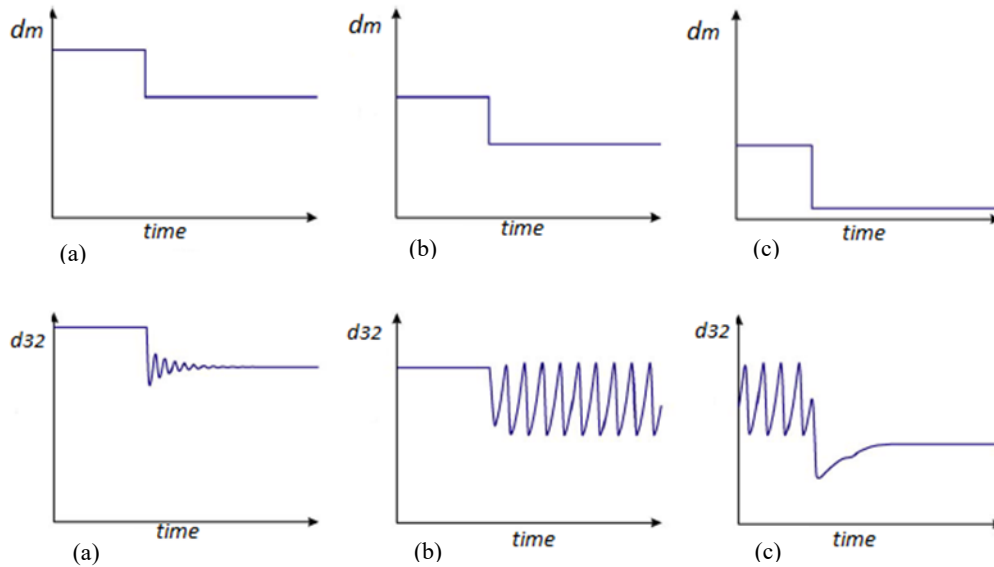
Fig. 3 Qualitative transient behaviour after a step-by-step decrease of d_m, taken from Radichkov et al. (2006).

4. MODELLING OF GRANULATION LOOP

The development of a dynamic model of the granulation loop is challenging. The most widely used approaches for modelling such systems include Discrete Element Modelling (DEM), Population Balance (PB) modelling, as well as hybrid PB-DEM. The combination of mass balance, energy balance and PB can give us a dynamic model for representing the behaviour of the granulation loop. The focus of this paper is on PB modelling.

4.1 General population balance equation

The Population balance equation (PBE) was originally proposed by Hulburt and Katz (1964) and Randolph and Larson (1962). Originally, PBE was based on the number density function. A simple derivation of the PBE can be found in Litster and Ennis (2004). The microscopic PB (particle property distribution varies with position in the vessel) can be expressed as follows:
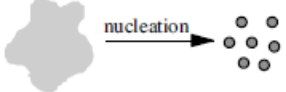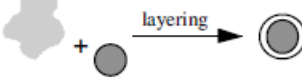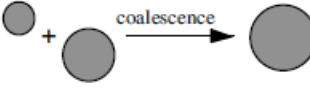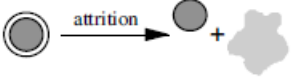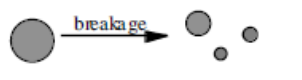
$$\frac{\partial n}{\partial t} = -\nabla . \bar{v}_e n - \nabla . \bar{v}_i n + \dot{b} - \dot{d}, \tag{1}$$

where n is the number size distribution (no·m^{-4}) and is a function of time, space and particle properties. The term $\dot{b}$ is the birth rate distribution (no·s^{-1}·m^{-4}) and $\dot{d}$ is the death rate distribution (no·s^{-1}·m^{-4}). The term $\bar{v}_e$ is the vector of the particle velocity components with respect to the external coordinates (x, y, z directions), $\bar{v}_i$ is the vector of the velocity components with respect to internal coordinates (particle properties such as size, density), and t is time.

4.2 Mechanisms of granulation process

The PBEs represented by Equation (1) are based on complex granulation mechanisms that are taking place inside the granulator. Sastry and Fuerstenau (1973) conducted early work on the mechanisms of granulation. They defined five mechanisms that may occur during granulation and those were nucleation, coalescence, breakage, abrasion transfer, and snowballing (layering). A modern approach for dividing the granulation mechanisms were proposed by Iveson et al. (2001). They divided the granulation process into three basic mechanisms, namely (i) nucleation and wetting, (ii) growth and consolidation and (iii) breakage and attrition. A typical categorization of the principal mechanisms for mathematical modelling purposes (PB modelling included) is summarized in Table 1.

Table 1. Principal mechanisms in granulation processes according to Litster and Ennis (2004).

Mechanism	Changes mass or number of granules	Discrete or Continuous process
nucleation	mass and number	discrete
layering	mass	continuous
coalescence	number	discrete
attrition	mass	continuous
breakage	number	discrete

Nucleation:

Nucleation is the first step in the granulation process. This mechanism is responsible for the formation of the initial aggregates (granules) from liquid or fine powder feed. In the spraying zone, the fine powder interacts with the binder spray droplets resulting in an increase of both mass and number of granules. This is a discrete process and a number of nucleation models have been proposed in literature, e.g., Wildeboer et al. (2005). However, nucleation is rarely identified and separated from other granulation mechanisms, such as granule growth due to layering and agglomeration (Iveson et al., 2001; Litser and Ennis, 2004).

Growth:

Granule growth occurs through two key mechanisms: layering and agglomeration. Agglomeration is alternatively denoted coalescence (Cameron et al., 2005).

Growth due to layering:

Layering is a particle growth that occurs due to successive coating of a liquid phase onto the granule. As a result, the granule grows and its mass increases, but the number of granules in the system remains unchanged. No collision between granules is assumed during this particle growth.

Layering is a continuous process and an assumption of size-independent linear growth rate is common in the PB modelling of granulation processes. This simplification implies that each granule has the same exposure to new feed material and that the volumetric growth rate is proportional to the projected granule surface area. Such linear growth rate can be assumed when there is no segregation of granule size (Cameron et al., 2005; Litster and Ennis, 2004).

Agglomeration (coalescence):

Agglomeration refers to a particle growth mechanism that occurs due to successful collision of two particles, resulting in the formation of a composite particle. Agglomeration is a discrete event that changes the number of granules, but not their mass. The formation of the new granule is represented as a birth term in PBEs and the disappearance of the two smaller particles as a death term (Litster and Ennis, 2004).

It is indeed challenging to model particle agglomeration. One of the approaches was proposed by Kapur and Fuerstenau (1969). Assuming that coalescence rate is proportional to the number density of granules of each size range and inversely proportional to the total number of granules, the birth rate and the death rate of new granules of size v is represented by Equation (2) and (3), respectively (Litster and Ennis, 2004).

$$\dot{b}(v) = \frac{1}{2N_{tot}} \int_0^v \beta(u, v-u, t) n(u) n(v-u) du, \qquad (2)$$

$$d(v) = \frac{1}{N_{tot}} \int_0^\infty \beta(v,u,t)n(v)n(u)du, \tag{3}$$

where u and $(u\text{-}v)$ are the volumes of the two colliding particles (m³), v is the volume of the new particle (m³), N_{tot} is the total number of particles (no·m⁻³) and β is the rate constant usually called as coalescence kernel. The term ½ before the integral is to avoid double counting of particle collisions.

The coalescence kernel is a key parameter that controls the overall rate of agglomeration. Various studies such as Adetayo and Ennis (1997), Adetayo et al. (1995), Liu et al. (2000) and Ouchiyama and Tanaka (1975) were devoted to finding formulations of coalescence kernels. From these studies, it was concluded that both the size-independent and the size-dependent coalescence kernels drive the coalescence process. In the beginning of the granulation process, i.e., in the non-inertial regime, the collision probability does not depend on the particle size but only on binder distribution. In contrast, in the inertial regime, particle coalescence and collision is a function of particle size and collision velocity (Litster and Ennis, 2004).

According to Adetayo et al. (1995), the extent of granulation in the inertial growth regime can be expressed using a model parameter k_{max}. The critical size d_{max} can be predicted using Equation (4) and (5). These formulations were derived by analysing the fertilizer production using a drum granulator.

$$d_{max} = d_0 \exp\left(\frac{k_{max}}{6}\right), \tag{4}$$

$$k_{max} = 6\ln\left(\frac{N_{St}\cdot 9\mu}{8\rho_g U_c d_0}\right) \propto \ln\left(\frac{\mu}{\rho_g U_c d_0}\right), \tag{5}$$

where d_0 and d_{max} are initial and critical particle diameters (m), N_{St} is viscous Stokes number, μ is viscosity (Pa·s), ρ_g is granule density (kg·m⁻³) and U_c is collision velocity (m·s⁻¹).

A number of other empirical and semi-empirical coalescence kernels for granulation are available in the literature (Cameron et al., 2005; Litster and Ennis, 2004). These include model parameters that should be fitted with experimental data.

Breakage and attrition:

Particle attrition is the opposite effect of layering. This granulation mechanism is more significant at high granule velocities and when drying occurs simultaneously with the granulation. Examples of such systems are fluidised bed and spouted beds. The attrition rate is a negative rate and is proportional to the bed conditions. Formulation of attrition rates for both fluidized and spouted beds are summarised in Litster and Ennis (2004).

Particle breakage by fragmentation is a discrete event and results in birth and death terms in the PB. Breakage effects are important in high shear devices, especially in high impact mixer granulation (Chaturbedi et al., 2017; Litser and Ennis, 2004; Ramachandran et al., 2009). A different type of the particle breakage also appears in continuous granulation loops, via particle crushing in the mill. Models of breakage effects are complex and were extensively studied by Ramachandran et al. (2009) and Chaturbedi et al. (2017).

4.3 Granulator model

The industrial granulation loop, which is mentioned in this paper, should be modelled as a dynamic system capable of showing the PSD dynamics of the granules. This implies the use of PBEs that were described in Section 4.1 and Section 4.2. A plug flow may be assumed with the particle size changing only in one direction (axial). The shape of a granule may be assumed to be spherical and thus, the diameter can be used to represent its size. Thus, a microscopic PB of Equation (1) with one internal coordinate (particle diameter) and one external coordinate (axial direction) may be utilized as shown in Equation (6) (Litster and Ennis, 2004):

$$\frac{\partial n}{\partial t} = -\frac{\partial}{\partial l}(un) - \frac{\partial}{\partial d_p}(Gn) + \dot{b} - \dot{d}, \tag{6}$$

where u is the particle velocity (m·s⁻¹), d_p is the particle diameter (m), l is the distance from the start of the granulator (m) and G is the particle growth rate (m·s⁻¹), and $n = (d_p, l, t)$.

Further development of the model should be based on the granulator type that is used in the granulation loop. The significance of each granulation mechanism described in Section 4.2 will determine the main model assumptions. Equation (6) represents number based PB. However, solving the number based PB numerically is time consuming. A relatively faster solution can be obtained if the mass distributed PB is used (Cameron et al., 2005; Radichkov et al., 2006).

For the development of a simplified model of the drum granulator, the change in the particle size growth may be assumed only due to layering, i.e. particle coalescence, attrition and breakage may be neglected ($\dot{b}$ and $\dot{d}$ terms in Equation 6 are set to zero). In addition, a size-independent linear growth rate may be assumed. In this case, the growth rate, G is proportional to the particle projected area, A_p i.e.,

$$G \propto A_p = d_p^2 \tag{7}$$

Another approach for modelling such complex system might be using the compartment based PB. This would represent the inhomogeneity of the system. The assumption of granule formation by linear layering of the particles where one liquid droplet can wet only one particle is quite unrealistic. The particles that are more wetted are characterised with increased aggregation rates compared to those particles with less moisture content (Chaturbedi et al., 2017; Li et al., 2012). In this perspective, it could be a good idea to separate the spraying zone from the other part of the granulator. However, in the case of continuous granulation process with simultaneous granule drying (especially when microscopic PB is used), it might not be significant.

A dynamic model of the granulator that includes all the mechanisms of the granulation process such as nucleation, growth due to layering and coalescence, particle attrition and breakage is more accurate in the sense that such kind of model is able to capture and exhibit complex operational dynamics. However, developing such kind of models may be difficult and in addition, obtaining the solution of the model numerically can be challenging as well as time consuming (Cameron et al., 2005). From the process control point of view, a very detailed model (although more accurate) but not real-time implementable simply becomes impractical. Thus, it is useful and essential to develop a mathematical model that is simple enough yet sufficient to capture the necessary (important) dynamics of the granulator. It is also important that the model can be solved sufficiently fast so that it can be used for real-time implementation. Such kind of models are well suited for online model based control strategies. Thus, a good balance between the model complexity (accuracy) and the model solution time should be considered during the development of the mathematical models of the granulator.

For developing a complete model of the granulation loop, it is also necessary to have mathematical models of other units present in the loop such as particle classifier (screens), dryer and crusher.

4.4 Models for classifier, dryer and crusher

Classifier and dryer:

Simultaneous drying of the particles inside the granulator may be modelled using for example evaporation function and combining it with the energy balance. The separation of the discharge from the granulator is performed using double check screens. Two sieves of different sizes are used to separate the granules flowing out of the granulator into three fractions – oversized, product size and undersized granule fractions. These may be implemented in the model by using probability density functions, e.g., Gaussian normal distribution function, uniform distribution etc.

Crusher:

The oversized particle fraction is sent to a roll-crusher where the granules are broken (crushed) to form fine particle feed which is then added to the undersized particle fraction stream and finally taken back to the granulator as a recycle stream. As was discussed in Section 3, the granulation loop stability is dependent on the recycle feed. Thus, the model of the recycle feed that also includes the crusher should be developed to reflect this characteristic. Among others, some models of the crusher that are available in the literature include Austin and Cho (2002), Kis et al. (2006) etc. In Cotabarren et al. (2008) a model for a double-roll-crusher for urea size reduction process is proposed. The developed mathematical model predicts the PSD by taking into account the crusher gap.

5. CONCLUSIONS

The recycle ratio is an important factor for the stability of the granulation loop. This ratio is partly dependent on the way the granulator drum functions. To stabilize the granulation loop, control algorithms that utilize the model of the process may be a good choice. Therefore, a proper understanding of the dynamics of the granulation loop is important. A mathematical model of the granulation loop can be developed and simulated to study various operational scenarios. This model can be further used for control purposes. By stabilizing the granulation loop, oscillatory behaviour may be supressed and hence the product yield may be improved.

Despite a number of studies on granulation processes, the available models have qualitative character rather than quantitative. Many of these models do not take into account particle agglomeration and to what degree recycled and fresh particles result in nucleation or agglomeration. Therefore, a more accurate yet a simple model of the granulation loop is essential.

REFERENCES

Adetayo, A., & Ennis, B. (1997). Unifying approach to modeling granule coalescence mechanisms. *AIChE Journal, 43*(4), 927-934.

Adetayo, A., Litster, J., Pratsinis, S. E., & Ennis, B. (1995). Population balance modelling of drum granulation of materials with wide size distribution. *Powder technology, 82*(1), 37-49.

Austin, L. G., & Cho, H. (2002). An alternative method for programming mill models. *Powder technology, 122*(2), 96-100.

Cameron, I., Wang, F., Immanuel, C., & Stepanek, F. (2005). Process systems modelling and applications in granulation: A review. *Chemical Engineering Science, 60*(14), 3723-3750.

Chaturbedi, A., Bandi, C. K., Reddy, D., Pandey, P., Narang, A., Bindra, D. Hussain, M. (2017). Compartment based population balance model development of a high shear wet granulation process via dry and wet binder addition. *Chemical Engineering Research and Design, 123*, 187-200.

Cotabarren, I., Schulz, P. G., Bucalá, V., & Piña, J. (2008). Modeling of an industrial double-roll crusher of a urea granulation circuit. *Powder technology, 183*(2), 224-230.

Hulburt, H. M., & Katz, S. (1964). Some problems in particle technology: A statistical mechanical formulation. *Chemical Engineering Science, 19*(8), 555-574. doi: https://doi.org/10.1016/0009-2509(64)85047-8

Iveson, S. M., Litster, J. D., Hapgood, K., & Ennis, B. J. (2001). Nucleation, growth and breakage phenomena in agitated wet granulation processes: a review. Powder technology, 117(1), 3-39.

Iveson, S. M. (2002). Limitations of one-dimensional population balance models of wet granulation processes. *Powder technology, 124*(3), 219-229.

Kapur, P., & Fuerstenau, D. (1969). Coalescence model for granulation. *Industrial & Engineering Chemistry Process Design and Development, 8*(1), 56-62.

Kis, P. B., Mihálykó, C., & Lakatos, B. G. (2006). Discrete model for analysis and design of grinding mill-classifier systems. *Chemical Engineering and Processing: Process Intensification, 45*(5), 340-349.

Li, J., Freireich, B., Wassgren, C., & Litster, J. D. (2012). A general compartment-based population balance model for particle coating and layered granulation. *AIChE Journal, 58*(5), 1397-1408.

Litster, J., & Ennis, B. (2004). *The science and engineering of granulation processes* (Vol. 15): Springer Science & Business Media.

Liu, L., Litster, J., Iveson, S., & Ennis, B. (2000). Coalescence of deformable granules in wet granulation processes. *AIChE Journal, 46*(3), 529-539.

Ouchiyama, N., & Tanaka, T. (1975). The probability of coalescence in granulation kinetics. *Industrial & Engineering Chemistry Process Design and Development, 14*(3), 286-289.

Radichkov, R., Müller, T., Kienle, A., Heinrich, S., Peglow, M., & Mörl, L. (2006). A numerical bifurcation analysis of continuous fluidized bed spray granulation with external product classification. *Chemical Engineering and Processing: Process Intensification, 45*(10), 826-837.

Ramachandran, R., Immanuel, C. D., Stepanek, F., Litster, J. D., & Doyle, F. J. (2009). A mechanistic model for breakage in population balances of granulation: Theoretical kernel development and experimental validation. *Chemical Engineering Research and Design, 87*(4), 598-614.

Randolph, A., & Larson, M. (1962). Transient and steady state size distributions in continuous mixed suspension crystallizers. *AIChE Journal, 8*(5), 639-645.

Sastry, K. V., & Fuerstenau, D. (1973). Mechanisms of agglomerate growth in green pelletization. *Powder technology, 7*(2), 97-105.

Wang, F., Ge, X., Balliu, N., & Cameron, I. (2006). Optimal control and operation of drum granulation processes. *Chemical Engineering Science, 61*(1), 257-267.

Wildeboer, W., Litster, J., & Cameron, I. (2005). Modelling nucleation in wet granulation. *Chemical Engineering Science, 60*(14), 3751-3761.

Comparing water treatment topologies in Recirculating Aquaculture Plants

Simon Pedersen [*] **Torsten Wik** [*]

[*] *Division of Systems and Control, Department of Electrical Engineering, Chalmers University of Technology, 412 96 Göteborg (e-mail: pesimon@chalmers.se, tw@chalmers.se).*

Aquaculture, the farming of fish and aquatic crops such as kelp and algae, is traditionally carried out in natural bodies of water. An alternative is land-based farming in tanks or raceways, which is particularly attractive when coupled with water treatment to form a recirculating aquaculture system (RAS). Benefits compared to traditional farming in open cages include reduced emissions of nutrients, small or no risk of escapes, and control of pathogens (Thorarensen and Farrell, 2011).

Water treatment takes place in a series of mechanical filters and biological reactors, where particulate and dissolved matter is degraded by microorganisms similarly to how municipal sewage is treated. The biological nature of recirculating aquaculture systems makes experimental process development troublesome. Contributing factors include very long time constants, biological variations, and concerns for animal welfare. This strongly motivates the use of dynamic simulations, and for that purpose a RAS simulator – called FishSim – was developed (Wik et al., 2009). However, the capabilities of that implementation were limited by numerical problems.

Using Modelica, a high-level object-oriented language for dynamic systems modeling (Modelica Association, 2012), we have developed a new simulation tool for recirculating aquaculture. Like FishSim, it is based on Activated Sludge Model 1 (Henze et al., 2000), but this implementation is numerically well-behaved and robust which allows a much greater variety in the simulated systems. It is also significantly faster, even after the models have been expanded with many more features, such as energy balances, different feeding options, and a separation of autotrophic bacteria into ammonia-oxidizing and nitrite-oxidizing bacteria. Since open-source Modelica tools are available, the software is also free to use.

Water treatment is central in recirculating aquaculture. Fish excrete ammonia, which is toxic to them. Aerated bioreactors are typically employed to remove ammonia and ammonium via nitrifying autotrophs, which require low levels of biodegradable organics to thrive. Nitrification creates nitrite (also toxic to fish at low levels) and nitrate, the latter which is removed by water exchange or denitrification. Denitrifcation conversely requires high availability of biodegradable organics, but only progresses rapidly in the absence of oxygen. The treatment systems often further contain particle filters and UV and/or ozone treatment against pathogens.

While it is reasonably clear to the industry which components should be present in the treatment system, the order in which they are best employed is still an open question. In the literature and supplier information material there is a large number of suggested configurations, but few studies comparing them. Some guesses can be made based on elementary chemical reaction engineering, but the very complex dynamics of the biological treatment leads to high uncertainty.

Using the simulator, we have investigated and compared several treatment topologies. Through parameter optimization based on a genetic algorithm (Haupt and Haupt, 2003) the minimal reactor sizes in each configuration was found which could maintain acceptable levels of ammonia and nitrate. The resulting sizes are an indicator of which topology is the most effective.

REFERENCES

Haupt, R.L. and Haupt, S.E. (2003). *Practical Genetic Algorithms*. John Wiley & Sons, Inc., Hoboken, NJ, USA. doi:10.1002/0471671746.

Henze, M., Gujer, W., Mino, T., and van Loosdrecht, M.C.M. (2000). *Activated Sludge Models ASM1, ASM2, ASM2d and ASM3*.

Modelica Association, 2012 (2012). *Modelica language specification 3.3*. Modelica Association.

Thorarensen, H. and Farrell, A.P. (2011). The biological requirements for post-smolt Atlantic salmon in closed-containment systems. *Aquaculture*, 312(1-4), 1–14. doi:10.1016/j.aquaculture.2010.11.043.

Wik, T.E., Lindén, B.T., and Wramner, P.I. (2009). Integrated dynamic aquaculture and wastewater treatment modelling for recirculating aquaculture systems. *Aquaculture*, 287(3–4), 361 – 370.

Utilization of generic consumer modeling in planning and optimization of district heating and cooling systems

Khalid Tourkey Atta & Wolfgang Birk

Control Engineering Group, Department of Computer Science, Electrical and Space Engineering, Luleå University of Technology, Luleå, Sweden.

Abstract

District heating and cooling (DHC) networks are large scale complex systems which are generally difficult to operate and optimize. The large thermal inertia in the systems leads to long reaction times on changes at the consumer side, which means that forecasting of consumer behaviour is a needed tool for efficient operation. Within the European Union many major research project target the energy reduction on the consumption side and peak load management while maintaining customer satisfaction.

The optimal operation of a DHC network can therefore be considered as an interesting area of investigation due to a number of aspects, like (i) the vast amount of the energy that is distributed by these networks, (ii) the demand to provide a better quality of services by the operators of these networks, and (iii) compliance with new environmental regulations.

In this presentation, we discuss a possible conceptual method that utilizes a simplified static model of different types of consumers in the network to design a decision support system that will guide the operators of the DHC network to optimally operate the network with different operational scenarios that include but not limited to: (i) energy consumption minimization, (ii) economic operation, (iii) peak load reduction/shifting, and (iv) environmentally friendly operation. In its current form, the operator will be informed, while in the future these actions could be fully automated in a closed loop context.

The DHC network in Luleå, Sweden will be used as a test case which represents a typical medium size network. The case has a number of properties which motivate its study like e.g. the distributed generation possibilities, the geographical distribution of the consumers, and the different types of consumers in the area. The presentation will be concluded with an outlook on future tracks of research and development.

Keywords: District heating, district cooling, thermal grids, demand forecast, Energy optimization, peak load management

Integrating microbial genome-scale flux balance models with JModelica and the Bioprocess Library for Modelica

Jan Peter Axelsson, senior consultant
Vascaia AB, 112 51 Stockholm, Sweden

Bioprocesses are complex and their products are still considered to be defined by the detailed production procedure by the authorities for pharmaceuticals. Still simplified models are of great value to facilitate design of these processes although computer simulation has still a limited spread. Data-driven methods dominate the field.

In this paper, a genome scale flux balance model FBA [1] of yeast from the Python open source framework COBRApy [2] is integrated with the JModelica [3] dynamical simulation software to simulate cells in a batch reactor. With the use of the Bioprocess Library for Modelica [4] the flux balance model can easily also be tested in fedbatch and perfusion reactors and be used in evaluation of control strategies.

The integration is done in the following way. The simulation interval is divided into a number of sub-intervals of equal length. At the start of each sub-interval the FBA LP-problem is solved given the concentration of substances in the reactor and results in metabolic flux rates that optimize cell growth. With these fluxes and optimal growth rate the reactor dynamics is simulated one sub-interval forward. The procedure is repeated until the total simulation interval is covered. A key assumption is that the dynamics of substrate is slow compared to the length of the sub-intervals.

Simple integration of COBRApy models and JModelica is possible since they can actually share the same Python environment. The computational time for the genome scale model shown in Figure 1 is about a minute on an ordinary laptop.

The results of simulation of the genome scale model is compared with results from the traditional simplified model available in the Bioprocess Library for Modelica [4]. For the major variables like glucose, ethanol, cell concentrations the results are similar. The genome scale provides prediction of a number of details, but not evaluated here.

The ease with which these ambitious genome-scale flux balance models can be integrated into dynamical simulation makes it possible to further test them in typical experimental setups that can be described in Modelica and where measurement data can be gathered.

References

[1] http://bigg.ucsd.edu/models
[2] Ebrahim A, J. A. Lerman, B. O. Palsson and D. R. Hyduke, "COBRApy: Constraints-Based Reconstruction and Analysis for Python, BMC Systems Biology 2013.
[3] Åkesson J. K-E Årzén, M. Gäfvert, T. Bergdahl, H. Tummescheit, "Modeling and Optimization with Optimica and JModelica.org – Languages and Tools for Solving Large-Scale Dynamic Optimization Problems, Computers & Chemical Engineering, 2009.
[4] Axelsson J. P., "Modelica library for simulation of bioprocesses", NPCW, Copenhagen, 2012.
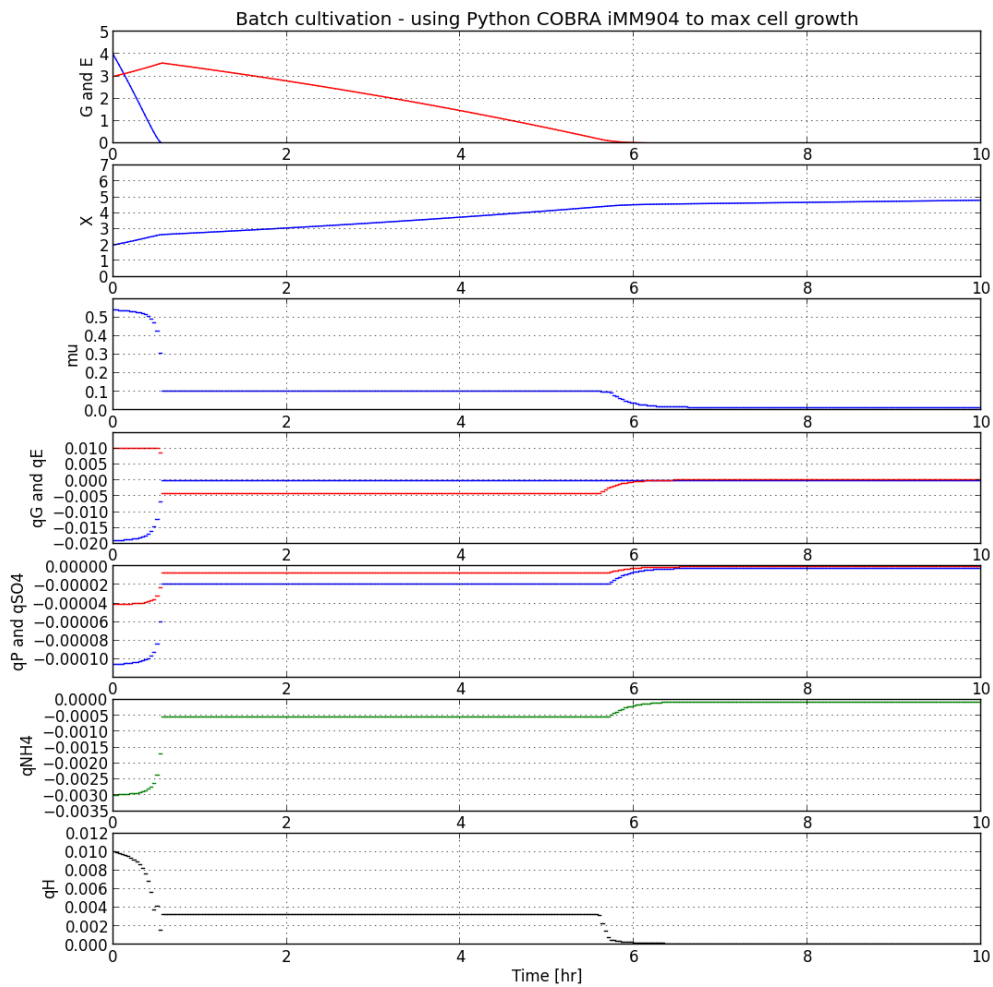
Figure 1. Simulation of growth of yeast in a batch reactor using a genome scale flux balance model iMM904. The diagrams show concentration of cells X, glucose G and ethanol E concentration over time in combination with metabolic fluxes of glucose qG, ethanol qG, phosphate qG, sulfate qSO4, ammonia qNH4 and hydrogen ions qH.